# Preliminary Scoping and Thermodynamic Modelling of $CO_2$ Compressors for Carbon Capture and Storage

**Matilda Lindroth**
**Maja Munktell**

April 2009
Thesis for the degree of Master of Science
Division of Thermal Power Engineering
Department of Energy Science
Faculty of Engineering, Lund University, Sweden

# Abstract

Power production represents one fourth to one third of all $CO_2$ emissions. Carbon Capture and Storage (CCS) in one way to approach the increasing problem with $CO_2$ emissions from fossil fuelled power plants. The $CO_2$ is separated, compressed and transported to a final storing site. To allow more efficient transport and to match the pressure of the final storing site, the $CO_2$ is compressed to a supercritical fluid. The additional equipment that a CCS system requires will have a negative effect on the overall power plant efficiency and it is of great importance to minimise this consequence. This thesis is a preliminary scoping of different $CO_2$ compression technologies and ways to improve them prior to transportation to a final storage site.

The report compares existing, adapted and novel compression technologies in terms of power consumption. $CO_2$ is currently being compressed in for example urea production using integrally bull geared compressors. In-line barrel compressors used in the gas industry show promising possibilities to be adapted for $CO_2$. Two novel ways that has been investigated are a high pressure ratio compressor that uses oblique shock waves to compress the gas and a cryogenic system where the $CO_2$ first is compressed, then cooled in chillers and then pumped to the required delivery pressure. The different compression technologies were modelled in IPSEpro, a thermodynamic simulation tool and the data was validated against TechUtils, a thermodynamic calculation tool. The result shows that compared to the current compression technologies for $CO_2$, novel or adapted methods can reduce the power consumption with approximately 7 %.

# Sammanfattning

Kraftproduktion står för en fjärdedel till en tredjedel av alla koldioxidutsläpp. “Carbon Capture and Storage” är ett sätt att minska koldioxidemissioner vid nyttjande av fossila bränslen i kraftverksanläggningar. Koldioxiden separeras, komprimeras och transporteras till slutförvaring. För att effektivisera transporten och anpassa trycket till slutförvaring komprimeras koldioxiden till en superkritisk fluid. Den extra utrustning som ett CCS-system medför kommer att sänka kraftverkets totalverkningsgrad och det är av yttersta vikt att minimera denna konsekvens. Examensarbetet är en förundersökning av olika metoder att komprimera koldioxid innan transport till slutförvaring samt hur dessa metoder kan förbättras för att minska effektbehovet.

Rapporten jämför existerande, anpassade och nya kompressionstekniker ur ett effektförbrukningsperspektiv. Koldioxid komprimeras redan inom till exempel ureaproduktion med så kallade integrally bull geared kompressorer. In-line barrel kompressorer som används inom gasindustrin har visats sig kunna anpassas för koldioxidkomprimering. Två innovativa metoder som undersökts är en kompressor som med hjälp av sneda stötar uppnår mycket höga tryckförhållanden per steg och ett system där koldioxiden först komprimeras för att sedan kylas genom tvåfasregionen. Den flytande koldioxiden pumpas därefter för att uppnå önskat tryck. De olika kompressionsteknikerna modellerades i IPSEpro, ett termodynamiskt simuleringsverktyg och beräknad data validerades mot TechUtils, ett termodynamiskt beräkningsprogram. Resultaten visar att med nya eller anpassade metoder kan effektbehovet minskas med cirka 7 % jämfört med nuvarande kompressionstekniker.

# Preface

This thesis for the Degree of Master of Science has been conducted at the Strategic Research Centre (SRC) at Rolls-Royce, Derby, England in corporation with the division of Thermal Power Engineering at the Faculty of Engineering, Lund University, Sweden.

During our time at Rolls-Royce we have developed a profound understanding of different compression technologies and the unique technical problems of compressing carbon dioxide. This experience has given us confidence in our roles as engineers.

There are many people who have contributed to making this thesis possible and made these six months the greatest adventure of our lives.

We would like to thank the following persons:

Paul Fletcher, our supervisor, who contributed not only with genuine knowledge and years of experience but also with many laughs.

Carrie Lambert, the project manager, who encouraged us to fill our potential and supported us both as a colleague and as a friend.

Andy Graham, our colleague, who always had time to answer our questions and challenged us to seek a deeper understanding by being inquisitive.

Fredrik Hermann, who guided us to the right people at Rolls-Royce and since then has helped and supported us immensely.

Jenny Persson, who helped us with the placement and became a true friend.

Magnus Genrup, our lecturer and supervisor, who gave us valuable comments on our work and progress.

All of our colleagues at the SRC who welcomed us with open arms.

Last but not least we would like to thank our families and friends who stood by us in good times and bad times. Without you this journey would never have been the same.

Derby 2009

Matilda Lindroth and Maja Munktell

# Table of Contents

## Nomenclature

| Symbol | Unit | Description |
|---|---|---|
| $C$ | [m/s] | Velocity |
| $c_p$ | [J/kgK] | Specific heat at constant pressure |
| $d$ | [m] | Diameter |
| $h$ | [kJ/kg] | Enthalpy |
| $h_0$ | [kJ/k] | Stagnation enthalpy |
| $H_{pump}$ | [m] | Head |
| $\dot{m}$ | [kg/s] | Mass flow |
| $N$ | [rev/s] | Rotational speed |
| $p$ | [bar] | Pressure |
| $p_0$ | [bar] | Stagnation pressure |
| $Q$ | [$m^3$/kg] | Volume flow |
| $\dot{Q}$ | [kW] | Heat transfer |
| $R$ | [J/molK] | Constant of proportionality |
| $T$ | [˚C] | Temperature |
| $T_0$ | [˚C] | Stagnation temperature |
| $U$ | [m/s] | Peripheral velocity |
| $W$ | [kJ] | Work |
| $Z$ | [-] | Compressibility factor |
| $A$ | [˚] | Angle between absolute velocity and axial direction |
| $\gamma$ | [-] | Specific heat ratio |
| $\eta_i$ | [-] | Isentropic efficiency |
| $\eta_p$ | [-] | Polytropic efficiency |
| $\omega$ | [rad/s] | Rotational velocity |

| Designations | |
|---|---|
| ASU | Air Separation Unit |
| CCS | Carbon Capture and Storage |
| COP | Coefficient of Performance |
| EOR | Enhanced Oil Recovery |
| FOD | Foreign Object Damage |
| IGCC | Integrated Gasification Combined Cycle |
| IGV | Inlet Guide Vane |
| LCT | Low Carbon Team |
| NPSHa | Net Positive Suction Head available |
| NPSHr | Net Positive Suction Head required |
| SRC | Strategic Research Centre |
| SWRI | South West Research Institute |

# 1 Introduction

Greenhouse gases like $CO_2$ and water vapor are a necessity to life on earth. Without greenhouse gases the earth's temperature would be more than 30 ˚C colder than current. During the last century the earth's temperature has increased with approximately 0.6 ˚C. It has been stated that the emissions of greenhouse gases from human activities is the primary reason behind the rising temperature. The use of fossil fuels and deforestation are two major contributors to the increase of $CO_2$ in the atmosphere and the greenhouse effect. If no actions are taken to prevent the increasing greenhouse effect the global warming will continue. [1]

There are a number of different approaches that can be used to address the problem of global warming. Since 1970 significant work has been carried out to improve the effectiveness of energy conversion by improving turbines, developing combined heat and power stations etc. The increased use of renewable energy has also helped to reduce the amount of green house gases released. [2]

It has been foreseen that until at least 2030 fossil fuel will remain being the dominant source when producing energy in the world. Developing countries like India and China will contribute to the prime increase in global energy use. It is predicted that by 2010 China will have overtaken The United States as being the world's largest energy consumer. [3]

The continuing increase of $CO_2$ emissions is a problem that has to be dealt with in the near future. Carbon Capture and Storage (CCS) is one way to handle the emission issue but is not the singular solution to the increased green house effect.

## 1.1 Problem Definition

### 1.1.1 Purpose

This thesis is part of a project managed by Rolls-Royce. Due to confidentiality this project will be referred to as 'The Project' throughout the thesis. The purpose is to survey existing, adapted and novel technologies for compressing $CO_2$ prior to transportation to investigate the power consumption.

### 1.1.2 Method

A literature survey on compressors, pumps and refrigeration plants will be undertaken to develop a general understanding of these technologies. The literature survey will also cover background material about different CCS separation methods and $CO_2$ properties.

Based on the literature review and the customer requirements, provided by a utility company, a benchmarking survey will be carried out to evaluate current technologies.

Compression solutions will be selected based on their suitability for $CO_2$ compression and the amount of information available. The selection will also ensure dissemination in method of compression. The selected technologies will be modelled in IPSEpro and TechUtils for predetermined conditions and then summarised and evaluated.

#### 1.1.2.1 Tools Used

**IPSEpro**

IPSEpro is a Windows-based thermodynamic modelling tool. It can be used for creating process models and for analysing processes in power plant engineering, chemical engineering and other related areas. Functions of the tool include:

- Calculating heat balances and predicting off design behaviour.
- Estimating costs on modelled designs.
- Validating and verifying estimates of calculations.
- Optimising plant performances.
- Planning modifications and repowering of existing plants.

IPSEpro consists of two parts; The PSE – Process Simulation Environment where simulations are preformed and the MDK – Model Development Kit where existing models are available. These models can also be changed or rebuilt in the model library. The standard library calculates gas properties by using the Perfect Gas Law. At elevated pressures and temperatures the working media will no longer behave as perfect gases and the law is not valid. To deal with this limitation other libraries has been developed where properties are calculated by using tabulated values. One example of this is the refrigeration library which is a convenient tool for modelling low temperature compression and refrigeration systems. For further information on IPSEpro see Appendix A. [4]

**TechUtils**

TechUtils is Rolls-Royce's set of software tools for thermodynamic calculations. The tools handle almost 200 different non-perfect gases and gas mixtures validated against NIST data. All thermodynamic and state equations are programmed with C++. For given inlet conditions, it calculates stage data such as pressure, temperature, enthalpy, and entropy for adiabatic processes but also isentropic and polytropic efficiencies, flow function, head estimates and power.

TechUtils uses Peng Robinson equations to model the properties of process gas mixtures. However 'pure $CO_2$' has been selected for the preliminary analysis due to the possibility to compare achieved results to IPSEpro.

**CompSelect**

CompSelect is a Rolls-Royce sales support tool that provides characteristics of current compressor products to the user. The tool facilitates selection of appropriate compressors for given pressures, inlet temperatures and mass flows.

### 1.1.3 Restrictions and Limitations

Due to limitations in IPSEpro, the modelling will be implemented using a pure $CO_2$ stream. When impurities are introduced to the stream, the properties will change. However the purpose is to compare different compression methods and the effect of using a pure $CO_2$ stream will be equal to all models. A small investigation of impurities was carried out to develop understanding of their impact.

This thesis only covers the compression after $CO_2$ separation prior to transportation for a power plant with post-combustion removal. The modelled compression methods will be compared by their power consumption for predetermined conditions. Other aspects such as unit costs, footprint and maintenance will be considered later on in The Project.

# 2 Rolls-Royce

Rolls-Royce is a global, world leading company which operates in four different markets: civil aerospace, defence aerospace, marine and energy. The business concept is 'invent once and use many times' where the Trent family of gas turbines is the best example, demonstrated in Figure 2.1.

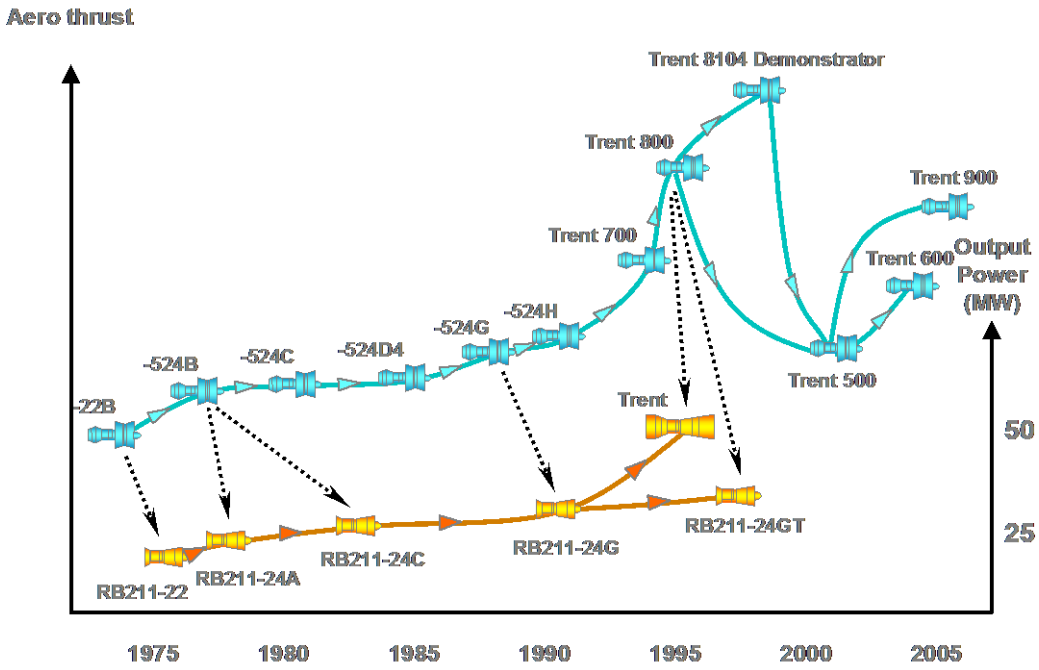


**Figure 2.1: Utilisation of components and technology from aero for industrial product development (note that the Trent 600 never was built)**

Rolls-Royce was founded in 1904 by Charles Rolls and Henry Royce with the goal of developing 'the best car in the world'. The first engines were internal combustion piston engines however, in the 1920's interest in jet engines evolved and in 1939 Rolls-Royce commenced activities. As time went by the aerospace industry grew to become Rolls-Royce's largest sector. In 1971 the company was divided and the car business was sold.

Today Rolls-Royce employs nearly 40 000 people in 50 different countries all over the world. The headquarters are situated in England however, 40 % of the workforce is based outside UK. Since 1996 Rolls-Royce has been run by Sir John Rose who joined the company 1984. The main market is civil aerospace, which accounts for 52 % of the sales followed by defence aerospace (21 %), marine (20 %) and energy (7 %) see Figure 2.2.To add value for customers an aftermarket service is provided in each of the business sectors. It represents 55 % of the Group sales and is continually growing. The remaining 45 % represents equipment sales. [5]

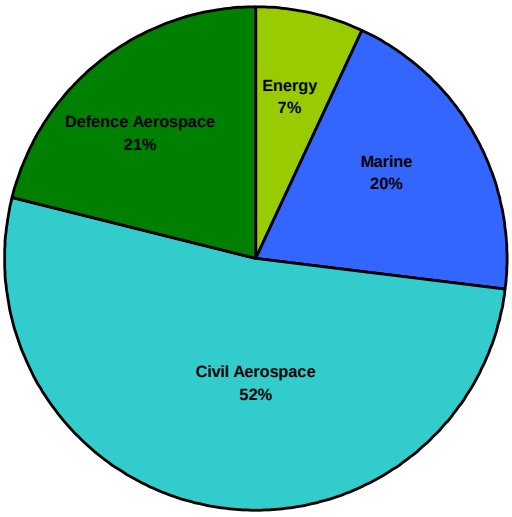


**Figure 2.2: Business market distribution**

## 2.1 Strategic Research Centre

The Strategic Research Centre, SRC, is a department that works across multiple disciplines within the entire business. The main objective is to investigate blue-sky technologies and create new business opportunities. SRC ensures that Rolls-Royce stays on top of potentially disruptive technologies whilst supporting existing products. The company concept of 'invent once and use many times' is visible through the department. For example the expertise in marine propulsion is applied within offshore wind power generation.

The department consists of four teams, as shown in Figure 2.3. To ensure a wide range of knowledge SRC employs professionals with degrees in physics, chemistry, maths, electronics, mechanics, manufacturing and information systems. Current projects include wireless sensors, nuclear power and anti-icing surface coating. Many of the projects are partly funded by the government.

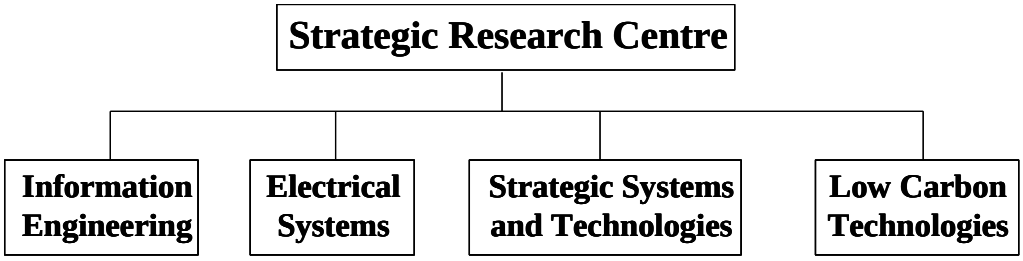


**Figure 2.3: Teams within SRC**

### 2.1.1 Low Carbon Team

90 % of Rolls-Royce's products rely on hydrocarbons. Therefore Rolls-Royce is committed to reducing the environmental impact of its products including its contribution to climate change. As part of its efforts, the Low Carbon Team (LCT) was founded in 2007. This was an initiative of Sir John Rose and the board of directors. Renewables is the fastest growing sector in the energy market and Rolls-Royce saw the opportunity to take hold of a leading position. LCT currently participates in projects on offshore wind power, tidal power and CCS.

#### 2.1.1.1 The Project

The Project is a joint venture between Rolls-Royce, a utility company and a university situated in UK. Due to a confidentiality agreement these two partners will be referred to as 'The Company' and 'The University'. The purpose of The Project is to find a compression solution optimised for $CO_2$ compression from a power plant with $CO_2$ separation in a CCS system.

Rolls-Royce manages the project and provides expertise regarding compressor technology. The Company contributes with data concerning power plant layout. The University is investigating $CO_2$ properties with and without the impact of impurities.

# 3 Carbon Capture and Storage

Carbon Capture and Storage (CCS) is a technique where the $CO_2$ in the flue gas stream from a power plant is separated from other flue gases and transported to a final storage site as illustrated in Figure 3.1. [6]

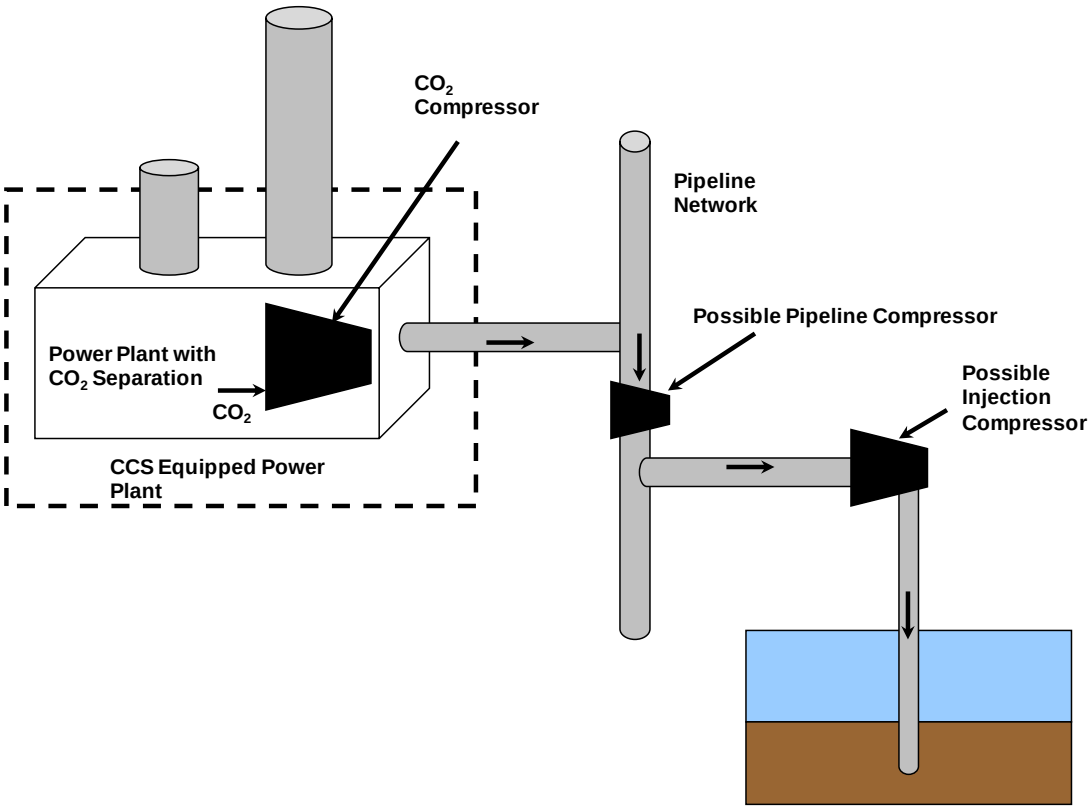


**Figure 3.1: CCS process chart**

## 3.1 Capture

To capture and compress 90 % of $CO_2$ emitted by the power plant 10 - 40 % additional energy is required. The exact energy increase will depend on the fuel and separation method used. As a result, the total amount of $CO_2$ produced will increase. [6]

### 3.1.1 $CO_2$ Capture Technologies

The amount of $CO_2$ in the flue gas emitted from a power plant varies from 3 -15 % of the total gas flow depending on the type of fuel and the capture technology used. Other flue gas constituents include nitrogen, oxygen and water vapour.

There are three different methods of $CO_2$ separation, see Figure 3.2. The first is post-combustion. As its name indicates, the technique strips the $CO_2$ from the flue gas after the combustion. As all of the flue gases are treated, the volume flow is large.

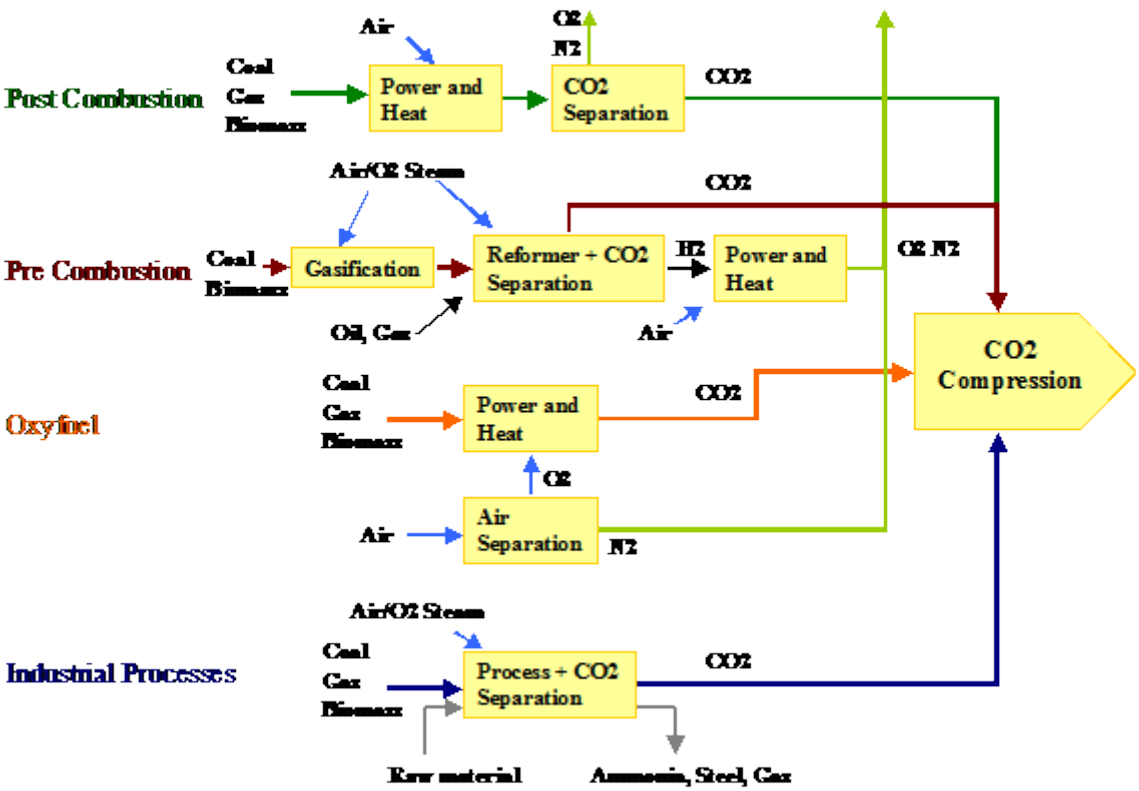


**Figure 3.2: Simplified flowcharts of the capturing processes, adapted from BP**

The second is pre-combustion capture that removes the carbon content in the fuel prior to combustion through gasification producing syngas. The syngas consists mainly of CO and hydrogen. The CO is transformed into $CO_2$ through a shift reaction. The $CO_2$ is then separated and compressed whilst the hydrogen is combusted in a gas turbine.

The third method is oxyfuel combustion capture. When the fuel is combusted in pure oxygen the flue gases consist mainly of $CO_2$ and water. The $CO_2$ is separated from the water by condensation and then compressed. [7]

#### 3.1.1.1 Post-combustion Capture

The most common way to separate the $CO_2$ from the flue gases is by chemical absorption. Post-combustion is a well-known method that has been in use for more than eighty years, separating $CO_2$ from industrial process streams.

The flue gas from a conventional power plant, produced by burning for example coal or natural gas, is cooled down and the excessive moisture is removed in a gas condenser. The flue gases are then treated to remove reactive impurities (e.g. sulphur and nitrogen oxides) before brought into contact with a solvent, usually monoethanolamine (MEA). The solvent chemically absorbs the $CO_2$. To remove residues of solvent, the remaining flue gas is water washed and then released. The method is called amine scrubbing.

The solvent, now containing $CO_2$, is pumped through a lean/rich heat exchanger and into the top of a stripper. More heat is added to produce steam, which acts as stripper

gas and the $CO_2$ contained in the absorbent is released. Before the lean absorbent is ready to be reused, it is fed through the lean/rich heat exchanger, see Figure 3.3.

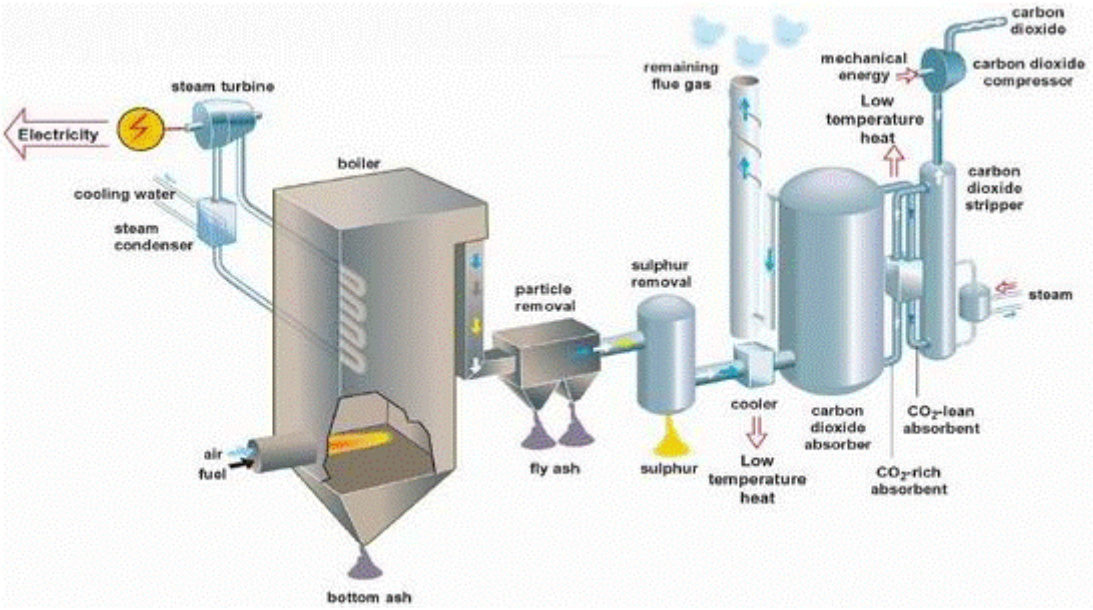


**Figure 3.3: Process flow chart for post-combustion removal of CO2**

The pressure of the $CO_2$ at the exit is close to ambient for an amine process. The separated $CO_2$ is then compressed and cooled down to a supercritical fluid for transport in pipelines to a final storage site. [8]

**Advantages and Disadvantages**

It is possible to remove a high percentage of the $CO_2$ using this method however, there is usually still about 10 % left in the flue gases leaving the absorber. It is not financially viable to remove more: the separation process is an economic trade-off. A higher recovery will increase the size of the absorption column and therefore the cost of the process. It will also increase the energy penalties associated with $CO_2$ capture.

The major drawback with post-combustion removal of $CO_2$ is the net electric efficiency decrease due to the amount of energy needed in the process. The regeneration of the amines using leading technology will need between 2.7 and 3.3 MJ/kg $CO_2$ for steam production. The compressor will need an additional 0.4 MJ/kg $CO_2$ when compressing $CO_2$ to 110 bar(a). Electrical requirements vary between 0.09 MJ/kg $CO_2$ for coal-fired power plants to about 0.27 MJ/kg $CO_2$ for natural gas fired. [6]

In total post-combustion capture can reduce the net efficiency of the power plant by 6-12%. The efficiency losses make it uneconomical to retrofit post-combustion capture to power plants that already suffers from low thermal efficiency. [9]

Another drawback is the large footprint of the separation and capture unit increasing the total area of the plant substantially.

**Technology Readiness Level**

Post-combustion capture is carried out on several pilot scale power plants (0.25 - 1.7 MW) for coal-firing and have been demonstrated in full scale gas-fired power plants.

The target is to have 20 full scale CCS demonstrations globally by 2015 and commercialised plants by 2020. [6]

#### 3.1.1.2 Pre-combustion Capture

Pre-combustion capture separates the coal from the fuel prior to combustion to produce hydrogen. Combustion of hydrogen produces no $CO_2$ emissions and water vapour is the main by-product.

As shown in Figure 3.4, the separation is performed in multiple steps. First, the hydrocarbon fuel is converted into hydrogen and CO to form a syngas. The fuel reacts with water at elevated pressures in a gasifier. If the fuel is natural gas the reaction is as follows

$$CH_4 + H_2O \Leftrightarrow CO + 3H_2 \qquad \text{Equation 3.1}$$

Reaction 2.1 is endothermic and hence heat is required for it to occur. To increase the efficiency, the gasification can be carried out in pure oxygen. This will require an Air Separation Unit (ASU) that separates the oxygen from the air, leaving an almost pure stream of oxygen entering the gasifier. Remaining particles in the syngas called ‘fly ash’ are removed with a filtering process.

Second, the CO is transformed in a shift reactor into $CO_2$, which is easier to capture and compress, see Equation 3.2. [9]

$$CO + H_2O \Leftrightarrow CO_2 + H_2 \qquad \text{Equation 3.2}$$

To remove sulphur, the syngas then passes through a mixture of limestone and water. The sulphur dioxide reacts with the mixture and forms gypsum that can be used in construction industries.

Third, a solvent absorbs the $CO_2$ in a similar way as in post-combustion. The releasing of the $CO_2$ from the solvent can be carried out either by heating the solvent or by decreasing the pressure in several steps with flash tanks. The number of flash tanks used to lower the pressure can vary and the process results in a number of $CO_2$ streams with different pressures. This makes the downstream compression of the $CO_2$ more difficult.

Once the $CO_2$ has been removed the syngas consists solely of hydrogen that can be combusted in a gas turbine, which drives a steam turbine to produce electricity. Excess heat from the combustion can be used to produce additional steam increasing the total efficiency. [10]

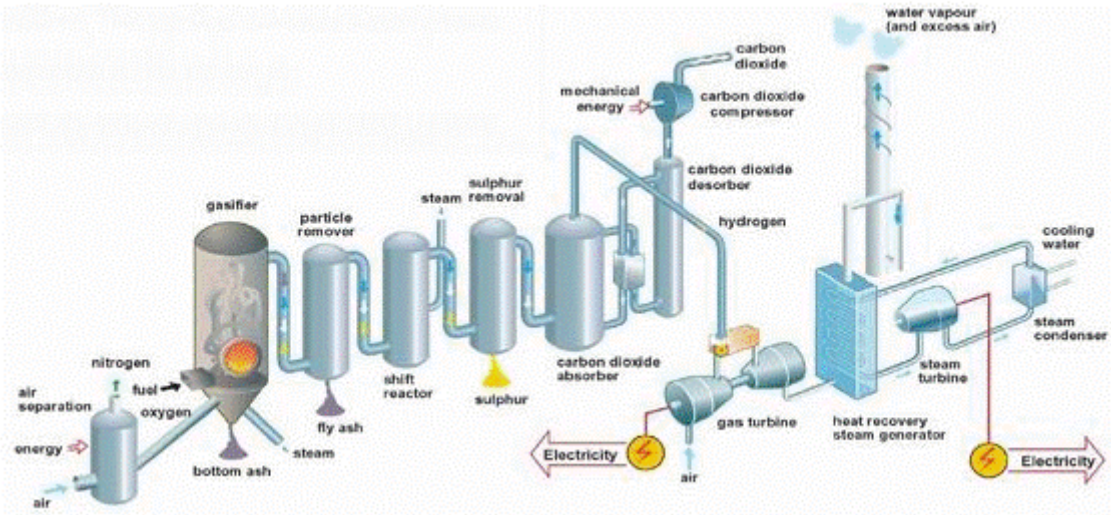


**Figure 3.4: Process chart for pre-combustion**

**Advantages and Disadvantages**

Pre-combustion separation produces a smaller volume of gas, which is richer in $CO_2$ than post-combustion. This will reduce the size of the separation plant and therefore the capital cost. However if an ASU is used this adds to capital costs.

The total efficiency of the overall plant will be reduced by 7 - 9 % with pre-combustion.

**Integrated Gasification Combined Cycle (IGCC)**

An IGCC plant uses gasification to transform pulverized coal into syngas. It then removes the remaining impurities from the syngas. It is called 'integrated' because its syngas is produced in a unit that is integrated in the combustion process. The efficiency of an IGCC typically reaches about 45 % but plant designs offering up to 50 % are achievable. Cost is a big drawback for IGCC plants, as they tend to be significantly more expensive than regular coal-fired power plants. [11]

**Technology Readiness Level**

The technology required for early applications is already available but needs to be demonstrated at large scale. [12]

### 3.1.1.3 Oxyfuel Process

As in pre-combustion the first step is to separate oxygen from air in an ASU. The fuel is then combusted in the pure oxygen, producing heat used for steam production as shown in Figure 3.5. When fuel is combusted in pure oxygen the resulting temperature is high. To avoid over heating in the turbine, flue gases (mainly $CO_2$ and water vapour) are recirculated to cool the process. The flue gases then pass through the same stages as in pre-combustion removing fly ashes and sulphur. After this the flue gases are cooled to condense the remaining water and then compressed and transported for final storage site.

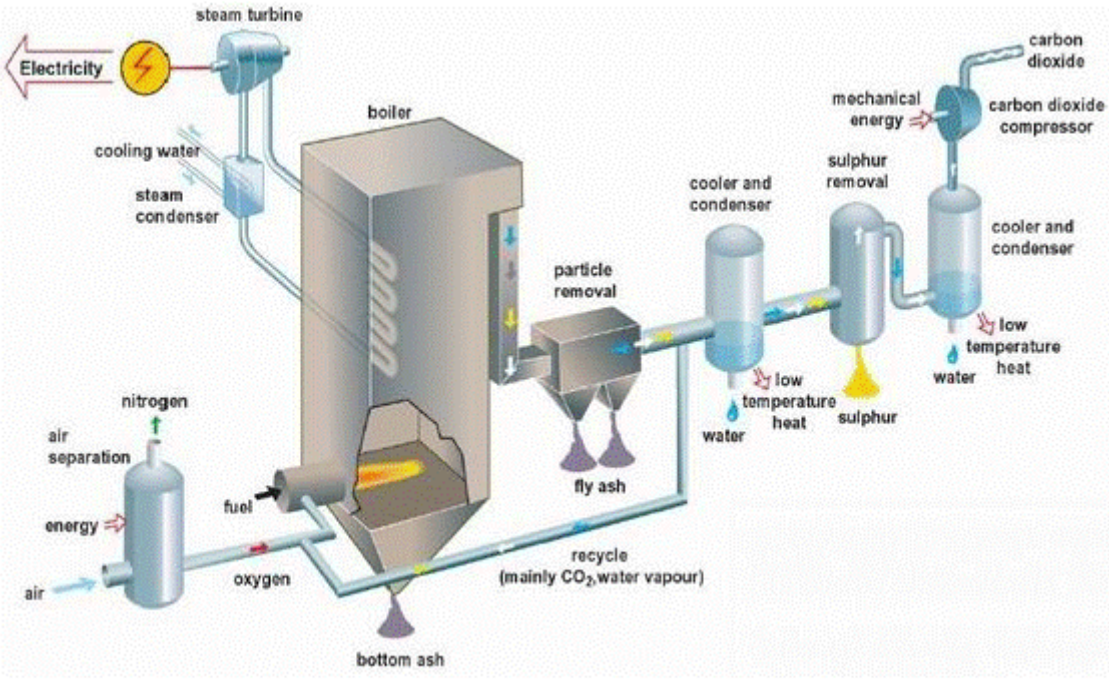


**Figure 3.5: Process chart for oxyfuel**

**Advantages and Disadvantages**

A major advantage is that the combustion occurs in a low nitrogen environment, which greatly reduces the forming of nitrogen oxides although there will be a larger amount of other impurities which increases the compressor work. [12]

The efficiency will be reduced by roughly 10 % for a power plant fitted with oxyfuel combustion. The major drawback of this method is the huge amounts of energy needed for air separation and the fact that an ASU is quite expensive to build. Novel technologies seek to eliminate the need for an ASU. [13]

**Technology Readiness Level**

Oxyfuel combustion has been proven in small scale and there are several ongoing tests. Oxyfuel combustion and capture still needs development and data from pilot and demo plants. The target is full scale demonstrations by 2012/2014 and commercialised plants by 2020. [12]

### 3.1.2 Compression

Prior to transport, the $CO_2$ is compressed to a pressure above 80 bar(a). This increases the density of the $CO_2$, reducing the work (i.e. the power consumption) required to transport it. .

There are different ways to approach this task. Until the mid 1990's the way of compressing $CO_2$ was either by using reciprocating compressors or multi-casing centrifugal barrel compressors. These methods are still used but new technologies have been developed. Today single casing integrally geared compressors are widely used for $CO_2$ compression in urea production plants and therefore one of the possibilities for $CO_2$ compression in CCS plants. Other, novel ways of reaching the required delivery pressure for transportation are also explored by actors on the market. [14]

## 3.2 Transport

Pipelines are anticipated to be the most common method for transporting $CO_2$. The pipelines can either be onshore or offshore depending on application and storage site. Factors that must be considered whilst planning onshore pipeline transportation include the interaction with the existing pipelines, the electrical grid and the infrastructure in general to ensure low impact on human and animal life if failure. [15] Pipelines placed under water must fulfil more difficult design requirements than those on land (high-pressure, corrosion, increased maintenance intervals etc.) [6] Another issue to consider is that the inlet pressure to the offshore pipelines must be higher than the onshore pipelines that are frequently provided with compressor boosting stations. [15]

Long distance pipelines have been used in the USA since 1970 for the transportation of $CO_2$ in the oil industry. The number of pipeline incidents has been relatively small. From 1972 to 2002 the rate of failure decreased from 0.0010 $km^{-1}year^{-1}$ to 0.0002 $km^{-1}year^{-1}$. These numbers are valid for small pipelines only. The study shows that larger pipelines are less likely to fail. [6] A third party, for example ship that collides with the pipeline, represents the greatest risk for pipeline damage. [15] One way to minimize the risks of failure is to build the capture sites close to the storage sites thereby reducing the length of the pipelines and the probability of failure.

Other ways to transport $CO_2$ is by ship, road or rail in large tanks. This method of transport does not require as high pressures as pipeline transport. Using ships for the transport of $CO_2$ is only in the early stages of development. There are four small ships operating worldwide for this purpose. During ship transportation the leakage of $CO_2$ to the atmosphere is estimated to be 3 - 4 % per 1000 km. Collision, foundering, stranding and fire are other risks that might occur. The effect of $CO_2$ leakage to the sea surface from a collision has not yet been investigated. [6]

## 3.3 Storage

After transport the dense $CO_2$ will be stored below the earth's surface in abandoned oil and gas reservoirs, deep saline formations (e.g. aquifers) or unminable coal beds. It is believed that aquifers have the largest capacity for $CO_2$ storage of at least 1 000 $GtCO_2$. Oil and gas reservoirs are estimated to have a storage capacity of 675 - 900 $GtCO_2$. It is still uncertain how big the overall capacity is. [6]

### 3.3.1 Geological Storage

The geological injection of $CO_2$ involves some of the same technology used for the oil and gas exploration and production industry such as well-drilling and injection-technology. The dense $CO_2$ will be kept about 800 m below surface in deep saline formations or hydrocarbon reservoirs. At this depth the $CO_2$ will be in a supercritical state and the density will be 50 - 80 % of the density of water.

Before selecting the geological storage area it must be characterized. Factors to consider include whether there is an overlying cap rock that will provide an effective seal, if there is enough volume and porous storage formation and if there are any abandoned or active wells that will affect the seal.

There are a number of ongoing projects where geological storage of $CO_2$ is demonstrated. Sleipner project in the North Sea, Weyburn project in Canada and In Salah project in Algeria are three of them. The Sleipner project was the first demonstration plant of $CO_2$ storage where 1 $MtCO_2$ annually has been injected since 1996. Statoil has been separating $CO_2$-streams from their natural gas production and storing it in deep saline formations 800 m below the seabed of the North Sea. In Salah is a joint venture between Sontrec, BP and Statoil and is the first large-scale storage site in a gas reservoir where the $CO_2$ is re-injected to sandstone 1 800 m underground. The Weyburn project aims to store $CO_2$, which is a by-product when producing syngas, the plan is to eventually use it for enhanced oil recovery (EOR). The geological storage stretches from the south of Canada to the north of the USA.

$CO_2$ leakage from geological storage can have local and global impacts. The main global impact is that the captured $CO_2$ is released to the atmosphere and will therefore contribute to climate change. Local impacts include effects on humans, ecosystems and/or groundwater. Leakage may occur as a result of injection failure or if abandoned wells create rapid and sudden release of $CO_2$. A leakage of 7 - 10 % of $CO_2$ is dangerous for human health and life. A detective system will need to be used to identify leakage of $CO_2$ before it reaches the surface. Some detection/prevention methods are available but more research needs to be done in the area.

Abandoned oil and gas reservoirs are desirable storage sites for a number of different reasons:

- The oil fields have already been extensively studied and characterised.
- Computer models are available that predict the movement and trapping of hydrocarbons.
- The infrastructure and wells in place could be used for handling $CO_2$ storage operations.
- The oil and gas has been stored for up to millions of years demonstrating the storage reliability and safety.

The abandoned oil and gas reservoirs have to be situated at least 800 m below earth to be technically and economically reasonable. [6]

### 3.3.2 Enhanced Oil Recovery

Using $CO_2$ for Enhanced Oil Recovery (EOR) provides further possible storage sites. In EOR $CO_2$ is injected into operating oil wells to displace the oil and bring it to the surface. The $CO_2$ that is produced with the oil recovery will be recycled into the formation. Things to consider with EOR are the phase behaviour of the $CO_2$ whilst mixing with the oil and how pressure and temperature in the reservoir will affect its behaviour. More than 50 % of the $CO_2$ generated will return with the oil and be re-injected into the reservoir. Using $CO_2$ for EOR will increase the recovery of oil by 7 - 23 %.

One project in $CO_2$-EOR is located in Colorado, USA and has been ongoing since 1986. $CO_2$ produced from natural gas is flooded through the sandstone reservoir for additional oil recovery. [6]

### 3.3.3 Ocean Storage

Another way of storing $CO_2$ is to inject it directly into the ocean at depths greater than 3 km. At this depth the $CO_2$ is denser than water and so most of it will remain at the bottom of the ocean, isolated from the atmosphere for centuries. The $CO_2$ will then slowly become a part of the global carbon cycle. This method is still in the research phase and has only been investigated in laboratories. There is no physical limit to how much $CO_2$ can be stored in the ocean; it will depend on the oceanic equilibrium with the atmosphere.

The greatest environmental concern associated with ocean storage is the change in the ocean's pH value. In short-term studies undertaken, it has been shown that $CO_2$ released in the ocean will affect the marine life however, the long-term environmental effect has still not been investigated and understood. [6] Due to this uncertainty experts on the subject advise against this method.

# 4 Carbon dioxide

## 4.1 Properties

Carbon dioxide, $CO_2$, is a colourless and odourless gas. It is composed of two oxygen atoms covalently bonded to a single carbon atom. It occurs naturally in the atmosphere in gaseous state with an average concentration of 387 ppm by volume or 582 ppm by mass in the Earth's atmosphere. The mass of the Earth's atmosphere is $5.14\times10^{18}$ kg leaving the total amount of $CO_2$ to be $3.0\times10^{15}$ kg. [16] The concentration varies slightly over the year. It increases during the autumn when the plants wither and die and decreases during spring when new plants consume greater amounts of the gas. The plants use $CO_2$ to produce sugar through photosynthesis that in turn is used directly for respiration or to produce compounds required for the growth and development of the plant.

Depending on pressure and temperature, $CO_2$ can be present in three phases, see Figure 4.1. At low temperatures, the gas turns solid forming dry ice through deposition. At atmospheric pressure and –78 °C, the dry ice sublimates into gas. At the critical point, 31.1 °C and 73.8 bar(a), $CO_2$ becomes a supercritical fluid i.e. it behaves as a gas but has liquid-like density.

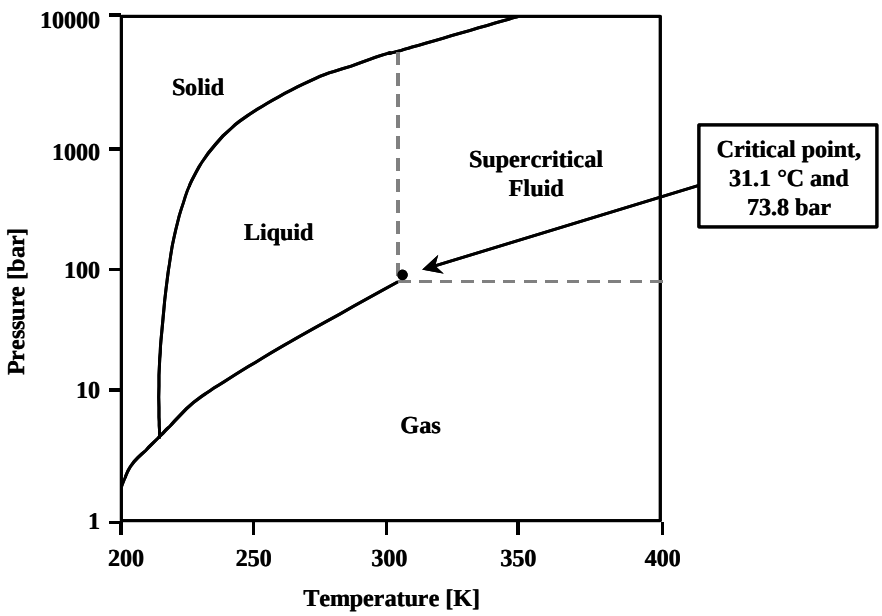


**Figure 4.1: Phase diagram for $CO_2$**

Properties of the gas around the critical point are very sensitive to changes in pressure and temperature making it hard to predict its behavior. Unlike ideal gases, the compressibility factor of $CO_2$ changes with the temperature and pressure of the system. Therefore, real gas behaviour must be considered when undertaking calculations involving $CO_2$. [17]

## 4.2 Impurities

Depending on the separation process and other factors such as fuel type, the $CO_2$ stream will contain different amounts and types of impurities. The impurities in the stream affect the thermodynamic properties and therefore the system design, operation and optimisation. The phase behaviour will also change as the impurities extend the two-phase region to higher pressures. Hence, the required operating pressures to keep the $CO_2$ out of the critical region will increase.

The primary separation process to be considered in the project is post-combustion capture. Typical impurities in a $CO_2$ stream from a coal-fired power plant fitted with post-combustion are $CO_2$, $H_2O$, $N_2$, Ar, $SO_2$ and $O_2$.

The water content in the stream is of high importance as the solubility of water in $CO_2$ changes depending on the phase. The solubility of water in liquid $CO_2$ is higher than the solubility in gaseous $CO_2$. Water removal (dehydration) is therefore best undertaken when the $CO_2$ is in gaseous phase at the pressure and temperature that corresponds to the minimum water solubility. Free water causes corrosion, which is a major problem in both the compression process and during transportation in pipelines. Other impurities such as $SO_x$, $NO_x$ and $O_2$ will not cause corrosion in absence of free water but might be harmful when water is present. [17]

# 5 General Overview of Compressors and Pumps

## 5.1 Information about Compressors

### 5.1.1 Compressor Work

A compressor is used to increase the pressure in a gas stream. This will also increase the density of the gas and therefore when calculations are done, the thermodynamic laws must be considered. Starting from the Ideal Gas Law (see Equation 5.1) and the first and second law of thermodynamics, the theoretical work of the compressor can be calculated.

$$pv = RT \qquad \text{Equation 5.1}$$

However $CO_2$ does not behave as an ideal gas at high pressures; therefore the ideal gas law must be corrected for deviations in terms of compressibility. $Z$ is introduced as the compressibility factor and defined as:

$$Z = \frac{pv}{RT} \qquad \text{Equation 5.2}$$

If a gas stream with the velocity $C$ and the enthalpy $h$ is brought to rest adiabatically without work transfer the total enthalpy it possesses is called the stagnation enthalpy, $h_0$. It is defined as:

$$h_0 = h + \frac{C^2}{2} \qquad \text{Equation 5.3}$$

For perfect gases, the enthalpy $h$ can be substituted with $c_pT$, transforming the equation to:

$$T_0 = T + \frac{C^2}{2c_p} \qquad \text{Equation 5.4}$$

The static temperature $T_0$ will not change or vary through the compression if there is no heat or work transfer. The energy equation can then be expressed as:

$$W = -c_p(T_{02} - T_{01}) \qquad \text{Equation 5.5}$$

The stagnation pressure $p_0$ can be expressed in a similar way provided the gas is brought to rest not only adiabatically but also reversibly:

$$\frac{p_0}{p} = \left(\frac{T_o}{T}\right)^{\frac{\gamma}{\gamma-1}} \qquad \text{Equation 5.6}$$

where $\gamma$ equals $c_p/c_v$.

For a non-perfect gas, $\gamma$ is not a constant value and must be calculated separately at both the start point and end point of the compression process. $C_p$ is rarely available at

high pressures and to accurately calculate thermodynamic properties required such as enthalpy and entropy, departure functions must be used. A departure function is defined as the difference between the thermodynamic properties calculated for an ideal gas and those calculated for the real state. Departure functions are calculated by integrating a function based on an equation of state and its derivative. For $CO_2$, the Peng-Robinson equation of state which relates pressure, temperature and molar volume is often used. [18]

Ideally, the compression process would be an isothermal process but this is not possible in real life as it would demand an infinite number of intercoolers. Isothermal compression represents the upper limits of cooling and power savings. The isentropic efficiency of the compressor is defined as the ratio of actual and ideal work transfer.

$$\eta_i = \frac{W_{ideal}}{W_{actual}} \qquad \text{Equation 5.7}$$

Assuming a value for the isentropic efficiency $\eta_i$ the work usefully employed in raising the pressure of the gas can be calculated. The compressor temperature rise follows as [19]

$$T_{02} - T_{01} = \frac{T_{01}}{\eta_i}\left(\left(\frac{p_{01}}{p_{02}}\right)^{\frac{\gamma-1}{\gamma}} - 1\right) \qquad \text{Equation 5.8}$$

### 5.1.2 Compressor Types

To handle the broad variety of compression requirements, several different types of compressors are available on the market. The most common way is to divide the compressors into two groups: *positive displacement* and *dynamic compressors* as shown in Figure 5.1. [20]

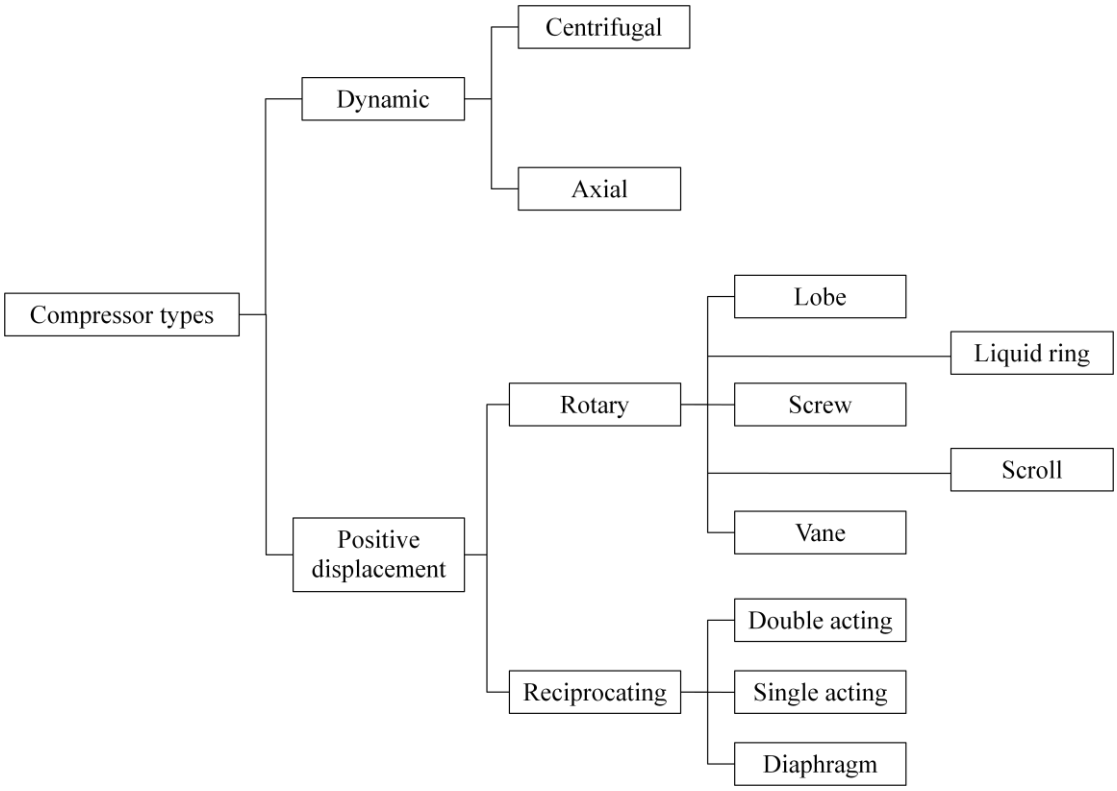


**Figure 5.1: Compressor types**

Selection of the appropriate compressor will mostly depend on the flow rate and compression ratio a compressor can provide however, other characteristics such as size, cleanliness, part load performance, maintenance etc. may also factor into the selection process.

#### 5.1.2.1 Dynamic Compressors

**Centrifugal**

A centrifugal compressor consists of a stationary casing with a rotating disc within, namely the impeller. The pressure rise is achieved by adding kinetic energy to a continuous flow going through the impeller. By slowing the flow down in a diffuser, the kinetic energy is transformed into an increase in static pressure. Pressure ratios of over 9:1 can be achieved by a single stage. [19] The flow range is approximately 0.2 $m^3/s$ to 90 $m^3/s$ [21].

Compared to axial compressors, centrifugals are less sensitive to Foreign Object Damage (FOD) and able to operate over a wider range of mass flows for a fixed rotational speed. Centrifugal compressors are less complicated than axial compressors and have fewer rubbing parts (e.g. interstage and tip seals). The flow rate for a given frontal area is however, smaller than for an axial compressor. For small gas turbines, turboprops and auxiliary power units, centrifugal compressors are the preferred compressor technology.

Centrifugal compressors cannot deliver as high pressure as reciprocating compressors without multiple stages but they handle higher airflow than a similarly sized reciprocating compressor.

Centrifugal compressors are used in natural gas pipelines and in air separation units. They can also be found in large-scale refrigeration plants. [20]

**Axial**

In an axial compressor, the airflow is parallel to the axis of rotation. It consists of several stages, each comprising a rotor followed by a stator. The rotor accelerates the working media, usually air, and adds kinetic energy to it, converting the shaft power input into an increase in total temperature. The stator then transforms the energy to an increase in static pressure by diffusion. [19]

The increase in pressure produced by a single stage is limited by the relative velocity between the rotor and the fluid, and the turning and diffusion capabilities of the aerofoils. The typical pressure ratio for an axial compressor is 1.15 - 1.6 per stage with a polytropic efficiency of 90 - 95 %. Higher pressure ratio is possible at the front stages if the relative velocity between fluid and rotors is supersonic. However this is achieved at the expense of efficiency and operability (stage pressure ratio > 2). As the pressure ratio increases, the required number of aerofoils increases, making the axial compressor more complex and expensive to construct.

The velocity vectors for each stage are shown in Figure 5.2. The length and direction of all vectors can be calculated by basic trigonometry and some assumptions. The peripheral speed, $U$, is assumed to occur in the tangential plane at the mean radius. $C_1$ is the approaching velocity and it has an angle, $\alpha_1$, from the axial direction. This results in a velocity relative to the blade, $V_1$, with an angle, $\beta_1$, from the axial direction. Leaving the rotor, the absolute velocity, $C_2$, of the air has increased. The air leaves the rotor with the velocity $V_2$ at an angle $\beta_2$. The stator reduces the air velocity typically such that $C_3 \sim C_1$ and $\alpha_3 \sim \alpha_1$. Another assumption is that the compressors are designed so that the axial velocity, $C_a$, is kept constant. [22]

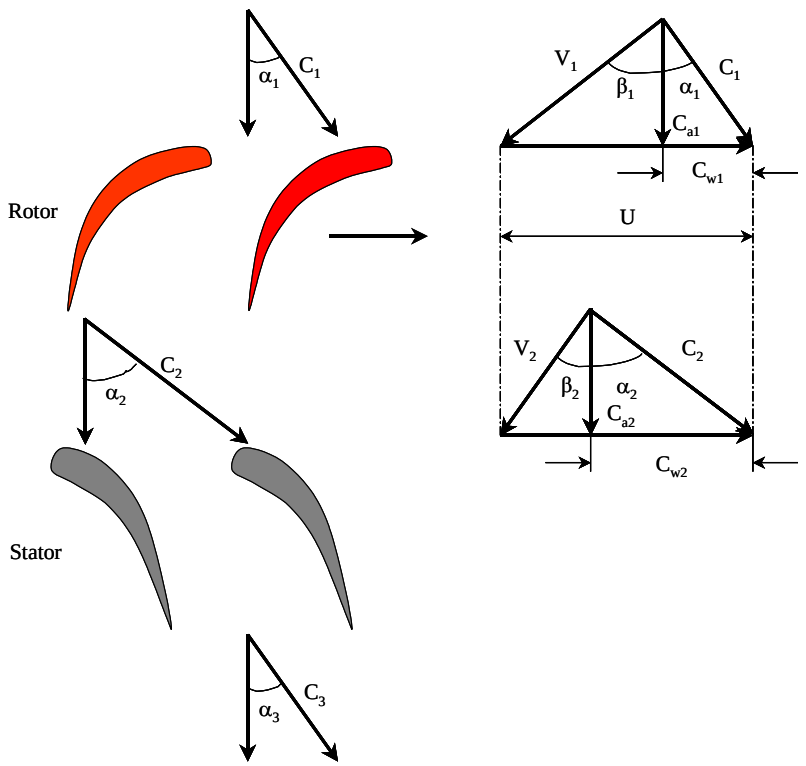


**Figure 5.2: Velocity triangles for axial compressors**

Axial compressors are used for high flow and low-pressure applications. The normal operating range is about 5 400 – 1 400 000 m³/h with pressures up to 55 bar(a) for aero engines at take off conditions. For land based power plants this number is lower, normally around 20 - 25 bar(a). [23]

#### 5.1.2.2 Positive Displacement Compressors

**Reciprocating**

A reciprocating compressor is a compressor that uses pistons driven by a crankshaft to produce compression. The piston traverses through the cylinder, sucking air at one end of its stroke and compressing it at the other end. These machines are capable of providing high pressure, up to 3 000 bar(a), along with variable loading. The flow rate is smaller than for centrifugal compressors, approximately 0.01 $m^3/s$ up to 3 $m^3/s$.

Reciprocating compressors are used in a wide variety of refinery, petrochemical and natural gas services. It is probably the oldest of the compressors in the process industry and is manufactured in a broad range of configurations. They have a good turn-down capability, maintaining efficiency levels at part-load similar to the levels achieved at full load. They are particularly suited for high pressures, high compression ratios and are the compressors of choice for refinery hydrogen services. [25]

### 5.1.3 Suitable Compressors for CCS

A typical $CO_2$ volume flow from a power plant will be approximately 160 000 $m^3/h$. According to Figure 5.3, it is possible to use either a centrifugal or an axial compressor for the first stage. For the later stages, where the volume flow is reduced

and the pressure is higher, centrifugal compressors appear to be the most appropriate choice.

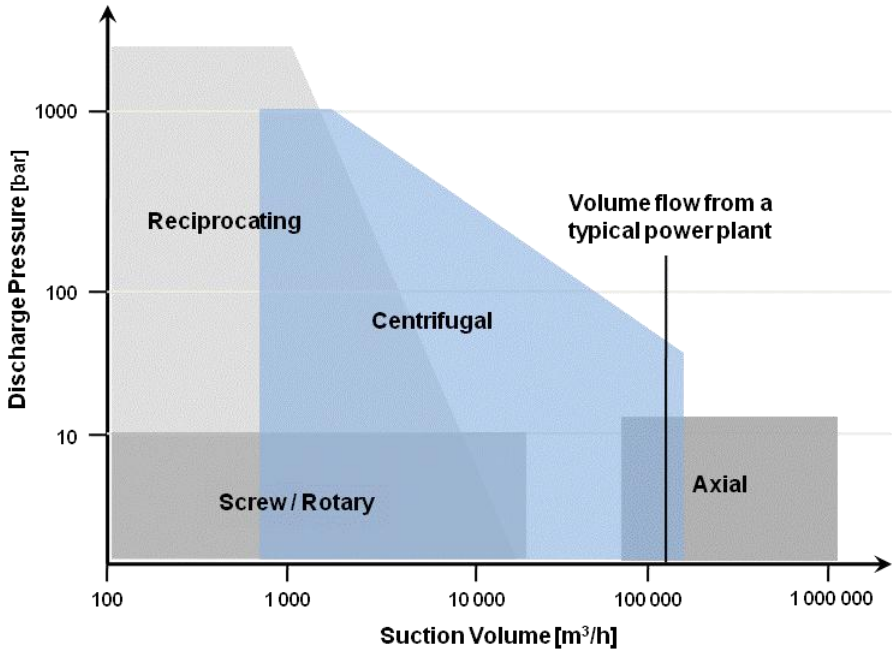


**Figure 5.3: Operating range for different types of compressors**

## 5.1.4 Compressor Suppliers

### 5.1.4.1 Rolls-Royce

**Overview**

Rolls-Royce provides the oil and gas industry with compressors. Their multi-stage[1] barrel compressors are found in a variety of applications such as gas gathering, re-injection and depletion. Rolls-Royce also produces pipeline compressors with high polytropic efficiencies claimed to be in the region of 89 – 91 %.

**Product Details**

Rolls-Royce barrel compressors (see Figure 5.4) are used for a variety of natural gas compressor applications, both on- and offshore. The installations range from single units to multiple-unit trains with a maximum delivery pressure of 450 bar(a) and a flow of 37 400 $m^3$/h. Four different standard frames are available and according to Rolls-Royce their internal aerodynamic design can be adapted to suit different customer requirements.

[1] Note that a stage is defined as a single impeller whereas a section is the set of impellers between coolers. In the case of single impeller section compressors (e.g. MAN Turbo's and Ramgen's) a stage is equivalent to a section.

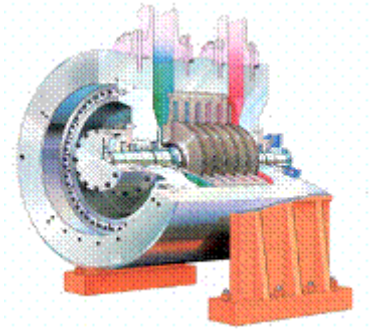

**Figure 5.4: Example of Rolls-Royce barrel compressor**

**Table 5.1: Details of Rolls-Royce compressors**

| | RBB | RCB | RDB |
|---|---|---|---|
| **Max Pressure [bar(g)]** | 310 (476) | 221 | 140 |
| **Number of stages** | 1 – 9 | 1 – 9 | 1 – 9 |
| **Design speed range [rpm]** | 8 000 – 13 800 | 5 000 – 11 500 | 4 500 – 7 500 |
| **Max flow [$m^3$/h]** | 10 200 | 23 000 | 37 400 |
| **Weight [kg]** | 11 300 | 20 400 | 34 000 |

Rolls-Royce pipeline compressors (see Figure 5.5) can handle large volume flows and are the preferred option for natural gas transmission. They are available in seven standard frames with custom designed interiors. The RFA 36 with an axial inlet has a polytropic efficiency of 91 % and is claimed to be the most efficient pipeline compressor in service.

The attributes of Rolls-Royce pipeline compressors are summarised below:

- Discharge pressure up to 220 bar(a).
- Head 15 - 180 kJ/kg.
- Flow 10 000 – 100 000 $m^3$/hr. [5]

### 5.1.4.2 MAN Turbo

**Overview**

MAN Turbo produces integrally geared compressors for urea production, air separation and other applications. The company claims that their integrally geared compressors (see Figure 5.6 below) consume 20 % less power compared to a conventional single shaft machine, which has been used hitherto for this application. MAN Turbo also supplied integrally geared compressors for the world's biggest coal based CCS project at the Great Plains plant in North Dakota. The plant delivers over 100 kg/s of compressed, pure $CO_2$ which is transported by pipeline to Canada and used in the project at Weyburn oilfield.

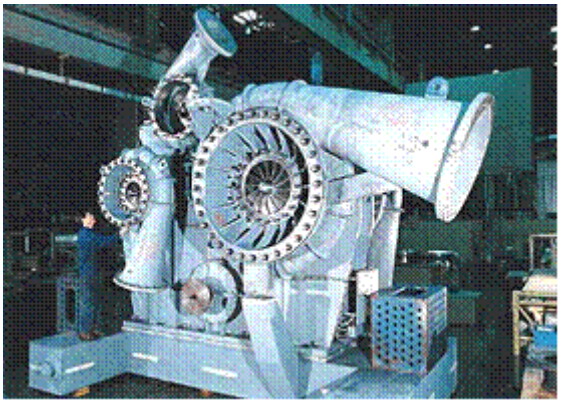

**Figure 5.5: Example of MAN Turbo's integrally geared compressors**

Another MAN Turbo product is its isothermal compressor. An isothermal compressor is a single-shaft centrifugal compressor with integrated cooling. These are suitable for air separation processes.

**Product Details**

The MAN Turbo integrally geared compressors consist of two to ten radial flow impellers that are mounted on a gear unit. There are a number of different compressor versions with 8 and 10-stages that are either already compressing $CO_2$ or can be adapted to handle it (i.e. the RG 080-08 and the RG 053-10 are currently compressing $CO_2$, the RG 140 is assumed to be operating with air but can be adapted for $CO_2$ compression).

**8-Stage, the Dakota Pipeline RG 080-08**

The RG 080-08 has eight overhung mounted impellers, four compressor pinion speeds and five intercoolers. In the picture above, compressor sections are single centrifugal stages mounted with one on each end of the shafts. MAN Turbo claims that compared to a conventional single-shaft machine, the power requirement is reduced by 20 % and according to MAN Turbo this could only be possible for single shaft machines with little intercooling or intermediate gearing.

***Pressure**:* Inlet: 1.15 bar Outlet: 187 bar(a)
***Flow rate**:* 68 760 $m^3$/hr

**10-Stage, the Novazot Urea Plant RG 053-10**

The RG 053-10 has five pinion speeds, the possibility to intercool after each stage and inlet guide vane control.

***Pressure**:* Inlet: 1 bar Outlet: 200 bar(a)
***Flow rate**:* 23 500 $m^3$/hr

**Table 5.2: Integrally geared compressors from MAN Turbo**

| | RG50 | RG80 | RG100 | RG125 | RG140 |
|---|---|---|---|---|---|
| **Volume flow [$Nm^3/h$]** | 20 000 | 65 000 | 100 000 | 130 000 | 160 000 |
| **Mass flow [kg/s]** | ~ 12 | ~ 34 | ~ 52 | ~ 68 | ~ 84 |
| **Power [MW]** | 5 | 14 | 20 | 28 | 33 |
| **PD [bar]** | 160 | 200 | 200 | 200 | 200 |

Their isothermal compressors (type RIK), single-shaft centrifugal compressors with integrated cooling can deliver a pressure < 18 bar(a) and flow rates of 66 000 – 700 000 $m^3/h$. [26] [14]

**Information and Contact Details**
Information on the MAN Turbo products was obtained from the proceedings from the IMechE *Carbon Capture and Storage Conference* held on the 12th of November 2008 and the MAN Turbo website, www.manturbo.com.

### 5.1.4.3 Ramgen Power Systems

**Overview**
The Rampressor represents the application of ramjet principles to the compression of $CO_2$. Ramgen Power Systems claim that the Rampressor's shock compression technology represents a significant advance in the state of the art for many compressor applications, specifically for the compression of $CO_2$. The company also claims that the Rampressor can achieve exceptionally high compression efficiency at high single-stage compression ratios.

**Product Details**
***Flow rate:*** 38 800 $m^3/h$ (18.9 kg/s – divide by density $CO_2$ of 1.754 $kg/m^3$)
***Pressure ratio:*** 10:1 [27]

### 5.1.4.4 Siemens

**Overview**
Siemens is prioritizing IGCC based pre-combustion capture. They offer compressors for air, nitrogen and $CO_2$ which are all necessary for an IGCC power plant. The company states that integrally geared compressors are more suitable for compressing large volume flows of $CO_2$ than single shaft compressors.

**Product Details**
The STC-GV is an integrally geared compressor with vertically split volute casing that is used for air separation. Siemens claims that it has high efficiency and outstanding operating range. It has intercooling between each stage and can be designed to suit all gases. The STC-GV product range is currently available in configurations with up to eight stages.

Details of the STC-GV are provided below:

***Pressure:*** Discharge up to 100 bar(a)
***Flow rate:*** up to 480 000 $m^3/h$

The STC-GC is the standard version of the customized STC-GV. It is used for air separation. It is an integrally geared centrifugal compressor in a compact single-lift unit. It is also available in a high-pressure version, STC-GC (H).

Details of the STC-GC's are provided below:

***Flow rate, STC-GC:*** 10 000 – 120 000 $m^3$/h
***Pressure, STC-GC:*** inlet 1.1 bar(a), pressure ratio up to 20
***Flow rate, STC-GC (H):*** 3 600 – 11 000 $m^3$/h
***Pressure, STC-GC (H):*** inlet < 8 bar(a), pressure ratio up to 8 [28]

#### 5.1.4.5 Dresser Rand

**Overview**
Dresser Rand offers centrifugal compressors for $CO_2$ compression in the urea production industry. They claim that their compressors have polytropic efficiencies exceeding 85 %. In November 2008 Dresser Rand announced that they had made a sizeable investment (circa $49 million) in Ramgen Power Systems.

**Product Details**
Dresser-Rand offer radially and axially split centrifugal compressors. Details of these products are given below:

*Radially split compressor*
***Flow rate:*** 611 650 $m^3$/h
***Pressure:*** 720 bar(a)

*Axially split compressor*
***Flow rate:*** 611 650 $m^3$/h
***Pressure:*** 55 bar(a) [29]

#### 5.1.4.6 General Electric

**Overview**
GE is currently looking into the compression of $CO_2$. They have on-going research on IGCC plants and experience with the compression of $CO_2$ from urea production. Their first commercial offering is likely to be a cryo-pump system (i.e. compressing the $CO_2$ using an integrally geared compressor with intercooling to 70 bar(a) before sub-cooling to liquid phase and pumping to desired delivery pressure and temperature). They also produce axial and single-shaft centrifugal compressors.

**Product Details**
The integrally geared compressors are designed for high flow and low pressure or high pressure and low flow. They are used for process air and gas services. GE offers up to four high-speed pinions with the possibility to mount two impellers on each one. According to GE the intercooled compression guarantees high efficiency.

Details of GE's integrally geared compressors are provided below:

***Flow rate:*** 900 – 350 000 $m^3$/h
***Pressure:*** < 70 bar(a)

GE offers axial compressors for LNG, air separation and air compression. Details of these are provided below:

***Flow rate:*** 100 000 – 900 000 $m^3$/h
***Pressure:*** Pressure ratio < 10 and discharge pressure < 25 bar(a)

GE has vertically split (barrel type) centrifugal compressors which are used for high and medium pressure applications such as natural gas compression, gas re-injection and urea production. Details of these compressors are provided below:

***High Pressure Applications***
***Flow rate:*** < 15 000 $m^3$/h
***Pressure:*** < 1 000 bar(a)

***Medium Pressure Applications***
***Flow rate:*** < 50 000 $m^3$/h
***Pressure:*** < 200 bar(a)

GE also provides horizontally split (barrel type) compressors for high flow, low pressure operations such as refrigeration compressors and $CO_2$ compressors in urea production. Details of these products are given below:

***Flow rate:*** < 500 000 $m^3$/h
***Pressure:*** < 40 bar(a) [30]

#### 5.1.4.7 Other Companies Contacted

The other companies that were contacted with limited/no response were:

Alstom: Contacted via telephone but no information was offered.

Hitachi: Completed online contact form and received auto response only.

Pratt and Whitney: Responded to online contact form but were reluctant to provide any information.

### 5.1.5 Summary of Compressors

A summary of the compressors investigated in Section 5.1.4 is provided in Table 5.3.

**Table 5.3: Table of existing compressor products**

| | Pressure Inlet [bar] | Pressure Outlet [bar] | Flow Rate [$m^3$/h] | Defining characteristics | Advantages | Dis-Advantages |
|---|---|---|---|---|---|---|
| **RAMGEN** | - | 10:1 | 38 800 | Supersonic shock compression | High pressure ratio, potentially low cost and small footprint | Low volume flow, un-proven technology |
| **GE Integrally geared** | - | < 70 | 900 – 350 000 | Integrally geared | High flow rate | Low discharge pressure |
| **GE Centri. Horizontal split** | - | < 40 | < 500 000 | Centrifugal, horizontal split | High flow rate | Low discharge pressure |

| | | | | | | |
|---|---|---|---|---|---|---|
| **GE Centri. Vertical split (l)** | - | < 200 | < 50 000 | Centrifugal, vertical split (l) | High discharge pressure | Low volume flow |
| **GE Centri. Vertical split (h)** | - | < 1000 | < 15 000 | Centrifugal, vertical split (h) | High discharge pressure | Low volume flow |
| **GE Axial** | - | Ratio 10, < 25 | 10 000 – 900 000 | Axial | High flow rate | Low discharge pressure |
| **Dresser Rand Axially Split** | - | < 55 | 611 650 | Centrifugal, axially split | High flow rate | Low discharge pressure |
| **Dresser Rand Radially Split** | - | < 720 | 611 650 | Centrifugal, radially split | High flow rate and pressure | - |
| **Siemens STC-GC (h)** | < 8 | Ratio 8 | 3 600 – 11 000 | High pressure Integral | High suction pressure | Low volume flow |
| **Siemens STC-GC** | 1.1 | Ratio 20 | 10 000 – 120 000 | Standardized Integrally Geared, Compact Design | Compact design | Low volume flow |
| **Siemens STC-GV** | - | < 100 | 480 000 | Integrally geared, vertically split | High efficiency, wide operating range | Low discharge pressure |
| **MAN Turbo Isothermal** | - | < 18 | 66 000 – 700 000 | Isothermal compression | Isotherm process, high efficiency | Low discharge pressure |
| **MAN Turbo 10-stage** | 1 | < 200 | 23 475 | Integrally geared | Internal cooling | Low volume flow |
| **MAN Turbo 8-stage** | 1.15 | < 187 | 68 760 | Integrally geared | Internal cooling | Low volume flow |
| **R-R RBB** | - | 310 (476) | < 10 200 | Centrifugal, Barrel | High delivery pressure, high efficiency, flexible design | Low volume flow |
| **R-R RCB** | - | 221 | < 23 000 | Centrifugal, Barrel | High delivery pressure, high efficiency, flexible design | Low volume flow |
| **R-R RDB** | - | 140 | < 37 400 | Centrifugal, Barrel | High efficiency, flexible design | Low volume flow |
| **R-R RFA** | - | 220 | 10 000 – 100 000 | Pipeliner | High efficiency, wide operating range, flexible design | - |

These compressor products were assessed against the following criterions:

- Available technical information.
- Ability to satisfy the proposed customer requirements.
- Level of product maturity.

Based on the above described criterions and the aspiration to cover a variety of compression technologies it was determined that the most appropriate products for further evaluation were the MAN Turbo integrally geared compressors, Ramgen's Rampressor and Rolls-Royce's centrifugal barrel compressors.

## 5.2 Information about Pumps

### 5.2.1 System Equation

The pressure rise achieved with by pumping is generally measured in metres of head. The difference between the discharge head and the suction head is called differential head. [31] To calculate the differential head, the energy conservation equation from Bernoulli's equation at two points is used [32].

$$p_1 + \frac{\rho v_1^2}{2} + \rho g h_1 + \Delta p_{pump} = p_2 + \frac{\rho v_2^2}{2} + \rho g h_2 + \rho g \left(h_t + h_f\right) \qquad \text{Equation 5.9}$$

Where $\Delta p_{pump}$ is the pressure rise achieved by the pump

$$\Delta p_{pump} = p_2 - p_1 + \frac{\rho\left(v_2^2 - v_1^2\right)}{2} + \rho g\left(h_2 - h_1\right) + \rho g\left(h_t + h_f\right) \qquad \text{Equation 5.10}$$

By dividing the pressure rise with density and constant of gravitation the head of the pump, $H_{pump}$ can be expressed in meters. [33]

$$H_{pump} = \frac{p_2 - p_1}{\rho g} + \frac{v_2^2 - v_1^2}{2g} + h_2 - h_1 + h_t + h_f \qquad \text{Equation 5.11}$$

### 5.2.2 Cavitation

One potential issue associated with pumps is cavitation. When liquids are sucked into the inlet of the pump the pressure acting at the surface of the fluid can decrease and the liquid will start boiling, as seen in Figure 5.7. Bubbles will then build up and travel further into the impeller. The pressure rise in the impeller will make the bubbles collapse or implode which will damage the pump, the phenomenon is called cavitation. Avoiding cavitations of high relevance when pumping all types of liquids as it significantly reduce the expected lifetime of a pump. [31]

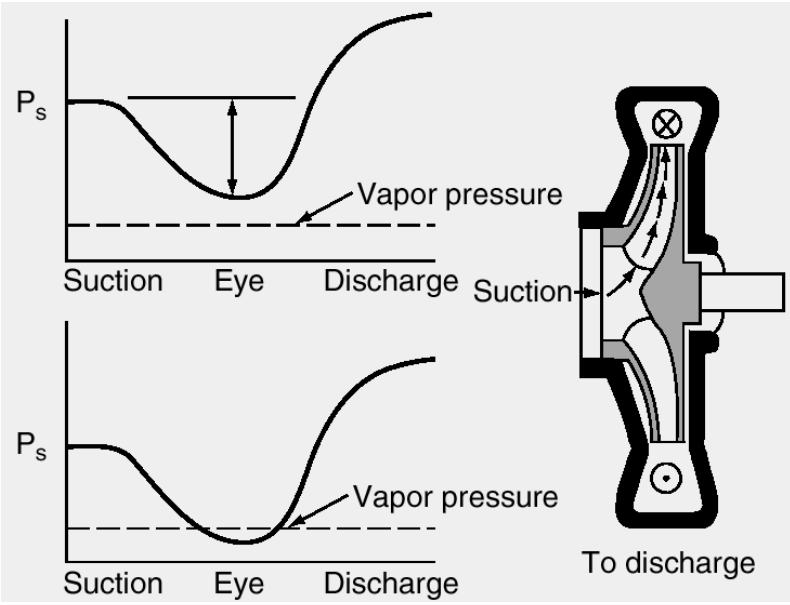


**Figure 5.6: Vapour pressure at the inlet of the impeller eye**

To avoid cavitation the available net positive suction head, NPSHa, has to be 3 % higher than the required net positive suction head, NPSHr [34]. However there is still a risk for cavitation to occur due to losses in the system (i.e. hydraulic losses, viscous losses and mechanical losses) [31]. For a given pump the NPSHa increases with increased flow rate. [32]

### 5.2.3 Pumps Types

Pumps are often classified according to their principle of operation. *Positive displacement pumps* include reciprocating and rotary pumps, *Roto-dynamic pumps* include centrifugal pumps and *other pumps* can be electromagnetic pumps, jet pumps or gas lift pumps, as seen in Figure 5.8. [31]

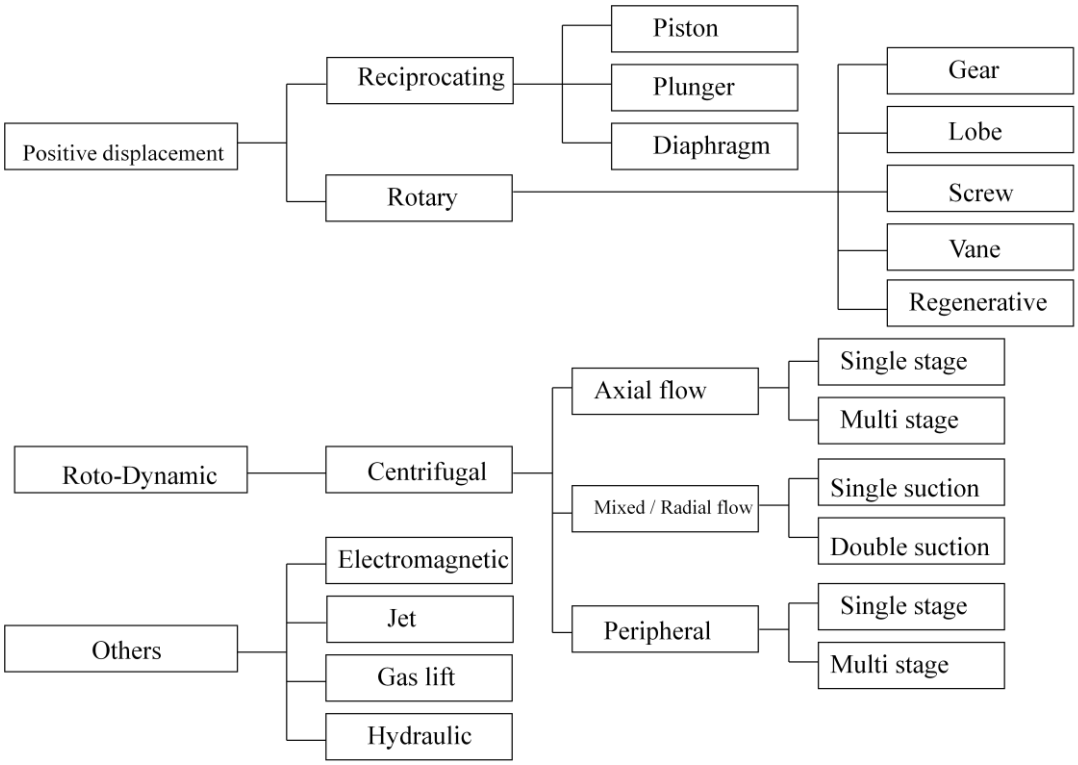


**Figure 5.7: Pump types**

### 5.2.3.1 Roto-Dynamic Pumps

**Centrifugal**

The most common pump type is the centrifugal pump. In a centrifugal pump the pressure of the fluid is raised by centrifugal force acting on the fluid [32]. Fluid enters the pump at the eye of the impeller and is accelerated radially which creates a vacuum and more fluid is drawn into the pump. Vanes will guide the fluid to the outlet of the impeller, as shown in Figure 5.9. The shape and angle of these vanes determines the flow rate the pump can handle. Diffusers are used to build up static pressure and to guide the flow in a different direction.

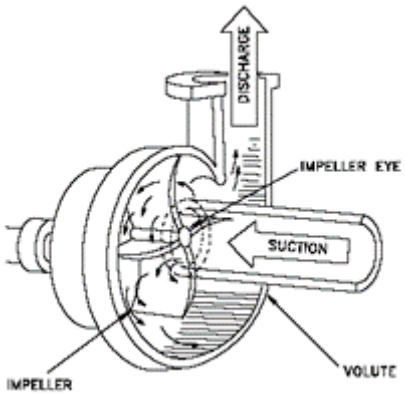


**Figure 5.8: Centrifugal pump**

The advantage with the centrifugal pump is its wide range of operating conditions. Variations can be made in flow rate, speed, suction and discharge heads, and type of fluid. However the pump is normally designed for specific parameters to give the best

efficiency and changes from this design point will affect the performance of the pump. During operation the flow rate and the differential head vary a lot. When the flow rate increases the head decreases i.e., $H = f(Q)$ which is the characteristic of any centrifugal pump. The *H-Q* curve is the most common way to describe the pump characteristics, see Figure 5.10. The shape of the curve depends on the specific speed, the shape and numbers of impeller blades and the pump casing. [31] It is valid for a specific rate of speed, and if the rate of speed changes so will the *H-Q* curve. A new curve can easily be achieved by using the affinity laws described below. [33]

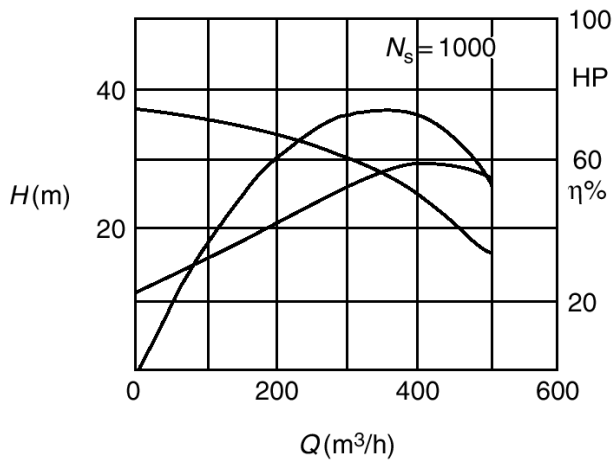


**Figure 5.9: Pump curve, head as a function of volume flow**

The curve can either be stable or unstable but the latter is not desirable. For a single-stage centrifugal pump stability can be achieved by:

- Reducing the numbers of blades/vanes.
- Modifying the vane geometry.
- Reducing the vane outlet angle.
- Modifying the diffuser shape. [31]

**Affinity Laws**

The affinity laws describe the relationship between the rotational speed, impeller diameter, capacity, head, power, and NPSHr and are used for predicting new curves for impeller diameter and speed.

The capacity of a centrifugal pump is directly proportional to the speed of rotation and the impeller diameter.

$$Q_2 = Q_1 \frac{N_2}{N_1} \quad , \quad Q_2 = Q_1 \frac{D_2}{D_1} \qquad \text{Equation 5.12 \& 5.13}$$

The head is proportional to the square of its speed and the impeller diameter.

$$Q_2 = Q_1\left(\frac{N_2}{N_1}\right)^2 , \quad Q_2 = Q_1\left(\frac{D_2}{D_1}\right)^2$$ Equation 5.14 & 5.15

The power consumption is the cube of speed and diameter. [32]

$$Q_2 = Q_1\left(\frac{N_2}{N_1}\right)^3 , \quad Q_2 = Q_1\left(\frac{D_2}{D_1}\right)^3$$ Equations 5.16 & 5.17

These laws are only valid when the efficiency is constant when the rotational speed is changed. If the change in rotational speed is small it is usually a good approximation.

**Volume Flow Regulation**
There are a few different ways to control the flow rate. The most common way to control the flow is by using a regulating valve. Another way is by controlling the rotational speed. This can be done by using a turbine, combustion engine or an electrical motor as the driving unit. A further option is to use a transmission that changes the rotational speed between the pump and the driving unit. Controlling the rotational speed requires larger unit costs than choking the flow but will be useful in applications where it is significant to keep a high efficiency in a wide operating range. [33]

**Classification**
The different types of centrifugal pumps are categorized in different ways:

- Vertical/horizontal, which refers to the plane where the shaft axis is placed.
- Single/dual/multiple stages, which depends on how many sets of impellers and diffusers.
- Vertical/horizontal, which refers to the orientation of the pump suction flange.
- Radial/Axial, which is based on the casing split. Radial – perpendicular to shaft axis, Axial – plane to the shaft axis. [31]

## 5.2.4 Pump Suppliers

### 5.2.4.1 Hitachi Plant Technologies, Ltd

**Overview**
Hitachi offers single or multiple stage pumps for thermal power plants.

**Product Details**
Hitachi offers barrel casing/multistage/turbine pump-sectional type. These pumps are used when high head is required and hence multiple impellers increase the pressure.

Product details for the barrel casing pumps and multistage pumps are as follows:

***Barrel casing pumps***
***Applications*:** Boiler feed pump, reactor feed, high pressure drain pump
***Flow rate:*** 150 – 2 500 $m^3$/h
***Head:*** 300 – 5 000 m

***Multistage turbine pumps***
***Applications*:** Boiler feed pump, control rod drive, descaling pump.
***Flow rate:*** 10 – 250 $m^3$/h
***Head:*** 100 – 2 000 m [35]

### 5.2.4.2 Flowserve

**Overview**
Flowserve produce pumps for a variety of different purposes such as boiler feed water pumping, offshore oil services and liquid natural gas.

**Product Details**
Details of Flowserve pumps are provided below:

**CS Between Bearing, Radially Split, Multistage, Ring Section Pump**
***Brand:*** IDP
***Applications*:** Boiler feedwater, desalination, water supply etc.
***Flow rate:*** 615 $m^3$/h
***Head:*** 1 465 m
***Pressure:*** 125 bar(a)
***Temperature:*** –30 to 165 °C

**WIK API 610 (BB5), Radially Split, Multistage Barrel Pump**
***Brands:*** IDP, Pacific
***Applications*:** Boiler feedwater, $CO_2$ injection, water injection etc.
***Flow rate:*** 400 $m^3$/h
***Pressure:*** 450 bar(a)
***Temperature:*** 450 °C

**DMX API 610 (BB3), Between Bearing, Axially Split, Multistage Pump**
***Brands****:* Byron Jackson, IDP, United Centrifugal
***Applications*:** Boiler feedwater, coolant injection, $CO_2$ injection etc.
***Flow rate:*** 1 500 $m^3$/h
***Pressure:*** 275 bar(a)
***Temperature:*** 200 °C [36]

### 5.2.4.3 Clyde Pumps

**Overview**
Clyde Pumps claims to be a world leader in the design and manufacturing of pumps for the power generation industry. They also have experience in designing pumps for the oil and gas industry, both onshore and offshore. The company claims that the flexibility of their product design allows the pump to fulfil a wide range of duties including standard water, oil and chemical applications and advanced water flood and boiler feed schemes.

**Product Details**
**H-OK**
***Applications:*** Main oil line pumps, water injection, produced water injection etc.
***Flow rate*** < 2 800 $m^3$/hr
***Pressure*** < 4 100 m
***Temperature*** < 180 °C
***Speeds*** < 7 000 rpm

**H-FH**
***Applications*:** Crude oil and product transfer, seawater injection, boiler feed etc.
***Flow rate*** < 1 250m$^3$/h
***Pressure*** < 3 000m
***Temperature*** < 120 °C
***Speeds*** < 6000 rpm

**FT**
***Applications:*** Boiler feed, reverse osmosis, mine dewatering, de-scaling
***Flow rate*** < 1 800 m$^3$/h
***Pressure*** < 3 500 m
***Temperature*** < 180 °C
***Speeds*** < 3 600 rpm

**FK**
***Applications*:** Supercritical and subcritical combined cycle power plants, cogeneration plants, industrial/refinery boiler feed
***Flow rate:*** < 2 500 m$^3$/h
***Pressure:*** < 4 000 m
***Temperature:*** 250 °C [37]

#### 5.2.4.4 General Electric

**Overview**
GE has experience with pumps for the oil and gas industry.

**Product Details**
The BFD and the MDW/MSW are horizontal multistage pumps with axially split cases. They are designed with a back-to-back configuration, minimising axial thrust. They are used for pipeline applications and other heavy-duty services.

Details of these products are provided below:

**BFD**
***Flow*** < 7 500 m$^3$/h
***Pressure (differential head)*** < 950m
**Pressure (maximum working pressure)** <150 bar(a)
***Speed*** < 4 500 rpm
***Temperature*** < 200 °C

**MDW/MSW**
***Flow*** < 3 600 m$^3$/h
***Pressure (differential head)*** < 830 m/stage
**Pressure (maximum working pressure)** <350 bar(a)
***Speed*** < 8 000 rpm
***Temperature*** < 260 °C [38]

#### 5.2.4.5 Summary of Pumps
Table 5.4 summarises the pumps currently available pumps on the market.

**Table 5.4: Pumps currently available pumps on the market that may be appropriate for $CO_2$ pumping.**

| | Min head [m] | Max head [m] | Min volume flow [$m^3$/h] | Max volume flow [$m^3$/h] | Temperature [°C] | Defining characteristics | Advantages / Disadvantages |
|---|---|---|---|---|---|---|---|
| **General Electrics MDW/MSW** | - | 830 / Stage | - | 3 600 | To 260 | Boiler feed pump, multi stage | |
| **General Electrics BFD** | - | 950 | - | 7 500 | To 200 | Boiler feed pump, multi stage | |
| **Clyde pumps (Weir pumps) FK** | 500 | 4 000 | 150 | 2500 | To 250 | Multi stage | |
| **Clyde pumps (Weir pumps) FT** | 650 | 3 500 | 100 | 700 | To 180 | Multi stage | |
| **Clyde pumps (Weir pumps) H-FH** | 100 | 3 000 | 85 | 1 250 | To 120 | Multi stage | Wide range of duties varying from water |
| **Clyde pumps (Weir pumps) H-OK** | 250 | 4 100 | 70 | 2 800 | To 180 | Multi stage | High head |
| **Flowserve** | - | 275 bar(a) | 20 | 1 500 | To 200 | Axially split multi-stage | Handles $CO_2$ |
| **Flowserve** | - | 450 bar(a) | - | 4 000 | To 450 | Radially split multi-stage | Handles $CO_2$ |
| **Flowserve** | - | 615 | - | 1 465 | -30 to 165 | Radially split multi-stage | Low temperature |
| **Hitachi plant technologies** | 100 | 1 000 | 10 | 300 | - | Multi stage turbine pump | High head |
| **Hitachi plant technologies** | 200 | 5 000 | 150 | 2 500 | - | Boiler feed pump, horizontal | High head |

Most of the above listed pumps are not used for pumping $CO_2$ or operating at cryogenic conditions however, they might be adaptable. Flowserve offers a radially split multistage pump for cryogenic applications which probably would be suitable for this purpose. The cryogenic pumping is a novel technology and many of the conditions are uncertain. Hence it is difficult to estimate the required pump capabilities.

### 5.2.5 Refrigeration Plant

A simple refrigeration plant consists of a compressor, a condenser, an evaporator and an expansion valve, see Figure 5.11.

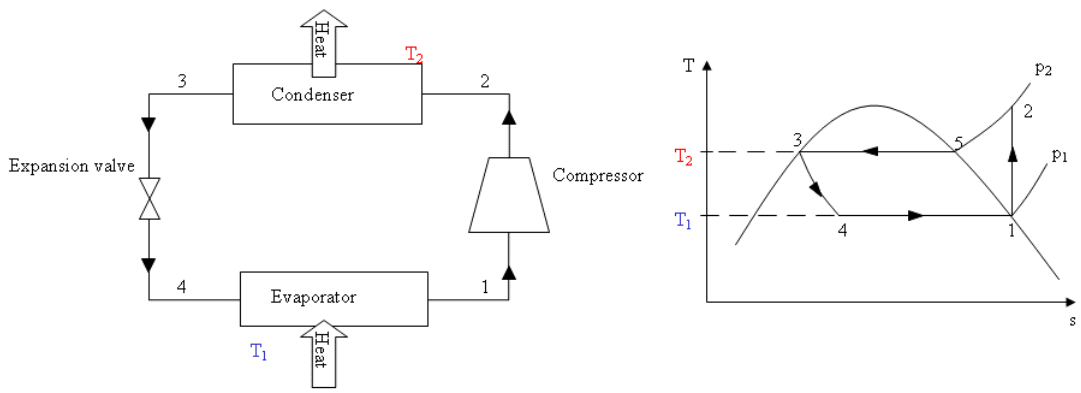


**Figure 5.10: Simple refrigeration plant with T-s diagram**

The compression (1-2) is assumed to be isentropic and the compressor work is calculated as

$$W_{in} = \dot{m}(h_2 - h_1) \qquad \text{Equation 5.18}$$

Since the refrigerant leaving the compressor is superheated (2) the condenser must first reach condensation temperature under constant pressure (2-5) prior to the condensation. The condensation will then take place during constant pressure, $p_1$, and temperature, $T_1$, until the refrigerant has reached the liquid phase (5-3). The heat leaving the condenser can be calculated as

$$\dot{Q}_{out} = \dot{m}(h_2 - h_3) \qquad \text{Equation 5.19}$$

If the velocity of the medium is the same before and after the expansion valve, the expansion is done whilst constant enthalpy $h_3 = h_4$ (3-4).

In the evaporator (4-1) the heat is transferred during constant temperature, $T_2$, and pressure, $p_1$. The heat that is transferred to the refrigerant can be expressed as

$$\dot{Q}_{in} = \dot{m}(h_1 - h_4) \qquad \text{Equation 5.20}$$

The total cooling work done by the refrigeration plant will be calculated as [33]

$$\dot{Q}_{out} = \dot{Q}_{in} + W_{in} \qquad \text{Equation 5.21}$$

The Coefficient of Performance, COP, is a measurement of how efficient the refrigeration cycle is. This value is typically in the range of 3-6 for a common refrigeration plant. [39] The COP is calculated as [40]

$$COP = \frac{\dot{Q}_{in}}{W_{in}} \qquad \text{Equation 5.22}$$

The COP will decrease when the difference between the cold and the hot temperatures increases, which will lead to higher compressor work. This work can be reduced by compression and expansion in two stages, as shown in Figure 5.12. [33]

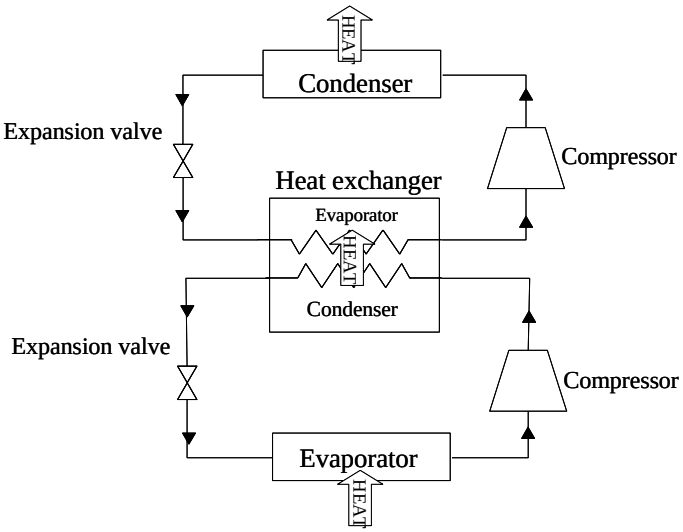


**Figure 5.11: Multi-stage refrigeration plant with heat exchanger**

Multi-stage refrigeration plants are used in industrial applications where high-pressure ratios are needed. In the two-stage refrigeration plant with a heat exchanger the refrigerants in the two stages will not mix. However when separation of the refrigerants is not required the heat exchanger can be replaced with a flash chamber as shown in Figure 5.13. The expansion will still be done in two stages but after the first expansion a liquid/vapour mix is present. The flash chamber leads the vapour back into the high-pressure cycle and the liquid will enter the second expansion valve. [41]

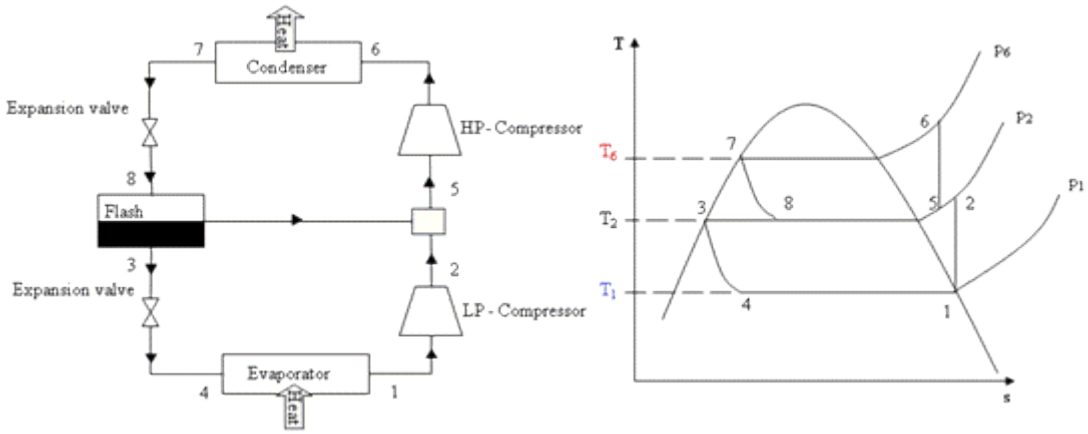


**Figure 5.12: Two-stage refrigeration plant with flash chamber**

### 5.2.5.1 Refrigerants

A refrigerant should have following characteristics:

- *Pressure* – To avoid leakage into the system the pressure of the refrigerant should be maintained above atmospheric pressure.

- *Boiling temperature* - The boiling point of the refrigerant must be lower than the system design temperature.

- *Freezing temperature* – must be well below the minimum temperature the system is operated in.

- *Critical temperature and pressure* – The operating pressure and temperature must be well below the critical point so the refrigerant can undergo phase change.

- *Latent heat* – using a refrigerant with high latent heat is favourable for not only the size of the plant but also the required mass flow of the refrigerant.

- *Safety aspects* – it is desirable to choose a refrigerant that is neither toxic nor flammable. [42]

- *Environmental* – The refrigerant must not affect the ozone layer or pollute the environment. [40]

There are advantages and disadvantages associated with every refrigerant. [40] The environmental impacts are one of the major reasons why a refrigerant is or is not used today.

Ammonia was one of the first refrigerants on the market and is still used in industrial refrigeration plants. [33] It has a low boiling point, is highly energy efficient and has zero impact on the ozone layer. [42] The disadvantages with ammonia however, are that it is highly toxic and explosive when mixing with air. [33]

Hitherto, halogen refrigerants have been used within the cooling industry but are gradually being phased out due to their negative impact of the ozone layer. [43] The main reason for using halogen refrigerants previously was their non-flammable and non-toxic properties. [42]

# 6 Customers requirements

As mentioned in Section 2.1 three different capture techniques are currently being considered for CCS separation – post-combustion, pre-combustion and oxyfuel combustion capture. The Company wants to be prepared for any of the options and provided typical data for the $CO_2$ streams for all alternatives.

The primary focus will be post-combustion, as this technology is required in the near future for retrofitting.

The following parameters were agreed by the partners to base the compressor design investigations on:

- The $CO_2$ mass flow separated from the flue gases from a typical coal fired power plant.
- Pure $CO_2$ for a preliminary evaluation.
- A typical delivery pressure from the separation process.
- A typical delivery temperature from the separation process.
- Fixed intercooling outlet temperatures, to ensure gaseous phase at the inlet of each compressor.
- A desired delivery pressure prior to pipeline transportation.

Power saving is the top priority since every kilowatt that can be saved equates to a large cost saving. Another important aspect to consider is the footprint since the CCS equipment will increase the size of the power plant. Heat recovery for power plant applications or for use in district heating is an opportunity for increased efficiency that will be evaluated later on in The Project.

## 6.1 Modelling Background

Four different methods where considered to attain the desired delivery pressure. The alternatives are as follows:

1. Cryogenic pumping where the gaseous $CO_2$ is compressed in a number of sections[2], cooled through the two-phase region and pumped to desired delivery pressure.
2. Semi-isothermal compression where the compression is undertaken in a series of compressor sections with intercooling.
3. Conventional integrally geared bull gear compressor where the compression is undertaken in a series of compressor stages with intercooling.

[2] Note the difference between a section and a stage. A stage is a single impeller and a section may consist of multiple impellers in one casing.

4. High-ratio compression where the compression is undertaken in stages with high pressure ratios.

The different compression alternatives are shown in Figure 6.1.

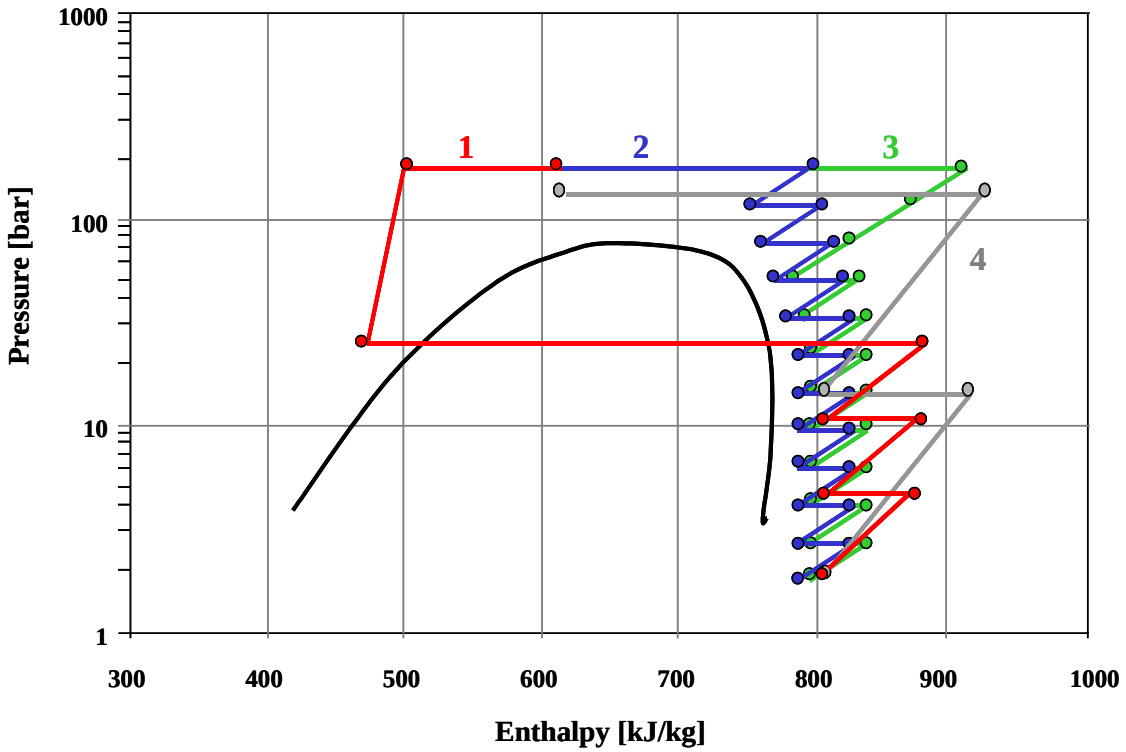


**Figure 6.1: Different alternative to achieve a delivery pressure above 140 bar(a)**

### 6.1.1 Assumptions

For each of the investigations, unless other explicitly stated, the following assumptions have been used:

- An inlet pressure of 1.8 bar(a).
- An inlet temperature of 40 ºC.
- A delivery pressure of 200 bar(a).
- Equal pressure ratios for all $CO_2$ compressors.
- $CO_2$ intercooler exit temperature of 38 ºC.
- Water as the cooling medium in the intercoolers with an inlet temperature of 20 ºC.

The heat exchanger pressure losses are assumed to be 1.5 % and internal piping losses to be 0.3 %. These losses were added as pipe losses after each heat exchanger in the IPSE model.

Other losses that were added to the calculated power in IPSEpro were:

- Motor losses 5 %.
- Mechanical losses 0.5 %.
- Heat leakage 1 %.

### 6.1.2 Compressor Efficiencies

To be able to calculate the power consumption accurate estimates of the compressor section efficiencies were needed. The Project is in an early stage and the compressors evaluated in the thesis might not be adapted for the required customer conditions. Some suppliers have existing $CO_2$ compressors for smaller flows and for purposes other than CCS. Compressor suppliers consider stage efficiencies as highly sensitive information and are therefore reluctant to give any precise figures. Hence it was necessary to estimate values in all models. Typical efficiencies for different types of compressors can be seen in Figure 6.2.

#### 6.1.2.1 Flow Coefficient

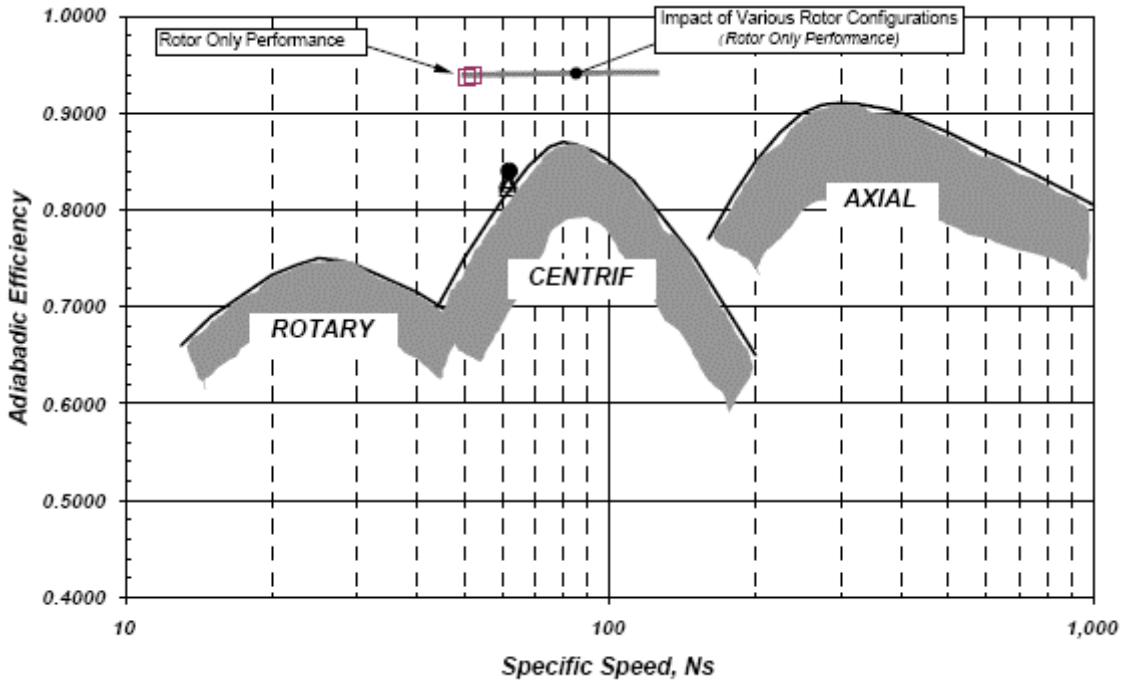


**Figure 6.2: Compressor efficiency versus specific speed**

The dimensionless flow coefficient can be used to estimate the polytropic efficiency for a centrifugal compressor without empirical data. The parameter describes the relationship between the inlet gas flow rate, the impeller diameter and tip speed as shown in Equation 6.1.

$$\delta = 700 \frac{\dot{Q}}{N d_2^{\,3}} \qquad \text{Equation 6.1}$$

Where $\dot{Q}$ is the volumetric flow in $ft^3$/min, $N$ is the rotational speed and $d_2$ is the impeller diameter in inches.

The value of the dimensionless flow coefficient ranges from 0.01 to 0.15 for a 3-D designed impeller blade and should not exceed 0.1 for a 2-D design. After determining the flow coefficient, the polytropic efficiency can be read directly off a flow coefficient versus efficiency chart (Figure 6.3.) [21]

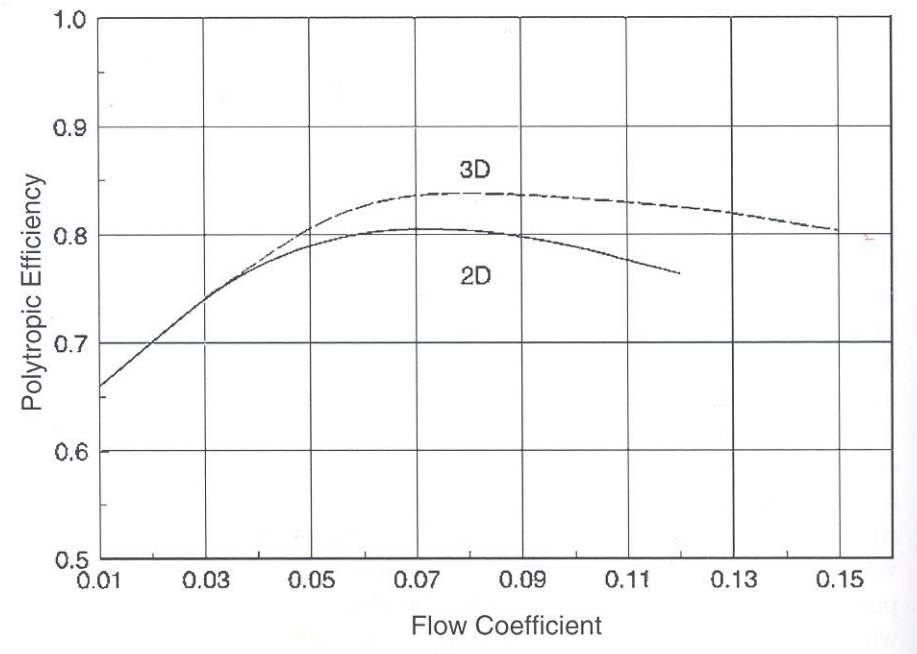


**Figure 6.3: Flow coefficient versus polytropic efficiency**

### 6.1.3 Power Calculation

Early attempts using available tools suggested typical polytropic efficiencies of 80 % to 85 %. Indications from compressor suppliers and experts within Rolls-Royce supported these values and they were therefore selected as a representative range.

The efficiencies only affect the outlet temperatures from the compressor. Therefore the polytropic efficiencies were used directly in IPSEpro to calculate inlet temperatures as well as inlet and outlet pressures for all sections. This was performed on all options modelled in ISPEpro. The polytropic efficiencies were transformed into isentropic efficiencies using TechUtils and applied in IPSEpro. The power consumption was calculated according to Equation 6.2 using isentropic efficiencies.

$$W = \dot{m}\sum_{k-1}^{n}(\Delta h)_n \qquad \text{Equation 6.2}$$

where $W$ is the total power and $n$ is the number of compressors.

### 6.1.4 Impact of Impurities

A basic test was performed in the standard library of IPSEpro to investigate the impact of impurities in the $CO_2$-stream. Due to limitations in the standard library the pressure could not exceed 35 bar(a), hence, only the first four sections in a 7-section compressor solution could be modelled. The conditions and assumptions for this investigation were as follows:

- Inlet pressure 1.8 bar(a).
- Inlet temperature 40 °C.
- Mass flow 84 kg/s.
- Outlet pressure 25.11 bar(a).
- 85 % polytropic efficiency
- The intercooling media was assumed to be water at 1.01 bar(a) and 15 °C.
- The intercooler outlet temperature ($CO_2$-stream) was set at 38 °C.

Pure $CO_2$ was used for the first simulation. A power consumption of 17.0 MW for the system was obtained[3]. The same simulation was carried out with a mixture corresponding to a typical flue gas composition from a power plant fitted with post-combustion capture technology. This resulted in a power consumption of 17.4 MW, which was an increase of 2.4 % compared to the pure $CO_2$ case of 17.0 MW.

According to The Company, Oxyfuel is the capturing process which contains the highest amount of impurities. Hence, an additional investigation of the 'worst case scenario' was undertaken. For this process the impact of the impurities resulted in a vast difference in power consumption. For the polluted $CO_2$ stream the power consumption was 21.4 MW which compared to the pure $CO_2$ of 17.0 resulted in 20.7 % higher power consumption than for the pure $CO_2$ stream.

[3] Note that the corresponding value in the refrigeration library was 16.6 MW for pure $CO_2$. The difference between the libraries is that in the standard library the properties are calculated assuming an ideal gas whereas the refrigeration library uses actual properties from tables.

# 7 Results

## 7.1 Investigation of MAN Turbo

MAN Turbo provides integrally geared centrifugal compressors for $CO_2$ compression. Their integrally geared compressors are constructed with overhung impellers mounted on pinion shafts that are driven by a central bull gear as shown in Figure 7.1.

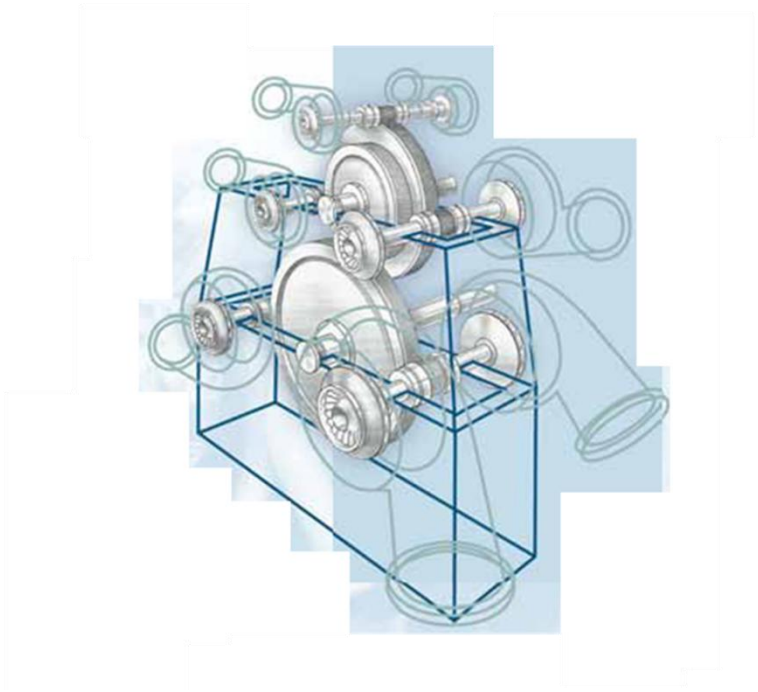

**Figure 7.1: MAN Turbo 10-stage integrally geared compressor**

MAN Turbo claims that this arrangement allows each impeller to run at its optimum speed, which gives an optimum flow coefficient and thereby high stage efficiency. Furthermore, according to MAN Turbo, high efficiencies are accomplished by adjustable inlet guide vanes (IGV's), small leakage losses and small hub/tip ratio.

Information about power consumption is available for a number of compressors, for both $CO_2$ compression and compressors designed for other purposes. To evaluate the reliability of these assertions models of 8- and 10-stage compressors were simulated in IPSEpro.

The pressure-temperature-entropy diagram in Figure 7.2 shows the pressure distribution for the MAN Turbo 10-stage integrally geared compressor, RG 053-10. After each impeller the $CO_2$ is cooled to below 40 °C except for the last two stages where intercooling is excluded presumably to ensure gaseous phase. [14]

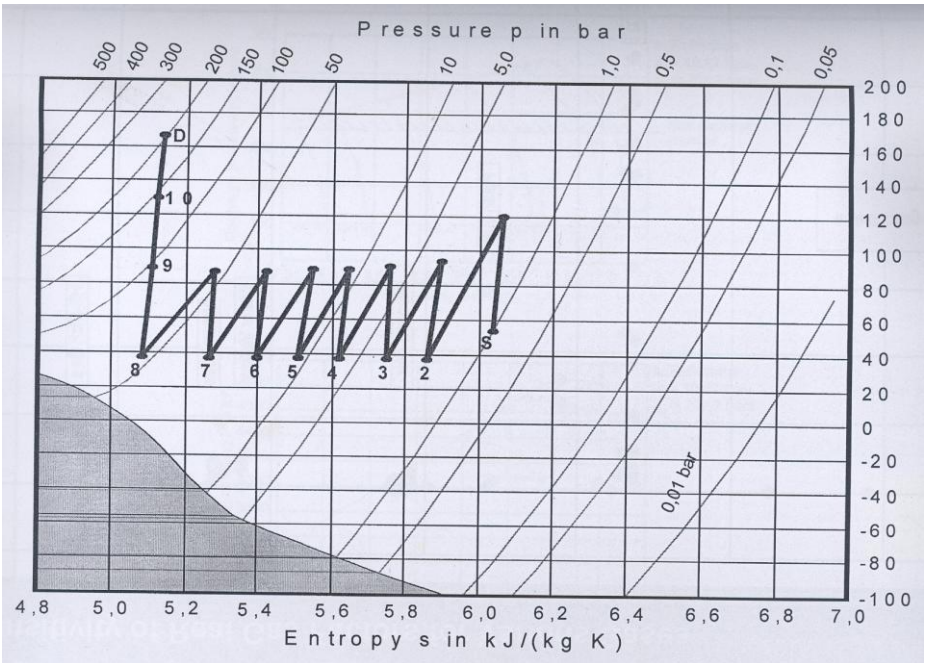


**Figure 7.2: Compression process for the 10-stage integrally geared compressor, RG 053-10**

The process is also illustrated on a pressure-enthalpy diagram, see Figure 7.3.

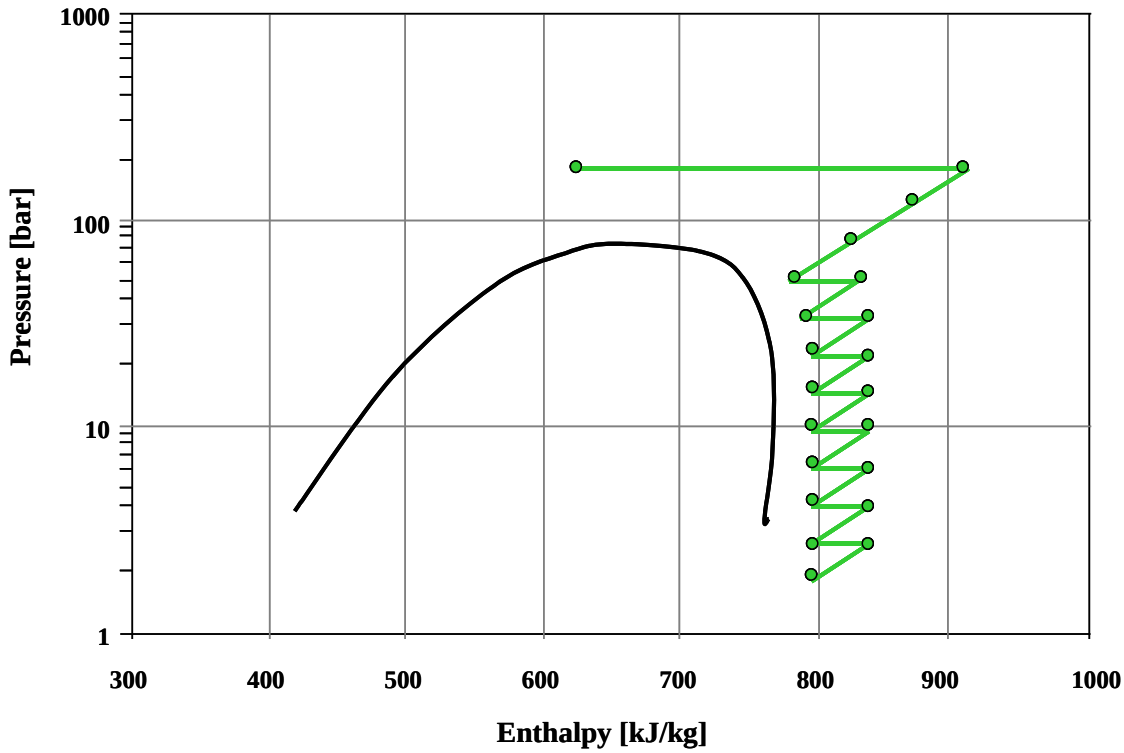


**Figure 7.3: p-h diagram for MAN Turbo 10-stage compression**

### 7.1.1 Determining Pressure Ratios

The pressure leaving each compressor stage was read from Figure 7.2. The difficulty associated with taking accurate readings from the figure indicates that assumptions for adjusting the pressure ratio per stage were required. A feasible design choice is to use

a smooth pressure ratio distribution. This assumption is further justified by the fact that in the figure above the temperature rise per stage is approximately the same. Using an exponential approximation the adjusted outlet pressures were calculated and are presented in Table 7.1.

**Table 7.1: Pressure rise for a 10-stage compressor**

| Stage | Outlet Pressure [bar(a)] | Ratio | Adjusted Outlet Pressure [bar(a)] | Adjusted Ratio |
|---|---|---|---|---|
| **1** | 2 | 2.00 | 2.0 | 2.00 |
| **2** | 3.5 | 1.75 | 3.8 | 1.90 |
| **3** | 7 | 2.00 | 7.0 | 1.84 |
| **4** | 12 | 1.71 | 12 | 1.73 |
| **5** | 20 | 1.67 | 21 | 1.73 |
| **6** | 35 | 1.75 | 35 | 1.67 |
| **7** | 56 | 1.60 | 56 | 1.60 |
| **8** | 90 | 1.61 | 90 | 1.61 |
| **9** | 140 | 1.56 | 140 | 1.56 |
| **10** | 200 | 1.43 | 200 | 1.43 |

The original pressure ratio and the adjusted pressure ratio were then plotted on a graph, see Figure 7.4.

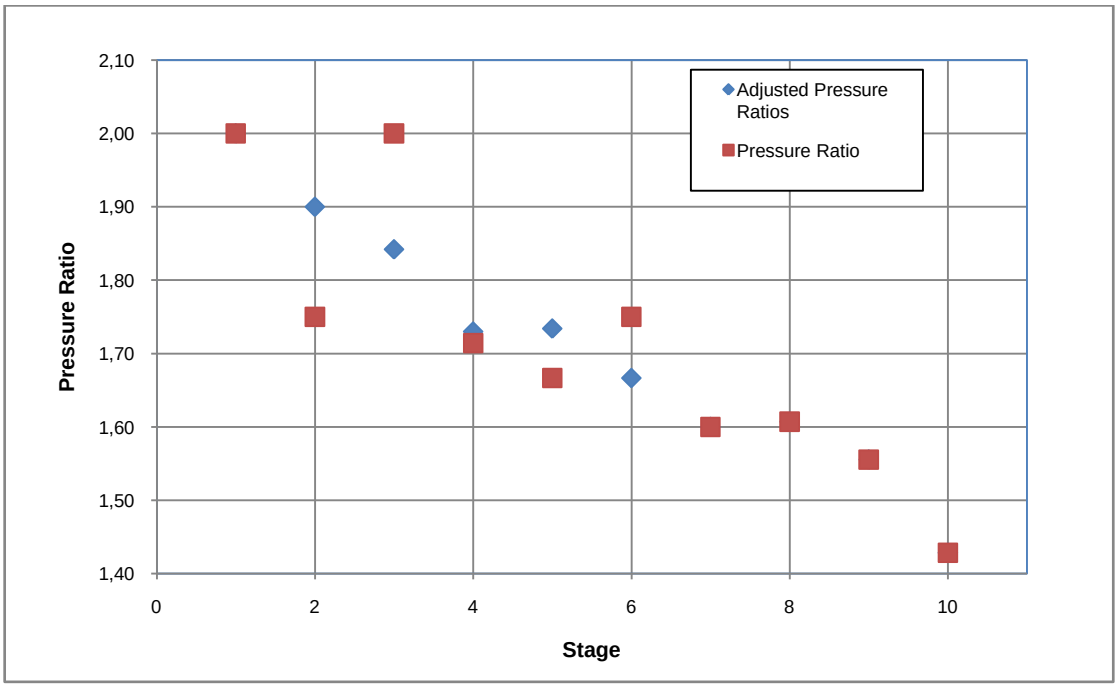


**Figure 7.4: Adjusted Pressure Ratios**

The assumption that this would be a typical pressure distribution for a 10-stage MAN Turbo was considered valid and thus these pressure ratios were used throughout the MAN Turbo calculations.

The MAN Turbo 10-stage integrally geared compressors have intercooling after the first seven compressors and have been modelled in IPSEpro according to Figure 7.5, with exit temperatures of 38 °C.

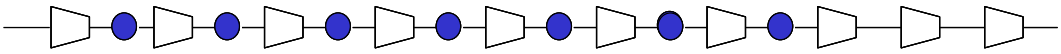

**Figure 7.5: IPSEpro model**

### 7.1.2 MAN Turbo Performance

The following three integrally geared compressors were evaluated in IPSEpro:

- RG 053-10.
- RG 080-08.
- RG 140.

#### 7.1.2.1 RG 053-10

This compressor is used for urea production in Novazot, Russia. The following information was available from Figure 7.2:

- The inlet pressure is 1.04 bar(a) and the delivery pressure is 200 bar(a).
- The inlet temperature is 50 °C.
- The $CO_2$ volume flow rate is 23 500 $m^3$/h which corresponds to a mass flow of 11.16 kg/s at inlet conditions.
- The stated power consumption for the RG 053-10 is 4.5 MW. [14]

#### 7.1.2.2 RG 080-08

Three RG 080-08 compressors feed the Beulah/Weyburn 200 mile pipe-line. The following statements were available:

- The inlet pressure is 1.15 bar(a) and the delivery pressure is 187 bar(a).
- The $CO_2$ volume flow is 68 760 $m^3$/h which corresponds to a mass flow of 34.00 kg/s at the inlet (for a density of 1.78 kg/$m^3$).
- The largest impeller diameter is 740 mm with the rotational speed of 7 400 rpm.
- The smallest impeller diameter is 115 mm with the rotational speed of 26 400 rpm.
- The stated power consumption for the RG 080-08 is 14 MW. [14]

#### 7.1.2.3 RG 140

The RG 140 is assumed to be used in the air separation industry. The following information was available:

- The inlet pressure is ~1 bar(a) and the delivery pressure is 200 bar(a).
- The mass flow is 84 kg/s.
- The stated power consumption is 33 MW. [14]

### 7.1.3 Efficiency Analyses

The power consumption depends on the efficiency of the compressor hence good knowledge about the stage efficiencies is necessary. There is insufficient public domain data to accurately determine the individual stage efficiencies. Therefore three different ways of estimating the efficiencies have been investigated.

#### 7.1.3.1 Efficiencies Claimed by MAN Turbo

A believable polytropic efficiency range per stage is 80 - 85 % according to Figure 6.2 in Section 6.1.2. Calculating the power consumption using the lowest and highest value will result in a range that most likely will cover the actual power consumption. In order to be used in IPSEpro the polytropic efficiencies were transformed to isentropic efficiencies in TechUtils, see Table 7.2.

**Table 7.2: Isentropic efficiencies transformed from 80 and 85 % polytropic efficiencies**

| Stage | $\eta_i$ ($\eta_p$ = 0.80) [%] | $\eta_i$ ($\eta_p$ = 0.85) [%] |
|---|---|---|
| **1** | 78.62 | 83.96 |
| **2** | 78.59 | 83.94 |
| **3** | 78.64 | 83.98 |
| **4** | 78.76 | 84.06 |
| **5** | 78.72 | 84.04 |
| **6** | 78.77 | 84.08 |
| **7** | 78.82 | 84.12 |
| **8** | 78.81 | 84.10 |
| **9** | 78.98 | 84.24 |
| **10** | 79.22 | 84.41 |

Without additional losses such as gearbox losses, motor and mechanical losses the corresponding shaft power result was 4.13 and 4.42 MW. Adding 5.5 % losses the result was 4.36 and 4.67 MW. MAN Turbo's stated power data of 4.5 MW lays within this range. [14]

The same calculations were carried out for an increased mass flow of 84 kg/s. The power excluding losses were then 31.37 and 33.54 MW respectively and with losses 33.10 and 35.38 MW respectively.

#### 7.1.3.2 Efficiency Calculated by Flow Coefficient

To estimate the polytropic efficiencies an attempt was made to calculate the flow coefficient of each impeller and then use the known correlation between flow coefficient and efficiency. The flow coefficient was calculated by using Equation 6.1 in Section 6.1.2.1. From the equation it follows that the volume flow, impeller diameter and rotational speed for each stage are required to retrieve the flow coefficient. Size data was not available for the RG 140 the calculations were preformed on an 8-stage compressor to evaluate efficiencies against claimed power consumption.

The following procedure shown as a flow chart in Figure 7.6 was undertaken

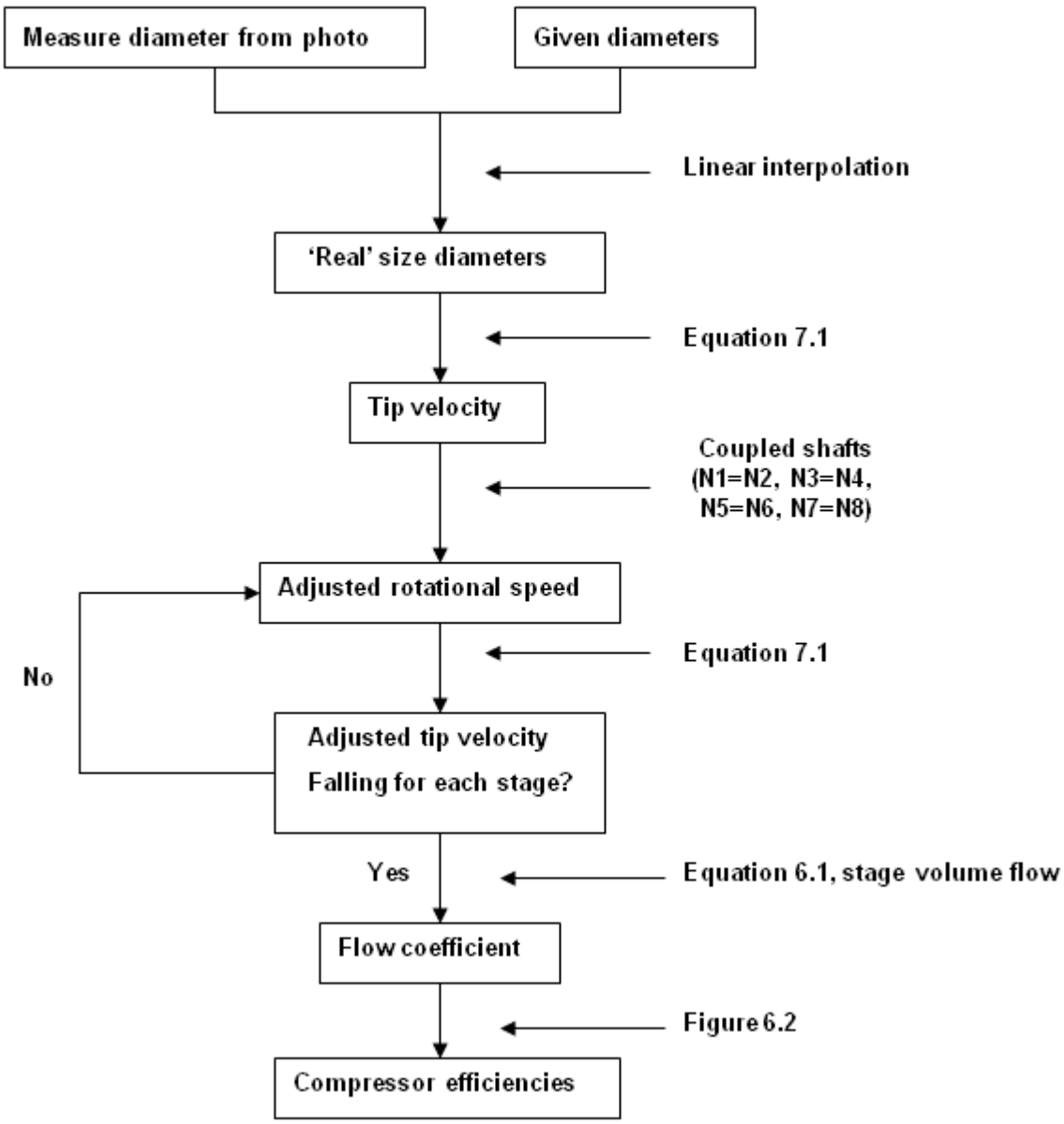


**Figure 7.6: Flow chart of efficiency calculations**

**Calculating Impeller Diameter, *d***

Measurements taken from an available photograph provided approximate sizing data for the 8-stage MAN Turbo RG 080-08 [14]. The measured diameters were converted to 'real' size diameters by using linear interpolation between the measured diameters and the given ones.

**Calculating Volume Flow, *Q***

To obtain the volume flow in each stage the density of the $CO_2$ was required. This was achieved by determining the inlet and outlet pressure to each stage and import them to TechUtils. To get an accurate assumption of how the pressure rise occurs in the eight-stage compressor the relationship between the pressure ratio for the first stage and the last stage was assumed to be equal to the corresponding ratios in the ten-stage compressor. Using the linear interpolation the pressure distribution over the other stages was calculated as a percentage of the last stage pressure ratio.

The delivery pressure was set to 187 bar(a) based on the stated information. By using the goal seek function in Excel the remaining pressure ratios were calculated and are presented in Table 7.3.

**Table 7.3: Possible pressure ratio distribution for an 8-stage compressor**

| Stage | Outlet pressure | Pressure Ratio | Interpolated distribution of pressure ratios |
|---|---|---|---|
| **1** | 2.5506 | 2.218 | 100% |
| **2** | 5.4263 | 2.127 | 96% |
| **3** | 11.0528 | 2.037 | 92% |
| **4** | 21.5129 | 1.946 | 88% |
| **5** | 39.9244 | 1.856 | 84% |
| **6** | 70.4789 | 1.765 | 80% |
| **7** | 118.0367 | 1.675 | 76% |
| **8** | 187.0000 | 1.584 | 71% |

The pressures were applied in TechUtils and the densities were obtained. By dividing the mass flow with the density the volume flow was calculated.

**Calculating Rotational Speed, *N***

The configuration of MAN Turbo compressors is to couple two impellers on the same pinion shaft. The impellers are distributed on shafts as follows:

**Table 7.4: Impeller distribution**

| Shaft | Impellers |
|---|---|
| **1** | 1&2 |
| **2** | 3&4 |
| **3** | 5&6 |
| **4** | 7&8 |

The tip speed, *v*, was calculated for the first and the last stage by using Equation 7.1 and the given rotational speed.

$$v = r\omega = \frac{d}{2} \cdot \frac{\pi}{30} N \qquad \text{Equation 7.1}$$

The tip speed for the remaining impellers was calculated by linear interpolation and estimated rotational speeds.

The tip velocity for the first impeller is higher than the tip velocity for the last impeller, which implies that there is a falling trend for the velocities. It is expected that the tip velocity will be higher for the first stage than the last stage in the coupling according to Equation 7.1 Therefore an iterative process was undertaken until a believable rotational speed with corresponding tip speed was found. The results are shown in Table 7.5.

**Table 7.5: Calculated tip speed and rotational speed**

| Stage | Dimension From Photo [mm] | Diameter [mm] | Speed [RPM] | Tip Speed [m/s] | Adjusted Speed [RPM] | Adjusted Tip Speed [m/s] |
|---|---|---|---|---|---|---|
| **1** | 71 | 740 | 7400 | 286.7 | 7400 | 286.7 |
| **2** | 64 | 666 | 7400 | 258.0 | 7400 | 258.0 |
| **3** | 32 | 327 | 11819 | 202.3 | 12000 | 205.4 |
| **4** | 32 | 327 | 11819 | 202.3 | 12000 | 205.4 |
| **5** | 19 | 189 | 17581 | 174.1 | 20000 | 198.1 |
| **6** | 17 | 168 | 19306 | 169.8 | 20000 | 175.9 |
| **7** | 13 | 126 | 26400 | 173.6 | 26400 | 173.6 |
| **8** | 12 | 115 | 26400 | 159.0 | 26400 | 159.0 |

**Determining Flow Coefficient and Efficiencies**

The values for *Q* and *d* were converted to $ft^3$/min and inches, so the values could be used in Equation 6.1. The efficiencies were then read from the flow coefficient – compressor stage efficiency graph, see Figure 6.3 in section 6.1.2.1. The results are presented in Table 7.6 below.

**Table 7.6: Flow coefficient calculations with corresponding efficiency**

| Stage | Density [kg/m$^2$] | Volume flow rate [m$^2$/s] | Inlet Flow [ft$^2$/min] | Diameter [in] | Flow Coefficient | Efficiency |
|---|---|---|---|---|---|---|
| **1** | 1.71 | 19.900 | 42166 | 29.13 | 0.161 | 0.79 |
| **2** | 3.91 | 8.695 | 18423 | 26.21 | 0.097 | 0.84 |
| **3** | 8.64 | 3.935 | 8338 | 12.87 | 0.228 | - |
| **4** | 18.52 | 1.836 | 3890 | 12.87 | 0.106 | 0.83 |
| **5** | 39.00 | 0.872 | 1847 | 7.447 | 0.157 | 0.8 |
| **6** | 83.47 | 0.407 | 863 | 6.613 | 0.104 | 0.83 |
| **7** | 129.95 | 0.262 | 554 | 4.945 | 0.122 | 0.82 |
| **8** | 204.9 | 0.166 | 352 | 4.528 | 0.100 | 0.83 |

Note that the flow coefficients for the first, third and fifth stages were above the recommended upper limit for the flow coefficient of 0.15, although in rare cases this limit can be exceeded. For the first and fifth stages, as the flow coefficient values were just slightly above the upper limit (0.161 and 0.157) values for efficiencies were extrapolated from the flow coefficient-efficiency graph. However for the third stage, a value for the flow coefficient could not be extrapolated from the graph so no efficiency was derived for this stage. The efficiencies were plotted as a function of stage number as shown in Figure 7.7.

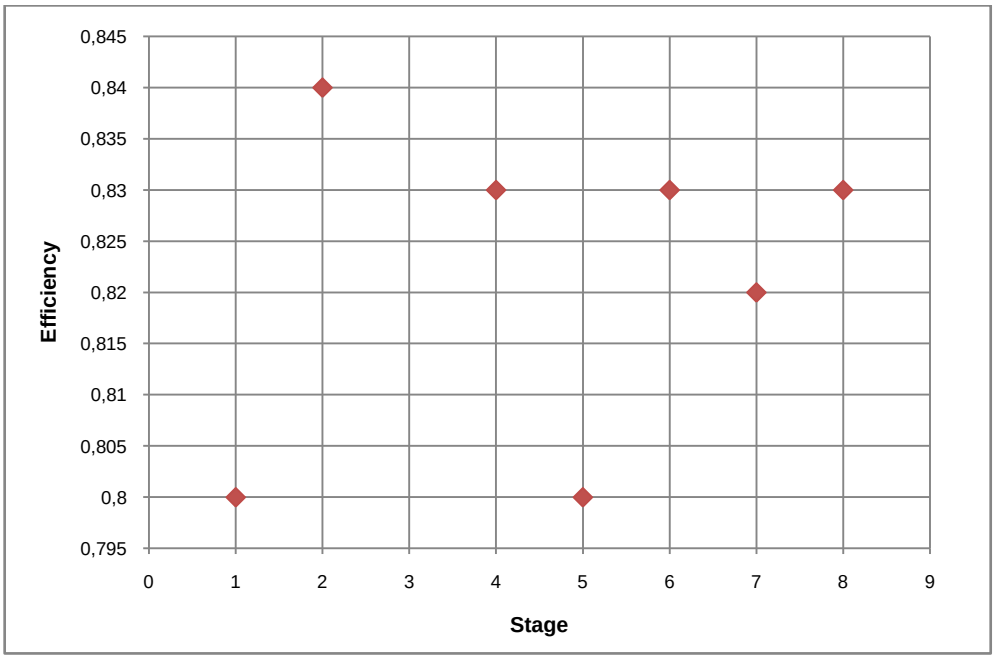


**Figure 7.7: Stage polytropic efficiency**

Figure 7.7 shows that the polytropic efficiencies vary significantly across the stages, which contradict the expected trend of reduced efficiencies through the compressor. This trend is expected as a result of smaller impeller sizes, the increased tip leakage and reduced volume flow towards the end of the compressor.

No power consumption was calculated due to the inconsistencies in the flow coefficient results. Although most of the efficiencies that were retrieved from this investigation falls within the 80 to 85 % range that is believed to be reasonable.

#### 7.1.3.3 Estimated Polytropic Efficiencies of 80 and 85 %

A simulation of a typical MAN Turbo 10-stage compressor was performed using best estimates of polytropic efficiencies. The efficiencies are shown in column 2 in Table 7.7. These values were transformed to isentropic efficiencies in TechUtils by providing the simulation tool with compressor inlet conditions and outlet pressures, see Table 7.7.

**Table 7.7: Polytropic efficiency estimations**

| Stage | $\eta_p$ [%] | $\eta_i$ [%] |
|---|---|---|
| **1** | 87.45 | 86.58 |
| **2** | 87.33 | 86.43 |
| **3** | 83.39 | 82.26 |
| **4** | 83.44 | 82.41 |
| **5** | 81.47 | 80.29 |
| **6** | 81.03 | 79.86 |
| **7** | 78.06 | 76.77 |
| **8** | 76.10 | 74.68 |
| **9** | 71.36 | 69.90 |
| **10** | 69.87 | 68.69 |

To evaluate if these efficiencies were a good approximation they were applied to the MAN Turbo RG 053-10 for a power comparison. As mentioned in Section 7.1.1, estimates for pressure and temperature were obtained from Figure 7.2.

All the data was imported to IPSEpro and the power was calculated to be 4.37 MW. The result was multiplied by 1.055 for assumed additional losses such as gearing, motor and mechanical losses, which gave a shaft power of 4.62 MW. The difference between the calculated power and the power consumption of 4.5 MW stated by MAN Turbo was +2.7 %. The relatively small difference between the two power consumptions validated the efficiencies and they were assumed to be good estimations.

To get an idea of the power required for a larger mass flow the same efficiencies were assumed for the RG 140. By using the same model as in previous case but with an increased mass flow the power consumption was calculated to 33.18 MW. With losses included the power consumption was 35.01 MW. This was 6.1 % higher than the stated power consumption of 33 MW.

### 7.1.4 Summary

Table 7.8 shows a summary of the power demands for each case investigated. Note that the shaft power includes losses.

**Table 7.8: Summary table of MAN Turbo performance**

| Type | MAN Turbo power data [MW] | Shaft power (estimated efficiencies) [MW] | Shaft power ($\eta_p$ = 0.80) [MW] | Shaft power ($\eta_p$ = 0.85) [MW] |
|---|---|---|---|---|
| **RG 053-10** | 4.5 (0.0 %) | 4.62 (+2.7 %) | 4.67 (+3.8 %) | 4.36 (-3.1 %) |
| **RG 140** | 33 (0.0 %) | 35.01 (+6.1 %) | 35.38 (+7.2 %) | 33.10 (+0.3 %) |

### 7.1.5 Discussion

For the RG 053-10, which is an actual compressor used for $CO_2$ compression, the power calculated using stated efficiencies match the MAN Turbo power data. The high efficiencies are therefore reasonable. The mass flow capacity for this compressor of 11.6 kg/s is below the required mass flow for a power plant which requires a number of compressors in parallel.

The RG 140 handles a mass flow which could be suitable for $CO_2$ compression although this compressor is assumed to be working with air and not yet adapted for $CO_2$. It is reasonable to believe that the greater difference between calculated and stated values for the RG 140 is due to operational area. According to Table 7.8 the difference in power consumption is small for 85 % polytropic efficiency compared with the stated 33 MW. The 85 % polytropic efficiency is higher than the efficiency calculated for the RG 053-10. However for the larger machine there would be lower losses due to tip clearances, hydraulic diameter, Reynolds number etc. Considering these aspects and MAN Turbo's experience in $CO_2$ compression, the stated power consumption of 33 MW is a believable figure.

## 7.2 Investigation of Ramgen

### 7.2.1 Overview of Ramgen Technology

Ramgen is a novel technology with supersonic 'shock' compression. It uses the same principles as a ramjet. A ramjet is an engine without rotating parts; instead it uses the engines forward motion to compress the air. At supersonic speeds, air is ingested into the engine. The air then flows around an obstructing centre-body that creates a ramming effect when the air is forced through the area between the body and the engine's sidewall as shown in Figure 7.8. As the airflow is slowed down to subsonic speeds, shock waves are created. The pressure increases dramatically, compressing the air prior to mixing with fuel. The mixture is then combusted and expanded through a nozzle to create forward thrust.

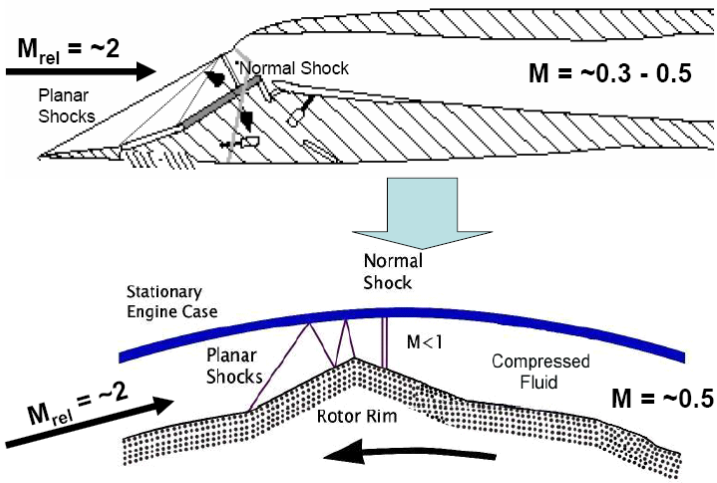


**Figure 7.8: Above supersonic F-15 inlet, beneath Rampressor rotor**

In the Rampressor a rotating disc (see Figure 7.9) mimics forward motion. It operates at high speed to create a supersonic effect. Raised sections on the rim of the disc create the same ramming effect as the centre-body in a conventional ramjet. The medium enters through a common inlet; flows into the annular space between the disc and the casing where the three raised sections create shock waves. As in a ramjet, the shock waves generate a pressure increase, compressing the medium to the desired level. The compression ratio is highly dependent on the strength of the shock wave, which increases exponentially with the Mach number, and where the oblique shock takes place. When the disc spins faster, the Mach number will increase.

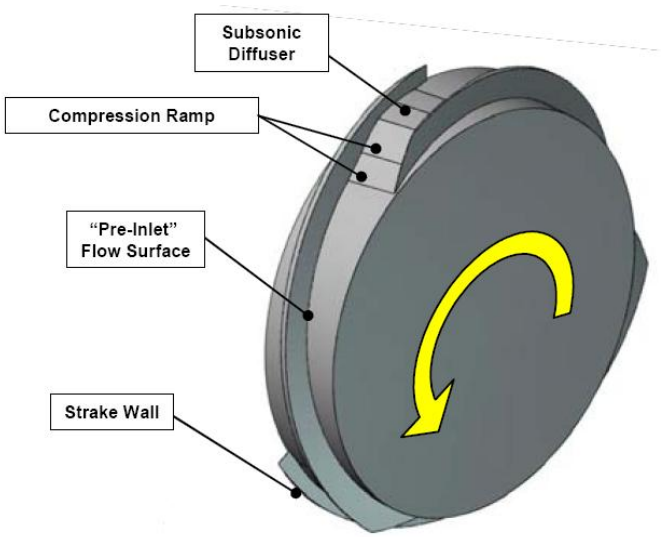


**Figure 7.9: Rotating disc with raised sections**

The compression is undertaken in two stages with a pressure ratio of 10:1. The compression process is shown in Figure 7.10.

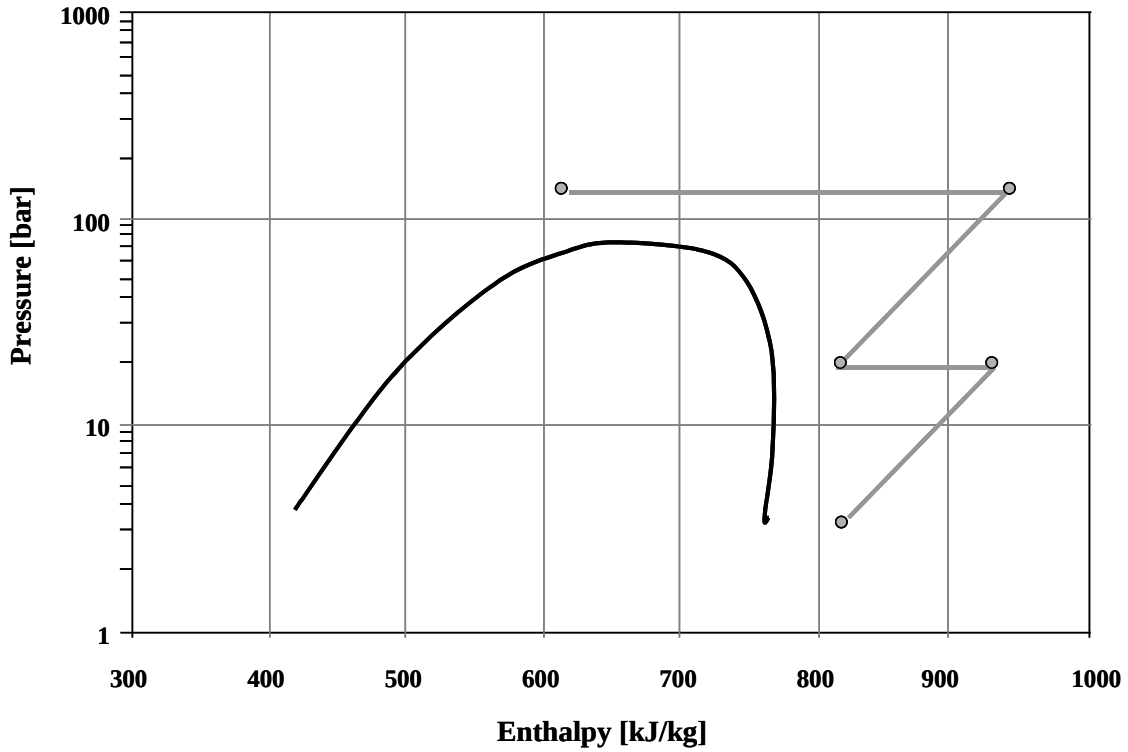


**Figure 7.10: Pressure-Enthalpy diagram for the Rampressor**

The configuration can be fitted with both an intercooler and an aftercooler if required for the application. The discharge temperature from the stages is ~ 470 ˚F (243 ˚C). This high-grade heat could be used in the power plant.

Ramgen claims high efficiency for their compressors as a result of its relatively simple design compared to axial and centrifugal compressors. The simple design with a small number of leading edges reduces the drag and therefore minimises the losses. Other advantages claimed over more conventional compressors are the high pressure ratios per stage, which reduces the footprint and the possibility to use the relatively high grade waste heat. [27]

## 7.2.2 Investigation of Ramgen Performance

### 7.2.2.1 Ramgen Statements

Ramgen claims that their compressors have high stage efficiencies. In reports published by Ramgen the isentropic efficiencies are claimed to be somewhere between 85 and 90 %. The company has also claimed an outlet temperature of 243 ˚C and a power consumption of 7.33 MW.

### 7.2.2.2 Assumptions

The initial investigation undertaken considered the two claimed efficiencies with a pressure ratio of 10:1 for each stage. This was a different approach than the one used for the other models where the delivery pressure was fixed. Therefore, the delivery pressure will not be the same for the Ramgen investigation as for the other models. The mass flow is set to 18.9 kg/s as stated by Ramgen.

### 7.2.3 Initial Investigation using Current Ramgen Product

A model with two compressors and intercooling after the first stage was created in IPSEpro. The power consumption for one compressor with two stages was calculated using the assumptions stated in Section 6.1.1 and those given above. Including losses, the values obtained for power consumption were 0.5 and 0.07 MW for 85 and 90% efficiencies respectively, greater than the stated 7.33 MW. The results including losses are provided in Table 7.9 below.

**Table 7.9: Summary of Ramgen performance**

| | RAMGEN power data [MW] | Shaft power ($\eta_i$ = 0.85) [MW] | Shaft power ($\eta_i$ = 0.90) [MW] |
|---|---|---|---|
| **1 Rampressor** | 7.33 (0.0 %) | 7.83 (+6.8 %) | 7.40 (+1.0 %) |

#### 7.2.3.1 Validation of Results

In an attempt to understand the discrepancy between the results obtained in this investigation and those obtained by Ramgen, some individual values within the IPSEpro model were examined. An investigation similar to the one undertaken in IPSEpro was also performed using TechUtils. The results for the efficiency analyses from both investigations are summarised in Table 7.10.

**Table 7.10: Validation of 85 % efficiency**

| | TechUtils | IPSEpro | RAMGEN |
|---|---|---|---|
| ***Matching efficiency*** | **0.85** | | |
| $T_{out}$ 1st stage | 267.75 | 266.26 | 243.33 |
| $T_{out}$ 2nd stage | 253.64 | 252.47 | 243.33 |
| **Total shaft power** | **7569.639** | **7564.78** | **7333** |
| ***Matching discharge temperature*** | **243.33** | | |
| Stage 1st Efficiency | 0.9044 | | 0.85 |
| Stage 2nd Efficiency | 0.9025 | | 0.85 |
| **Total shaft power** | **6916.644** | **6912.14** | **7333** |
| ***Matching absorbed power*** | **7333** | | |
| Stage 1st Efficiency | 0.9044 | | 0.85 |
| $T_{out}$ 1st stage | 255.18 | 253.86 | 243.33 |
| Stage 2nd Efficiency | 0.8538 | | 0.85 |
| $T_{out}$ 2nd stage | 254.73 | 253.48 | 243.33 |
| **Total shaft power** | **7338.87** | **7333.02** | **7333** |

It was discovered that for an isentropic efficiency of 85 % the discharge temperature was 10 ºC higher than the discharge temperature claimed by Ramgen. As a result of this the power consumption, without any losses added, was 3.2 % higher than the stated 7.33 MW. To achieve the claimed compressor discharge temperature of 243 ºC the isentropic compressor efficiency needed to be 95 % for the first stage and 90 % for the second stage. This resulted in power consumption 5.7 % lower than the power consumption stated by Ramgen. The results from TechUtils matched those achieved here and thus the discrepancy with Ramgen's claims was considered valid.

### 7.2.4 Discussion

The Rampressor compression is performed in two stages, resulting in power consumption that is much greater than the theoretical minimum of isothermal compression. The power consumption calculated in this investigation exceeded the stated value of 7.33 MW despite the highest stated efficiency being used.

The high pressure ratios in the Rampressor give high compressor outlet temperatures which Ramgen claim can be used elsewhere in the process to improve the overall power plant thermal efficiency.

The Rampressor is a novel technology that has not been proven at full scale. This lack of validation in addition to the difference between stated figures and calculated results gives a high degree of uncertainty.

## 7.3 Investigation of Potential Solution Based on Rolls-Royce Barrel Compressors

Rolls-Royce claims that their compressors offer a high degree of flexibility to meet customer requirements. Their idea is to use standard frames, vary the number of sections and custom design the internal aerodynamics to tailor their products to different applications. This provides the opportunity to vary the degree of intercooling, machine footprint and turn down capabilities. The barrel compressors also offer an opportunity to introduce internal cooling between impellers within the casing in addition to intercooling between the sections.

The required mass flow falls within a region where both axial and centrifugal compressors can be used as described in Section 5.1.3. Different solutions for the process have been considered by Rolls-Royce depending on whether the process is optimised for power consumption, footprint or heat recovery.

This investigation covers the effect of number of sections with intercooling, the possibility to introduce integral cooling and the effects of lowering the compressors inlet temperature with more efficient intercoolers and precooling. It also covers an investigation on efficiencies calculated in CompSelect to obtain a more accurate approximation of what Rolls-Royce compressors would be able to accomplish.

### 7.3.1 Isothermal Compression

The best theoretical compressor work for a process is the isothermal process, which is equivalent to an infinite number of intercoolers [44].

For a perfect gas the compressor work is calculated according to Equation 7.2

$$w_{in} = \int_1^2 v\, dP \qquad \text{Equation 7.2}$$

$CO_2$ cannot be considered a perfect gas due to its compressibility. Therefore the isotherm reversible work will be calculated according to Equation 6.3

$$w_{in} = h_2 - h_1 - \int_1^2 T\, ds = h_2 - h_1 - T(s_2 - s_1) \qquad \text{Equation 7.3}$$

The isothermal power consumption was calculated for compression from 1.8 bar(a) to 200 bar(a) at 40 °C. The entropies and enthalpies were retrieved from TechUtils at entry and delivery conditions. To calculate the specific work for a compressor, the isothermal work was multiplied by the mass flow and divided by the compressor efficiency.

### 7.3.2 Investigation of Number of Sections

To develop an understanding of the power saving additional intercooling between each compressor section will accomplish, several models were built in IPSEpro, an example is available in Appendix B. Thirteen models were constructed, beginning with two compressors with intercooling and then adding one compressor / intercooler at a time until 14 sections were built. To allow a fair comparison between thermodynamic properties for the different methods, the same efficiencies used for MAN Turbo and the cryogenic option were used for the Rolls-Royce model. The polytropic efficiencies of 80 and 85 % were transformed into isentropic using TechUtils. The shaft powers were calculated in IPSEpro and plotted in Figure 7.11.

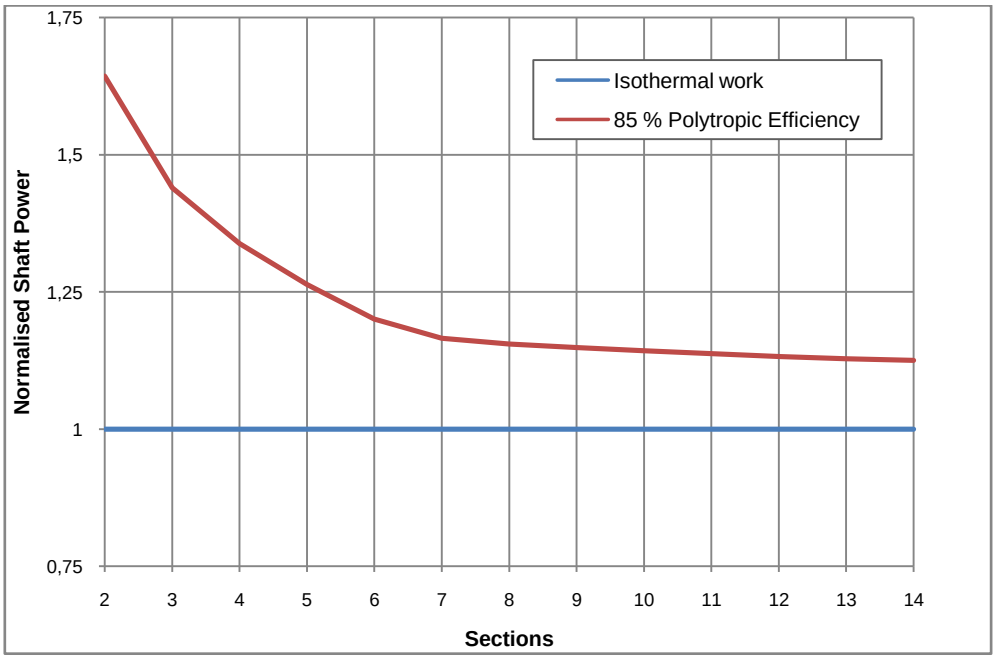


**Figure 7.11: Number of sections versus power consumption**

As seen in Figure 7.11, an increased number of intercoolers results in lower inlet temperature to each compressor, which reduces the power consumption of the compressor. As the temperature difference across each compressor moves towards

zero the shaft power approaches the theoretical minimum i.e. isothermal work. Up to seven sections, the intercooling results in a great power saving. Using more than seven intercoolers gives relatively small change in consumed power. Based on the investigation, additional modelling work was carried out using a 7-section model with intercooling after each section.

### 7.3.3 Investigating the Effect of Integral Cooling

As shown in the previous section introducing more cooling in the compression process can save a vast amount of power. However adding more intercoolers increases the footprint and unit cost and hence other cooling options were also considered. One alternative is to use integral cooling within the barrel compressors. This was done by dividing the compression process into sections with multiple impellers with cooling between each stage and intercoolers after each section as shown in Figure 7.12.

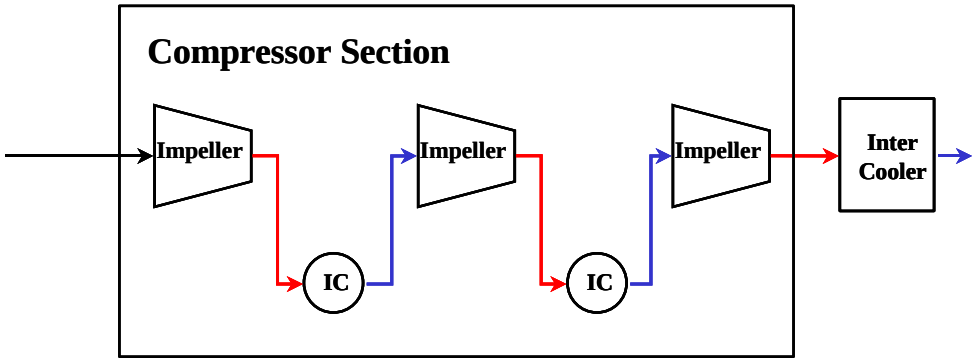


**Figure 7.12: Compressor section with three impellers**

To determine how much power saving integral cooling will achieve, two models were created in IPSEpro. These models simulated a seven-section compression process with and without integral cooling. The model with integral cooling was assumed to have two impellers in each section. Due to the limited space for coolers and hence smaller heat transfer area; it was assumed that the inlet temperatures of the second impellers would be higher than those of the first impellers in each section. To get an understanding of how big the temperature difference between external and internal intercooling is heat exchanger effectiveness was introduced according to Equation 7.4 The equation describes the relationship between the actual heat transfer to the maximum possible heat transfer available in the heat exchanger.

$$\varepsilon = \frac{\dot{Q}}{\dot{Q}_{\max}} = \frac{C_h (T_{h,\,in} - T_{h,\,out})}{C_{\min} (T_{h,\,in} - T_{c,\,in})} \qquad \text{Equation 7.4}$$

Where $Q$ is the actual heat transferred between the fluids and $Q_{max}$ is the maximum heat transfer. $C_h$ and $C_{min}$ are the heat capacity rates (mass flow multiplied by specific heat). $h$ denotes the hot medium ($CO_2$) and $min$ is the smallest of the heat rates for the two mediums in the heat exchanger. A reasonable heat exchanger effectiveness for external intercoolers is 0.7 and for the internal cooling the effectiveness is assumed to be somewhere between 0.1 and 0.3. [45]

The heat exchangers are cooled with water that has a specific heat approximately four times bigger than $CO_2$. In addition, the mass flow of water is bigger than the mass

flow of $CO_2$. As result, $C_h$ will be smaller than $C_c$ (heat capacity rate for water in this case) and $C_{min}$ can be assumed to be equal to $C_h$.

Using water with an inlet temperature of 20 ˚C as cooling medium the heat exchanger outlet temperature for the $CO_2$ was calculated for both internal and external coolers with an effectivity of 0.3 and 0.7 respectively.

For 85 % polytropic efficiency it was found that the integrally cooled compressor could save up to 4.3 % compared to an identical compressor without internal cooling.

### 7.3.4 Investigating the Effects of Intercooling Temperatures and Precooler

The compressor work is proportional to the inlet temperature hence reducing the inlet temperature will reduce the compressor work. An investigation on intercooling temperature was performed to determine how much the temperature affected the power consumption. Special attention was paid to high pressures, above 50 bar(a), where low intercooling temperatures may cause phase transformation. This is of particular concern for real $CO_2$ mixtures where the exact location of phase boundary is unknown. Therefore for this investigation the outlet temperatures of the final two intercoolers were set to 38 ˚C. The cooling medium was assumed to be water with an inlet temperature of 20 ˚C and thus a reasonable limit for the $CO_2$ stream leaving the intercoolers was 25 ˚C, giving a pinch point of 5 ˚C.

The $CO_2$ stream has a temperature of 40 ˚C leaving the separation process. This introduces the possibility to use a precooler. Hence the possible advantage of using a precooler was evaluated.

The baseline case for the investigation was the 7-section compressor train with each intercooling outlet temperature set to 38 ˚C. The outlet temperature from the intercoolers was decreased by one degree at the time to the limit of 25 ˚C with and without precooler. The power was calculated and plotted against intercooling temperature as shown in Figure 7.13.

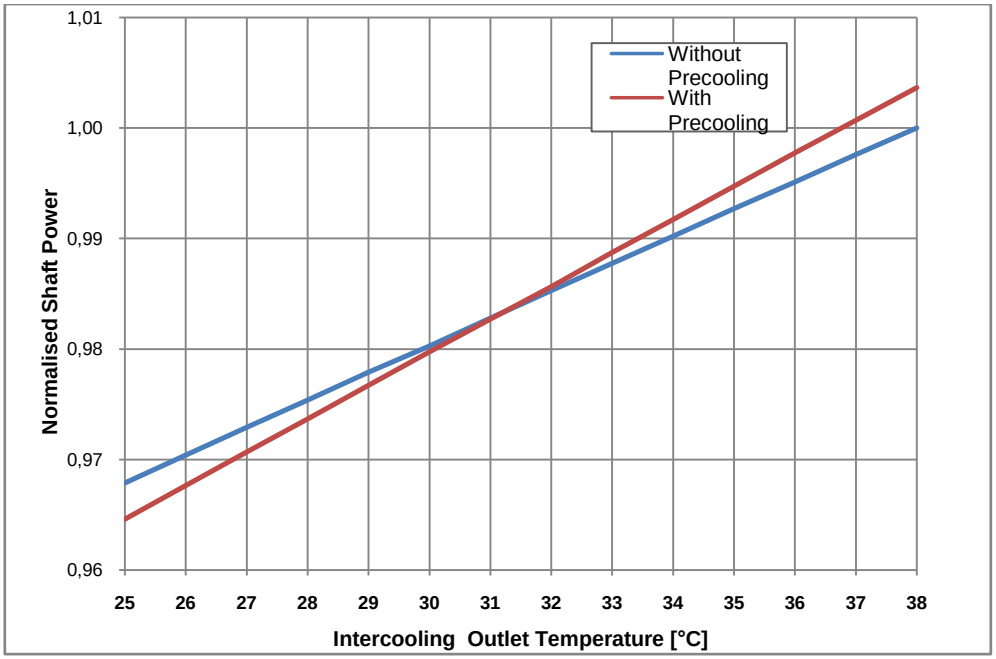


**Figure 7.13: Intercooling temperature versus power**

According to Figure 7.13, the average power saving is 0.23 % per ˚C without precooling and 0.28 % per ˚C with precooling. Adding a precooler to the system will however result in increased pressure losses, which is why the expected power savings will not occur until below 30 ˚C for this option. Parasitic pressure losses in the early stages affect the overall system more significantly than a pressure loss introduced later in the system.

### 7.3.5 Investigating Efficiencies from CompSelect

The efficiencies used in previous investigations (80 and 85 %) were assumed in order to compare the Rolls-Royce solution with competitive products. To obtain a more realistic understanding of the compressor performance the efficiencies for the 7-section model were calculated in CompSelect. The inlet and outlet pressures to the sections were determined using IPSEpro.

Speed of sound was determined using TechUtils with the pressures and the compressor inlet temperature. The ratio of tip speed to speed of sound (i.e. the Mach number) is limited to 0.9 therefore a maximum tip speed was calculated. For this velocity, the rotational speed was calculated for a number of different typical Roll-Royce impeller diameters.

The pressures and the mass flow were applied in CompSelect that provided polytropic efficiencies for actual compressors as shown in Table 7.11. A compressor that matched the maximum rotational speed was selected. The isentropic values for the efficiencies were calculated in TechUtils.

**Table 7.11: Isentropic efficiencies for a 7-section compressor process**

| Section | $\eta_p$ | $\eta_i$ |
|---|---|---|
| **1** | 88,56 | 87,73 |
| **2** | 88,07 | 87,20 |
| **3** | 86,44 | 85,44 |
| **4** | 86,12 | 85,07 |
| **5** | 84,66 | 83,44 |
| **6** | 78,73 | 77,00 |
| **7** | 70,00 | 68,97 |

Using IPSEpro, the corresponding power consumption was calculated. The power consumption increased with 0.8 % compared to using 85 % polytropic efficiency. The process is summarised in Figure 7.14.

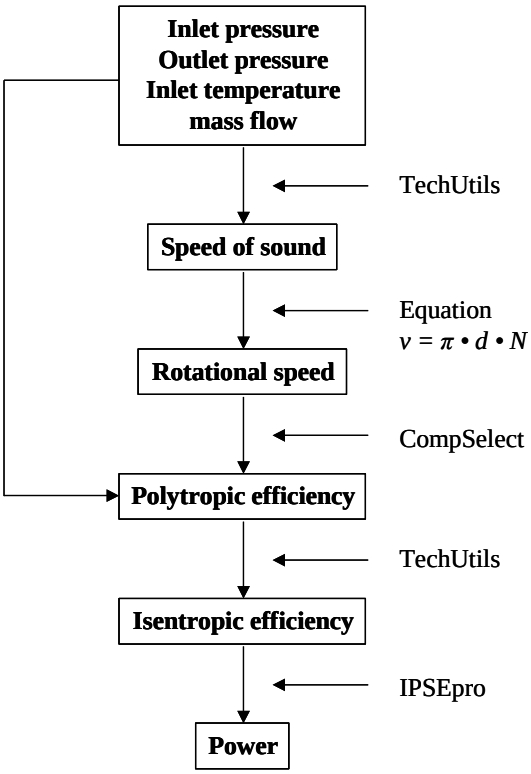


**Figure 7.14: Flow chart of CompSelect calculations**

### 7.3.6 Summary of Results

Additional losses of 5.5 % in total were added to the total power consumption and the results are shown in Table 7.12.

**Table 7.12: Summary table of Rolls-Royce performance**

| | Base line case (7-sections with cooling to 38 ˚C) | Integral cooling | Inter-cooling to 25 ˚C | Inter-cooling to 25 ˚C with pre-cooler | Efficiencies from CompSelect |
|---|---|---|---|---|---|
| **Difference [%]** | 0.0 % | -4.3 % | -3.2 % | -3.5 % | +0.8 % |

### 7.3.7 Discussion

According to Figure 7.11 the power saving achieved through intercooling beyond 7-sections is less than 1 %. Given the increased cost and footprint associated with additional sections the 7-section option was considered to be the most sensible alternative.

According to the results, using integrally cooled compressors is proved to be a good way of saving power without dividing the compressing process into more sections with intercooling.

Lowering the intercooling temperature resulted in a major power saving. However adding a precooler to the system made an insignificant change in power saving due to additional pressure losses. As mentioned in Section 3.2 impurities in the $CO_2$ stream will cause changes in thermodynamic properties for the $CO_2$ mixture. Hence, there is uncertainty regarding how low intercooling temperature that is possible to use and still stay clear of the two-phase region.

The power consumption calculated with efficiencies from CompSelect was higher than the baseline case. It is reasonable to believe that this was caused by the low efficiencies in the final sections.

## 7.4 Investigation of a Cryogenic System

### 7.4.1 Overview of Cryogenic Option

One way of achieving a delivery pressure above 140 bar(a) is to use a refrigeration and pumping system. The total power consumption for this method of $CO_2$ compression can be divided into two parts. The first part consists of a number of compressors that compress the gaseous $CO_2$. In the second part, the $CO_2$ is chilled at constant pressure into liquid phase in a refrigeration plant and then pumped to the desired delivery pressure as shown in Figure 7.15. By using the cryogenic method the area around the critical point where the properties are difficult to define is avoided. Furthermore, less power is required to achieve the equivalent pressure rise in the liquid phase as in the gas phase due to the smaller changes in enthalpy. This is partly because the work done in a pump is close to isothermal.

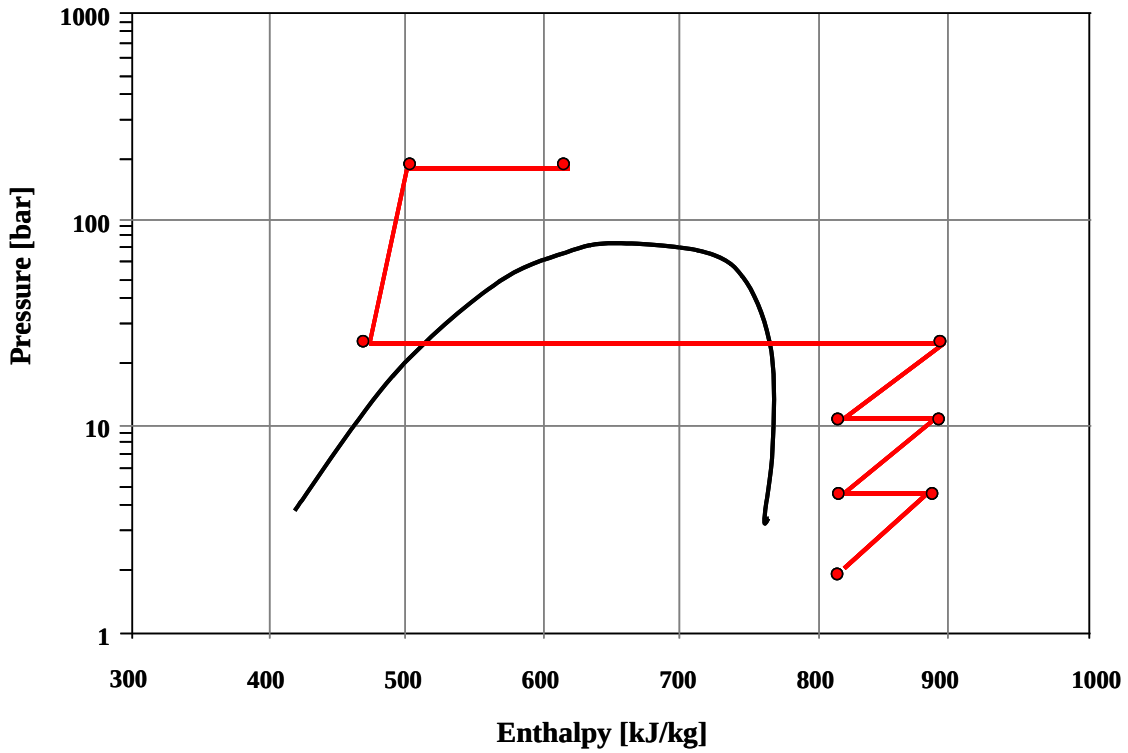


**Figure 7.15: Pressure - Enthalpy for $CO_2$**

An investigation previously performed by South West Research Institute (SWRI) showed that this method can save 35 % compared to a conventional compression method using centrifugal compressors. In this investigation the $CO_2$ was compressed from atmospheric pressure to 17 bar(a) in two stages prior to chilling and pumping to 153 bar(a). These conditions were based on a 700 MW(e) power plant and assumed pure $CO_2$ [46].

### 7.4.2 Investigation of Cryogenic Performance

There are many different factors influencing the performance of a cryogenic system. This investigation considers four key aspects:

- The number of $CO_2$ compressor sections prior to refrigeration.
- The pressure of the $CO_2$ entering the two-phase region.
- The reuse of cold $CO_2$.
- The $CO_2$/$CO_2$ heat exchangers pinch point.

#### 7.4.2.1 Assumptions

The following assumptions were made:

- Ammonia was used as the cooling media in the refrigeration cycle.
- The ammonia cycle was simulated as a two-stage refrigeration plant with a flash chamber.

- The high pressure (HP) ammonia was saturated at 10.5 bar(a) and 25 °C (10 °C above assumed atmospheric temperature) and sub cooled after the condenser.

- The intermediate pressure (IP) ammonia was superheated after the separator to ensure that only gaseous phase was present in the HP compressor.

- The low pressure (LP) ammonia had a 10 °C temperature difference to the $CO_2$ in the evaporator and was superheated to gaseous phase.

- The LP and HP ammonia compressors had equal pressure ratios and isentropic efficiencies of 85 %.

- The ammonia cycle had a COP of approximately three.

- Pinch points for the liquid to gaseous $CO_2$ heat exchangers were 10 °C on the hot side.

- The mass flow was the same through each of the liquid to gaseous $CO_2$ heat exchangers.

- The $CO_2$ inter cooling exit temperature was set to avoid liquid $CO_2$ in the compressors.

- The liquid $CO_2$ pump had an efficiency of 50 %.[4]

- The mechanical losses in the condenser fan were 2 % of the heat transferred.

### 7.4.3 Investigation Description

#### 7.4.3.1 Ammonia Cycle

The ammonia cycle was simulated as a two-stage refrigeration plant with a flash chamber as described in Section 5.2.6. An example of how the cycle was modelled in IPSEpro is available in Appendix B.

The choice of ammonia as the refrigerant was based primarily on its high thermal conductivity. The coefficient of performance (COP) for an ammonia cycle will be more than 1.5 times better than using, for example, $CO_2$ as the refrigerant. The only refrigerant that would give a higher COP than ammonia is Chloro-Methane. However due to the associated environmental issues and its extreme flammability, Chloro-Methane was not considered. [47]

According to a refrigerator supplier the compressors in the refrigeration cycle will most likely be screw compressors. As stated in Section 7.4.2.1, the compressors had assumed isentropic efficiencies of 85 %.

[4] This low figure was assumed because the pump will have to provide a very high pressure rise and hence have a large number of stages reducing efficiency. Also, it will be pumping a dense and highly viscous fluid and will probably require stronger thrust bearings, both factors further contributing to reduced efficiency.

#### 7.4.3.2 $CO_2$ Compression Prior to Refrigeration

The investigation covered three, four and five sections of compression of $CO_2$ prior to chilling. For each case, five different entry pressure levels were investigated (from 20 to 40 bar(a) in 5 bar increments). With increased entry pressure to the refrigeration cycle, the compressor shaft power will increase whilst the refrigeration shaft power will decrease and vice-versa.

The upper limit on final delivery temperature was set to 50 °C as this was requested by The Company. The temperature of the liquid $CO_2$, after pumping, was however significantly lower than the requested limit. In an attempt to minimise the shaft power, the excess cold of the high-pressure liquid $CO_2$ was fed through a heat exchanger to cool the gaseous $CO_2$ before each compressor stage as shown in Figure 7.16. It was anticipated that this would assist in reducing the power consumption of the cycle. However it was also noted that adding extra heat exchangers would increase the parasitic pressure losses in the cycle and result in a higher system cost and a larger footprint.

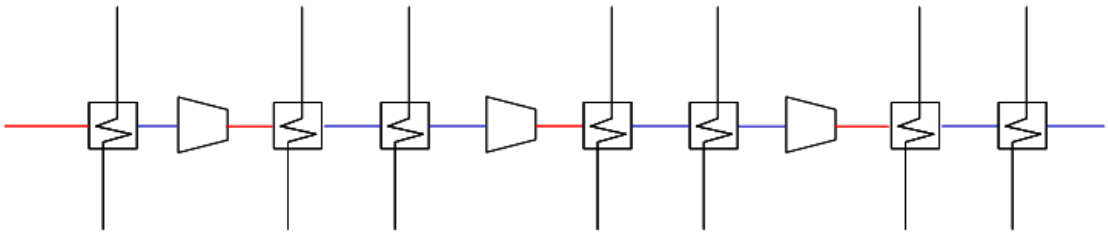

**Figure 7.16: Placement of liquid to gaseous CO2 HX**

Preliminary modelling work showed that when the pressure entering the refrigeration cycle increased, the temperature of the liquid $CO_2$ leaving the pump increased. This was expected since higher saturation pressure corresponds to higher temperature. Above 40 bar(a), there was no appreciable temperature difference between gaseous $CO_2$ and liquid $CO_2$, eliminating the benefit of using the extra heat exchangers to recover the cold from the liquid $CO_2$.

To evaluate the benefits of using the excess cold, the models were run both with and without $CO_2/CO_2$ heat exchangers. In the cases without recovery the 40 bar(a) upper limit is redundant and therefore 45 and 50 bar(a) were also investigated for these cycles.

### 7.4.4 Refrigeration and Cryo-Pumping Calculations and Results

#### 7.4.4.1 Estimated Polytropic Efficiencies of 80 and 85 %

Using two different polytropic efficiencies for the compressor sections, an investigation was undertaken to evaluate how the number of compressor sections affected the power consumption with and without reusing the excess cold in the liquid $CO_2$.

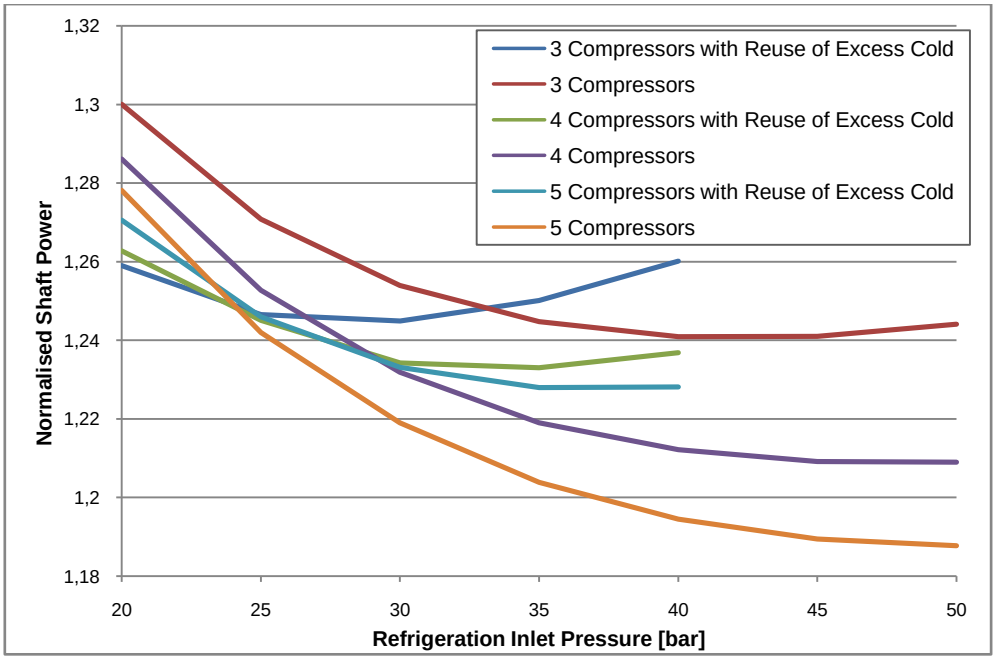


**Figure 7.17: Refrigeration inlet pressure versus shaft power for 3, 4 and 5 compressor sections with and without cold recovery, 85% polytropic efficiency**

As shown in Figure 7.17 an increased number of compressor sections was shown to reduce the overall power consumption of the system. It also follows that using a greater number of compressor sections increases the optimum refrigeration inlet pressure. When high pressures are used in the evaporator both $CO_2$ saturation temperature and the COP for the ammonia cycle will increase as shown in Figure 7.18.

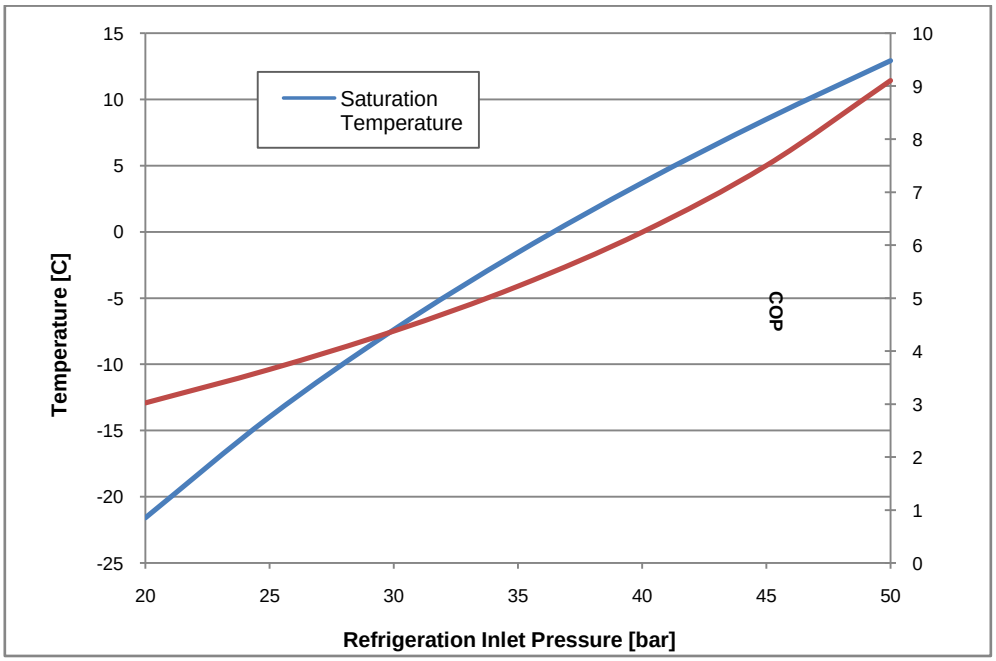


**Figure 7.18: Variation in temperature and COP for increased refrigeration inlet pressure**

Figure 7.17 also shows that there is no benefit associated with using the excess cold from the liquid $CO_2$ in heat exchangers prior to the compression sections above 22

bar(a) for the 5-section model. This is due to the additional parasitic pressure losses associated with each heat exchanger. To illustrate the penalty associated with these losses the two simulations were carried out without losses for a 5-section compressor system. The power consumption was plotted against refrigeration inlet pressure as shown in Figure 7.19.

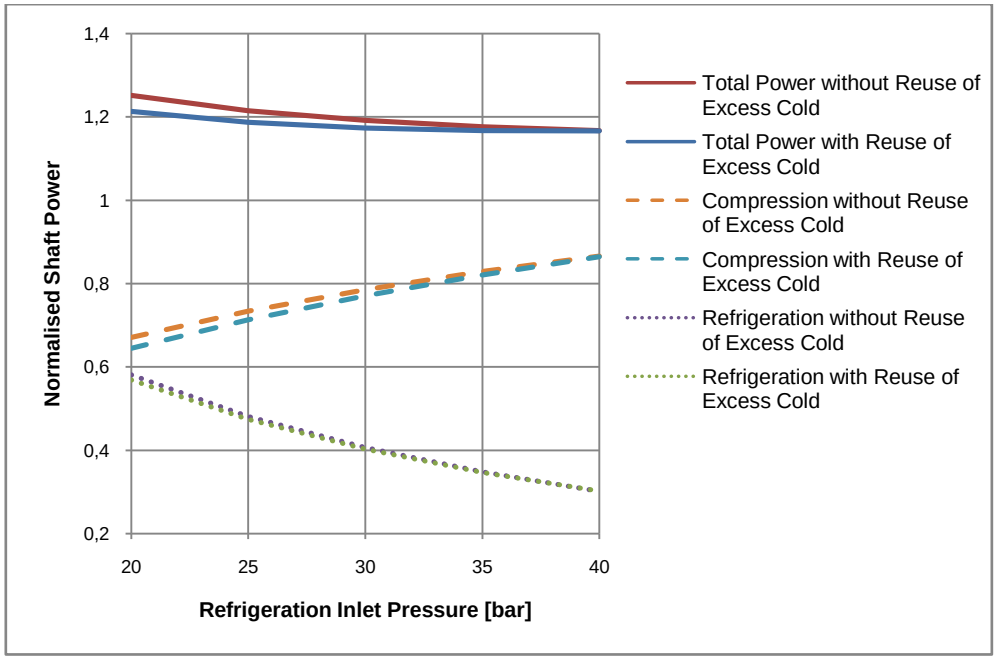


**Figure 7.19: Power consumption for a 5-section compressor cryogenic system without losses**

Figure 7.19 shows that without losses there will be power savings for the 5-section compressor model when reuse of the excess cold is introduced. For this model reuse of cold can save up to 3 % when entering the refrigeration plant at low pressures (i.e. low temperatures leaving the pump). For the same refrigeration inlet pressure this difference is 5 % for a 3-section compressor model. The difference between the 3- and 5-section models results is due to the higher pressure and temperature rise for each compressor in the 3-section model.

Figure 7.18 also shows that for increased pressures entering the refrigeration plant, the liquid $CO_2$ leaving the pump is warmer (i.e. less cold is available). Hence there is no significant difference in power consumption between the systems with and without cold recovery.

#### 7.4.4.2 Using Compressor Efficiencies from CompSelect

A second investigation was carried out in which the efficiencies for the compressors were obtained using CompSelect. The following modelling procedure was carried out:

1. For the three different models (3, 4 and 5 compressor sections with and without reuse of excess cold) the inlet pressure, inlet temperature and outlet pressure of the compressors were obtained from IPSEpro for each refrigeration inlet pressure and imported to TechUtils. A fixed efficiency was used as default value.

2. The maximum rotational speed for eight typical Rolls-Royce impeller diameters was calculated by assuring that the tip speed would not exceed a

Mach number of 0.9. The speed of sound for each section was determined in TechUtils.

3. Pressures and temperatures were then imported to CompSelect, which provided a range of possible compressor candidates.

4. The compressor with the highest polytropic efficiency that accommodated both the Mach number limitation and the desired design feature of having all impellers on a common shaft (i.e. same rotational speed) was therefore selected.

5. The polytropic efficiencies from CompSelect were transformed into isentropic efficiencies using TechUtils. This was done for every stage of each model at each pressure level.

6. The stage efficiencies for the different pressure levels in the different models were compared. It was found that the entry pressure to the refrigeration plant did not significantly alter the isentropic efficiencies. Hence a representative mean isentropic efficiency was chosen for every compressor stage.

7. To cover the small changes in efficiencies associated with pressure levels, a range of ±1 % was also employed.

8. All isentropic efficiencies were applied in IPSEpro and the total power consumption was calculated.

9. The cases were evaluated and compared on the basis of total shaft power consumption.

**CompSelect Summary**

The minimum power consumption for three compressors with and without recirculation was found at 30 bar(a) and 45 bar(a) respectively. For four compressor sections with recirculation a minimum power consumption could be identified at 35 bar(a). For the rest of the cases no minimum was found. It was noted that the power consumption decreased with additional compressor sections. This also resulted in higher refrigeration inlet pressure.

By adding losses such as fan losses, mechanical losses, motor losses and heat leakage to the system the power consumption was increased by 8 - 9 %. Motor losses, heat leakage and mechanical losses will have a negative impact on both compression and refrigeration whereas the fan losses only affect the refrigeration cycle. The higher penalty for the refrigeration cycle results in a less pronounced power consumption minimum.

### 7.4.5 Sensitivity Analyses

An investigation on the effect of heat exchanger pinch point (i.e. the temperature difference between the hot and the cold side either on the inlet or the outlet of the heat exchanger) on power consumption was also undertaken. Liquid to gaseous $CO_2$ heat exchangers as well as the evaporator was covered in this study. Changing the pinch point in the $CO_2/CO_2$ heat exchangers will affect the compressor power. Whereas the pinch point in the evaporator will affect the refrigeration power.

One way to reduce the shaft power for the $CO_2$ cycle is to reduce the pinch point by increasing the heat exchanger area. This will lower the temperature leaving the heat exchanger i.e. lower the compressor inlet temperature. When the pinch point approaches zero the heat exchanger area will move towards infinity. The choice of heat exchangers is therefore a trade-off between shaft power, cost and footprint of heat exchangers.

The pinch point analysis involved two stages. First, the effect of pinch-point on power was estimated using a theoretical approach. Second, the effect of pinch-point was calculated by changing the heat exchanger values in IPSEpro.

#### 7.4.5.1 Theoretical Pinch-Point Analysis

The total compressor work for a compressor is calculated as according to Equation 7.5

$$W = \frac{\dot{m} T_1 c_p}{\eta} \left( \left( \frac{p_2}{p_1} \right)^{\frac{\gamma-1}{\gamma}} - 1 \right) \qquad \text{Equation 7.5}$$

Where $\gamma$ is the relation $c_p/c_v$ and $c_v = c_p - R$.

At low pressures $CO_2$ is assumed to be a perfect gas with constant $c_p$, hence a change in the compressor inlet temperature is proportional to a change in power. For the case with 3 compressors at 20 bar(a) the power required to compress the $CO_2$ prior to refrigeration represents 55 % of the total power. The change of inlet temperature in percent was calculated for a 5 degree pinch point decrease, which corresponded to a total power change of 0.94 %. For the case of five compressors at 40 bar(a), the compression part represents 73 % of the total power and the same change in pinch point gives an expected change in total power of 1.18 %.

Changing the pinch point in the evaporator will result in an increase in the lower pressure limit for the ammonia cycle. Since the upper limit is fixed by the 10-degree difference to ambient the total pressure rise for the ammonia cycle will decrease and thereby result in less compressor work. To achieve the same heat transfer in the evaporator the mass flow in the ammonia cycle must increase.

At the approximate mean temperature of 300 K, the $c_p$ for ammonia is 4.86 J/kgK [48]. By dividing the universal gas constant with the molar weight, the gas constant for ammonia was calculated. Assuming constant $c_p$ and efficiency and using a 5-degree temperature difference, the power savings for the ammonia cycle can be approximately calculated according to Equation 7.6.

$$Savings = \frac{\dot{m}_{5°C} T_{in,5°C} \left( \left( \frac{p_2}{p_1} \right)^{\frac{\gamma-1}{\gamma}} - 1 \right)}{\dot{m}_{10°C} T_{in,10°C} \left( \left( \frac{p_2}{p_1} \right)^{\frac{\gamma-1}{\gamma}} - 1 \right)} \qquad \text{Equation 7.6}$$

For the case with three compressors at 20 bar(a) the lowest pressure in the ammonia cycle increased by 0.30 bar when the pinch point was decreased by 5 degrees. This corresponds to a power saving of 13 % for the ammonia cycle. Since the ammonia cycle represents 34 % of the total power, savings over the whole cycle are predicted to be 3.86 %.

The same calculations were undertaken for the case with five compressors at 40 bar(a). Increasing the lowest pressure within the ammonia cycle by 0.72 bar resulted in an 18 % power saving. In this case the ammonia cycle represents almost 14 % of the total power therefore the total power saving were predicted to be approximately 2.30 %.

#### 7.4.5.2 Calculated Pinch-Point Analysis

The pinch-point analysis investigation was carried out in IPSEpro. To evaluate the pinch point variation 5 and 10 °C pinch points for both 20 bar(a) with three compressors and 40 bar(a) with five compressors were simulated.

To evaluate the benefits of changing the pinch points for the heat exchangers and the evaporator a percentage change from the baseline was calculated. For the case with three compressors and 20 bar(a) an improvement of the evaporator to achieve a pinch point of 5 °C resulted in a power saving of 3.95 %. The same change for the liquid to gaseous $CO_2$ heat exchangers gave a power saving of 0.9 %. For a higher pressure with five compressors the saving were smaller, 2.30 % for the evaporator and 0.64 % for the $CO_2$ heat exchangers.

#### 7.4.5.3 Results and Discussion of Theoretical and Calculated Approaches

Figures from both investigations are summarised in Table 7.13.

**Table 7.13: Power consumption for decreased pinch point**

| | Shaft Power 10 ˚C Baseline | HX 5 ˚C Expected | HX 5 ˚C IPSEpro | Evaporator 5 ˚C Expected | Evaporator 5 ˚C IPSEpro |
|---|---|---|---|---|---|
| **3 Sections, 20 bar** | 0 % | - 0.94 % | - 0.90 % | -3.86 % | - 3.95 % |
| **5 Sections, 40 bar** | 0 % | - 1.18 % | - 0.64 % | -2.30 % | - 2.38 % |

The slight difference in expected and calculated values for the evaporator pinch point power savings could be attributed to the two compressor stages in the ammonia cycle used in the IPSEpro model, whereas in the theoretical calculations a single stage compression was assumed. The greater difference in power savings for the 5 section calculations is due to the additional losses that are introduced with extra heat exchangers which are not included in the theoretical analysis.

### 7.4.6 Summary

Minimum power consumption for the cryogenic solution depends on:

- The number of compressor sections in the gaseous phase.
- Phase transformation pressure.

- Refrigeration plant design i.e. number of compression stages, type of refrigerant, heat transfer area in the evaporator and the condenser.
- Efficiencies for all compressors and the cryogenic pump.
- System losses.
- Heat exchanger effectiveness and COP.

### 7.4.7 Discussion

The power consumption for the refrigeration plant can be divided into three parts; the compression, the chilling and the pumping. The power consumption for the pump is roughly the same for all cases and represents approximately 11 % of the total power. An efficiency of 50 % was used in the model, which is a relatively low pump efficiency. However the pump represents a small proportion of the total power the major power savings will come as a result of improving the refrigeration cycle and the compressors.

There are different things that can be considered for improvements of the compression process. The reuse of the excess cold is one of them. By adding heat exchangers after the intercoolers prior to the next compression section the compressor inlet temperature will reduce (i.e. reduced compressor work). However every heat exchanger introduces additional parasitic pressure losses. The 1.5 % pressure loss for each heat exchanger might be a pessimistic estimation that penalises the models with reuse of the excess cold unfairly.

Reducing the heat exchanger pinch point was another improvement considered for the compression process. A pinch point reduction from 10 to 5 °C gave an improvement of less than 1 %.

The refrigeration cycle can also be improved by reducing the pinch point in the evaporator. When this pinch point is reduced the ammonia enters the evaporator at a higher temperature. To accomplish the same liquid $CO_2$ temperature entering the pump, a higher ammonia mass flow is required. An increased mass flow will increase the compressor work in the ammonia cycle. However the higher ammonia temperature also gives a higher saturation pressure leaving the evaporator i.e. the pressure ratio in the ammonia cycle reduces since the high pressure is fixed. Based on results from the investigation the pressure rise has a greater positive impact than the negative impact of the increased mass flow.

When the $CO_2$ refrigeration inlet pressure increases more work is carried out in the compression process than in the refrigeration cycle. A high $CO_2$ condensing pressure corresponds to a high low-pressure for the ammonia cycle and a decreased mass flow.

The greatest advantage with the refrigeration and pumping option is that the critical area is avoided, therefore the phase of the $CO_2$ is known and the behaviour is easier to predict.

## 7.5 Summary of the Different Compression Option

Since the conditions for each compression method varies the best calculated results from all investigations are normalised and compared to the isothermal work and listed in Table 7.4.

A summary of all assumptions for each method are listed below:

**MAN Turbo**

- Mass flow 84 kg/s.
- Compression from 1 - 200 bar(a).
- 85 % polytropic efficiency.

**Ramgen**

- Mass flow 18.9 kg/s.
- Compression from 1.8 - 173.6 bar(a).
- 85 % isentropic efficiency.

**Barrels and Croygenic**

- Mass flow 84 kg/s.
- Compression from 1.8 - 200 bar(a).
- 85 % polytropic efficiency.

**Table 7.4: Summary of best calculated results**

| Isothermal work | MAN Turbo | Ramgen | Barrels | Cryogenic |
|---|---|---|---|---|
| **1.0** | 1.3 | 1.6 | 1.2[5] | 1.3 |

Compared to the existing compression techniques, up to 7 % power savings can be achieved by different technologies according to calculations based on table 7.4.

[55] This value was calculated using a 7-section compressor without further improvements such as integral cooling.

# 8 Discussion

The main objective from the Company was minimal power consumption and all options have primarily been assessed against this criterion. Other requirements such as footprint, use of waste heat, cost and maintenance have not been considered although there has been an awareness of these aspects.

The Rampressor is a novel technology that has not been proven in full scale although Ramgen Power Systems claims that their supersonic shock compressor would be appropriate for CCS applications. The numbers stated by Ramgen Power Systems and the results from the investigations shows high power consumption compared to the other options. The high pressure ratios results in high work load per stage and high exit temperatures. When the two-stage compression is plotted in a pressure – enthalpy diagram it is clear that the process is far from the isothermal work. However the waste heat can be used elsewhere in the power plant or for district heating to increase the overall thermal efficiency. The Company claimed that the use of additional waste heat is limited since there are plenty of low grade heat sources in the power plant. Hence this aspect was not considered.

An integrally geared compressor offers the opportunity to choose the optimum speed for each impeller, which gives an optimum flow coefficient and thereby high polytropic efficiencies for all stages. A major disadvantage for this type of compressor is the diffuser and return channels, which requires a 180° turn causing significant losses. Integrally geared compressors are used in urea production industry and it is well proven $CO_2$ compression method.

An in-line barrel solution gives the opportunity to alter the number of compressor sections. By plotting power versus sections, the power saving per additional section was obtained. After seven sections the power consumption approaches isothermal work and the power saving of additional sections with intercooling will be less than 1 % per section. Comparing the relatively small power saving for each section with the increase in total cost and footprint, a 7-section solution is a reasonable choice. Further improvements such as integral cooling, pre-cooling and lowering the intercooling temperature will reduce the power consumption. The most beneficial of these the improvements was the integral cooling where the power consumption approaches the 14-section compression but with significantly smaller footprint.

When comparing a Rolls-Royce in-line barrel solution with a MAN Turbo integrally geared bull wheel compressor some major attributes are notable. An in-line solution offers standard frames with flexible interior i.e. number of impellers per section, inlet guide vanes, possibility of integral cooling, number and placement of intercoolers. The integrally geared compressors offer a more compact design with high polytropic efficiencies throughout the compressor and optimised speed for each impeller.

With a cryogenic solution the critical region is avoided. The intercooling exit temperatures will be well above the saturation temperature ensuring compression in gaseous phase. The $CO_2$ phase transformation from gas to liquid will occur in chillers designed for this purpose. After the chilling is completed the liquid $CO_2$ can be pumped to required pressure. The pump will have to withstand cryogenic temperatures and a relatively high mass flow which may require adaption of current

products. These three parts (compressing, chilling and pumping) can be studied separately to find the driving force behind power savings.

All calculations in this thesis are based on pure $CO_2$ and the effects of impurities need more thorough investigations. Although, the small investigation of impurities shows that the power consumption most likely will increase due to changes in thermodynamic properties. Water removal and recirculation of non-condensables will further increase the power consumption.

# 9 Conclusion

The major conclusions of the investigations undertaken in the thesis are as follows:

- According to results in this thesis the Rampressor was not a suitable option due to the high power consumption and the unproven technology.

- The MAN Turbo products available for $CO_2$ compression require power consumption above the isothermal work.

- The cryogenic solution is a safe option which has low power requirements although the increased footprint and cost argues against it.

- The best option according to the results was the 7-section in-line barrel solution which can be further improved by integral cooling or lower intercooling outlet temperatures.

- Models that have been simulated in IPSEpro show that the power consumption can be reduced with approximately 7 % when improvements are made.

# 10 References

## 10.1 Literature References


[1] **Chalmers and Göteborg University.** [Online] [Cited: 20 April 2009.] http://www.miljoportalen.se

[2] **International Energy Agency.** *World energy outlook 2007*. France. 2007.

[3] **Commission of the European Communities.** *Supporting Early Demonstration of Sustainable Power Generation from Fossil Fuels.* Brussels. 2008.

[4] **Sim Tech.** [Online] [Cited: 4 November 2008.] http://www.simtechnology.com

[5] **Rolls-Royce.** [Online] [Cited: 2 March 2009] http://www.rolls-royce.com

[6] **Metz B, et. Al.** *IPCC Special Report on Carbon Dioxide Capture and Storage.* Cambridge, New York: Cambridge University Press. 2005.

[7] **Vattenfall.** [Online] [Cited: 6 November 2008.] http://www.vattenfall.com/www/co2_en/co2_en/399403facts/399433captu/index.jsp

[8] **International Energy Agency, Clean Coal Centre.** [Online] [Cited: 31 October 2008.] http://www.iea-coal.org.uk/site/ieacoal_old/publications/newsletter/current-issue-a/newsletter-3

[9] **Fredriksson Möller, B.** *A Thermoeconomic Evaluation of $CO_2$ Capture with Focus on Gas Turbine-Based Power.* Doctoral thesis, Division of Thermal Power Engineering, Department of Energy Science. Lund University Sweden. 2005.

[10] **BBC News.** [Online] [Cited: 7 November 2008.] http://news.bbc.co.uk/2/hi/science/nature/7584159.stm

[11] **World Coal Institute.** [Online] [Cited: 7 November 2008.] http://www.worldcoal.org/pages/content/index.asp?PageID=422

[12] **UK Advanced Power Technology Forum.** *Clean Fossil Power Generation in the 21st Century – a technology for carbon capture and storage.* APGTF workshop, London. 2009.

**[13] Fredriksson Möller B.** *$CO_2$-avskiljningsteknik och metoder*. Division of Thermal Power Engineering, Department of Energy Science. Lund University Sweden. 2005.

[14] **Institution of Mechanical Engineers.** *Carbon Capture and Storage – Event Proceedings, 12 November 2008.* London: Institution of Mechanical Engineers. 2008.

[15] **Watt James.** AMEC, *APGTF workshop*. London. 11-12 February 2009.

[16] **Earth System Research Laboratory.** [Online] [Cited: 23 February 2009.] http://www.esrl.noaa.gov/gmd/ccgg/trends/

[17] **Confidential correspondence with UK University**

[18] **Reid RC, Prausnitz JM, Poling BE.** *The Properties of Gases & Liquids.* Fourth Edition. New York: McGraw-Hill Inc. 1987.

[19] **Walsh P.P, Fletcher P.** *Gas Turbine Performance*. Second edition. Oxford, Malden, Carlton: Blackwell science Ltd. 2004.

[20] **eCompressedair.** [Online] [Cited: 23 October 2008.] http://www.ecompressedair.com/library/aircompressors.shtml

[21] **Aungier RH.** *Centrifugal compressors – A Strategy for Aerodynamic Design and Analysis*. New York: The American Society of Mechanical Engineers. 2000.

[22] **Cohen, Rogers GFC, Saravanamutto HIH.** *Gas Turbine Theory*. Fourth edition. Essex: Addison Wesley Longman Limited. 1996.

[23] **Direct Industry** [Online] [Cited: 8 October 2008.] http://www.directindustry.com/prod/man-turbomaschinen/axial-compressor-19648-43111.html

[24] **Davis, A.** *Reciprocating Compressor Basics.* Machinery Lubrication Magazine. July 2005.

[25] **General Electric Oil & Gas.** [Online] [Cited: 27 October 2008.] http://www.geoilandgas.com/businesses/ge_oilandgas/en/prod_serv/prod/compressors/en/index.htm

[26] **MAN Turbo.** [Online] [Cited: 27 October 2008.] http://www.manturbo.com

[27] **Ramgen Power systems.** [Online] [Cited: 4 March 2009.] http://www.ramgen.com

[28] **Siemens.** [Online] [Cited: 27 October 2008.] http://www.siemens.com

[29] **Dresser Rand.** [Online] [Cited: 27 October 2008] http://www.dresser-rand.com

[30] **General Electric.** [Online] [Cited: 27 October 2008] http://www.gepower.com

[31] **Girdhar P, Moniz O, Mackey, S.** *Practical Centrifugal Pumps.* Oxford, Burlington: Newnes An Imprint of Elsevier. 2005.

[32] **Gas Processors Association.** *Engineering Data Book.* Tulsa: The Gas Process Supplier Association. 2004.

[33] **Alvarez H.** *Energiteknik, del 1*. Lund: Studentlitteratur AB. 2006.

[34] **Karassik IJ et. Al.** *Pump Handbook.* Fourth edition. New York: The McGraw-Hills Companies, Inc. 2008.

[35] **Hitachi Plant Technologies, Ltd.** [Online] [Cited: 28 October 2008.] http://www.hitachi-pt.com

[36] **Flowserve.** [Online] [Cited: 29 October 2008.] http://www.flowserve.com

[37] **Clyde pumps.** [Online] [Cited: 29 October 2008.] http://www.clydepumps.com

[38] **General Electric Oil & Gas.** [Online] [Cited: 27 October 2008.] http://www.geoilandgas.com

[39] **University of Newcastle upon Tyne.** [Online] [Cited: 12 March 2009.] http://lorien.ncl.ac.uk/ming/cleantech/refrigeration.htm

[40] **University of Plymouth.** [Online] [Downloaded: 12 November 2008.] www.tech.plym.ac.uk/sme/THER205-web/refrig.pdf

[41] **Dr Çengel YA, Dr Boles MA.** *Thermodynamics – An Engineering Approach*. Third edition. New York: The McGraw Hill Companies Inc. 1998.

[42] **Perry RH, Green D.** *Perry's chemical engineers' handbook.* Fourth edition. New York: The McGraw Hill Companies Inc. 1984.

[43] **BOC.** [Online] [Cited: 17 November 2008.] http://www.boc-gases.com/products_and_services/by_product/refrigerants/index.asp

[44] **Brown RN.** *Compressors, Selection and Sizing.* Oxford: Elsevier Inc. 2005.

[45] **Sundén B.** *Kompendium i kondensation, förångning och värmeväxlare.* Lund: Avd. för värmeöverforing – VoK, Lunds Tekniska Högskola. 2002.

[46] **PhD Moore JJ, Nored MG.** *Novel concepts for the compression of large volumes of carbon dioxide. GT 2008-50924.* Berlin: South West Research Institute. 2008.

[47] **Confidential Email from utility company.**

[48] **Mayhew YR, Rogers GFC.** *Thermodynamic and Transport Properties of Fluids.* Second edition. Oxford: Blackwell Science Ltd. 1969.

[49] **UNC Chemistry Fundamentals.** [Online] [Cited: 31 October 2008.] http://www.shodor.org/UNChem/math/newton/index.html

[50] **WolframMathWorld.** [Online] [Cited: 31 October 2008.] http://mathworld.wolfram.com/NewtonsMethod.html

## 10.2 Figure References

2.1 Courtesy to **Rolls-Royce**

2.2 Produced by authors

2.3 Produced by authors

3.1 Produced by authors

3.2 Produced by authors, adapted from **[6]**

3.3 Courtesy to **Vattenfall** [Online] [Cited: 9 March 2009.] www.europeanenergyforum.eu

3.4 Courtesy to **Vattenfall** [Online] [Cited: 9 March 2009.] www.europeanenergyforum.eu

3.5 Courtesy to **Vattenfall** [Online] [Cited: 9 March 2009.] www.europeanenergyforum.eu

4.1 Produced by authors, adapted from **[17]**

5.1 Produced by authors, based on **[20]**

5.2 Produced by authors, adapted from **[22]**

5.3 Produced by authors, adapted from **Rolls-Royce**

5.4 Courtesy to **Rolls-Royce**

5.5 Courtesy to **MAN Turbo**

5.6 Courtesy to **[31]**

5.7 Produced by authors, adapted from **[31]** and **[38]**

5.8 Courtesy to **[31]**

5.9 Courtesy to **[31]**

5.10 Produced by authors, adapted from **[41]**

5.11 Produced by authors, adapted from **[41]**

5.12 Produced by authors, adapted from **[41]**

6.1 Produced by authors

6.2 Courtesy to **Ramgen** [Online] [Cited: 4 March 2009.] www.ramgen.com

6.3 Courtesy to **[21]**

7.1 Courtesy to **MAN Turbo**

7.2 Courtesy to **[14]**

7.3 Produced by authors

7.4 Produced by authors

7.5 Produced by authors

7.6 Produced by authors

7.7 Produced by authors

7.8 Courtesy to **Ramgen**

7.9 Courtesy to **Ramgen**

7.10 Produced by authors

7.11 Produced by authors

7.12 Produced by authors

7.13 Produced by authors

7.14 Produced by authors

7.15 Produced by authors

7.16 Produced by authors

7.17 Produced by authors

7.18 Produced by authors

7.19 Produced by authors

A1 Courtesy to **[4]**

A2 Produced by authors

A3 Produced by authors

B1 Produced by authors

B2 Produced by authors

# Appendix A

## IPSEpro

IPSEpro is a set of software modules used as a tool for creating process models and process analyzing in power plant engineering, chemical engineering and other related areas. The programme can be used to:

- Calculate heat balances and to predict off design behaviour.
- Estimate costs on consistent designs.
- Validate and verify estimates.
- Optimize plant performances on-line.
- Plan modifications and repowering of existing plants.

As shown in Figure A1, IPSEpro consists of two parts. The PSE – Process Simulation Environment where simulations are done for different projects and the MDK – Model Development Kit where existing models are available. These models can also be changed or rebuilt in the model library. [4]

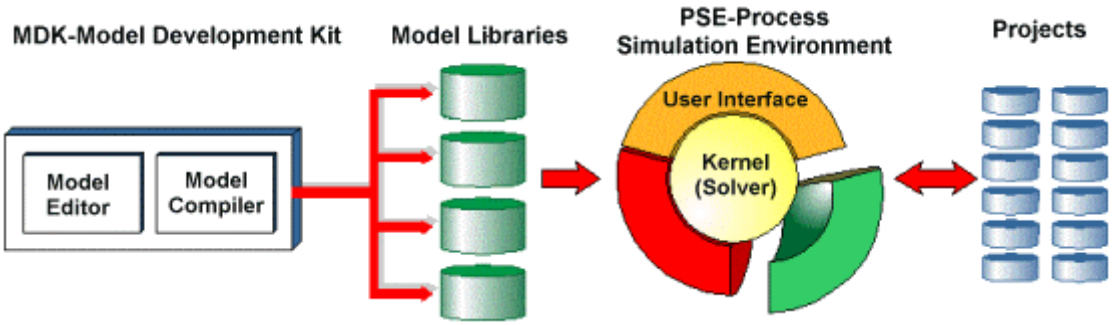


**Figure A1: IPSEpro system structure**

## Model Development Kit

A standard model library is provided in the software although in the MDK it is possible to create new models or modify existing ones. MDK consists of two functional units, a model editor and a model compiler. In the model editor the user can change icons as suitable for the model and describe their function mathematically. The model compiler will translate the code written in the editor to binary format. [4]

### Refrigeration process library

The refrigeration library is a model library where thermodynamic calculations can be done for over fifty different refrigerants. It can be used for calculations requiring refrigeration systems and vapour compression systems. This model can be used in combination with both the advanced power plant and the gas turbine library, which gives the user wider opportunities to explore different areas. [4]

### Process Simulation Environment

In PSE the user can create a model based on the components from the different libraries. Different concepts can be built up in a flow sheet where all data is added and the results of the calculations that have been done are shown directly on the flow sheet, see Figure A2. A colour scheme is used for definition of the values: black

means that the value is a converged variable or parameter, red means that the variable did not convert and blue means that the value was not calculated.

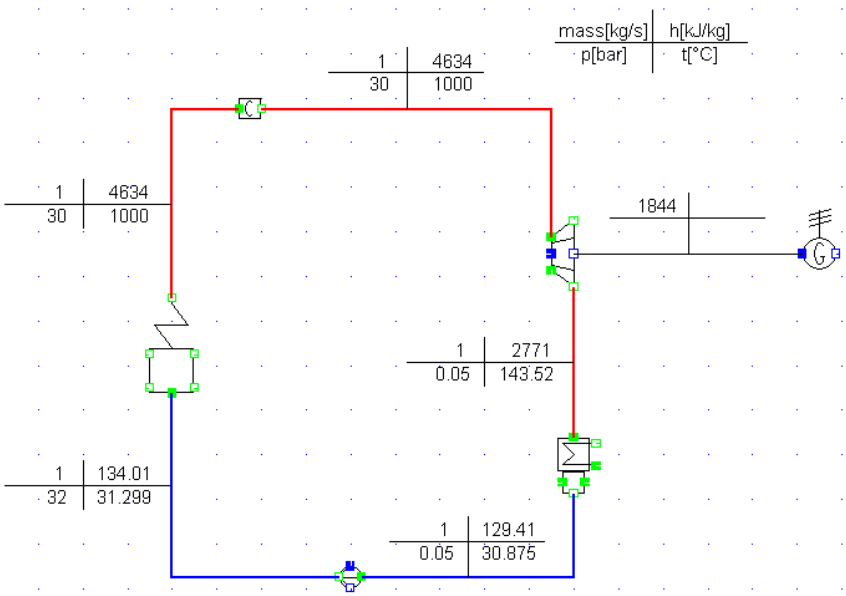


**Figure A2: Simple Rankine cycle simulated in IPSEpro**

IPSEpro defines three types of models: units, connections and globals. These objects have a hierarchical structure and can only reference other objects of lower level as shown in Figure A3.

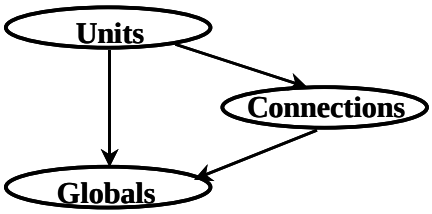


**Figure A3: Hierarchy of the model classes**

Units represent actual pieces of equipment, i.e. compressors or pumps, and are the nodes in the network structure. Connections represent the information that is transferred between two units and are the connections between the nodes. Globals contains information that is shared by other objects. A typical example of a global is a chemical composition. [4]

## PSExcel

PSExcel is an extension to the program, that, in cooperation with excel makes it possible to investigate a variety of different parameters (e.g. pressure, temperature, power etc.) It can also be used to apply existing excel data to simulations in PSE. [4]

## Solution method

The Newton-Raphson method

All nonlinear equations need a solving method that depends on an initial value and an iterative process. In IPSEpro the Newton-Raphson solver is used. The Newton-

Raphson solver is an iterative nonlinear method that uses the first few terms of the Taylor series for a function *f(x)* in the vicinity of a suspected root. [49]

The Taylor expansion of $f(x)$ at the point $x = x_0 + \varepsilon$ is

$$f(x_0 + \varepsilon) = f(x_0) + f'(x_0)\varepsilon + \frac{f''(x_0)}{2}\varepsilon^2 + \ldots \qquad \text{Equation A1}$$

Using only the terms of the first order gives

$$f(x_0 + \varepsilon) \approx f(x_0) + f'(x_0)\varepsilon \qquad \text{Equation A2}$$

Set $f(x_0 + \varepsilon) = 0$ and solve for $\varepsilon = \varepsilon_0$ results in

$$\varepsilon_0 = -\frac{f(x)}{f'(x)} \qquad \text{Equation A3}$$

which is the first order adjustment to the root's position. Using

$$\varepsilon_n = -\frac{f(x_n)}{f'(x_n)} \qquad \text{Equation A4}$$

the process can be repeated until it converges.

So the general iterative formula is formulated as

$$x_{n+1} = x_n - \frac{f(x_n)}{f'(x_n)}, \quad n = 1, 2, 3 \ldots \qquad \text{Equation A5}$$

How quickly convergence is reached highly depends on the initial value. If the initial value is far from the root the method delivers incorrect values. The more initial values the bigger risk that the system will fail. Because of this, a large equation system represents major problems and therefore this method is not always reliable. It is still a good solver and the main advantage is its ability to rapid convergence. When the method converges, it does so quadratically [50].

# Appendix B

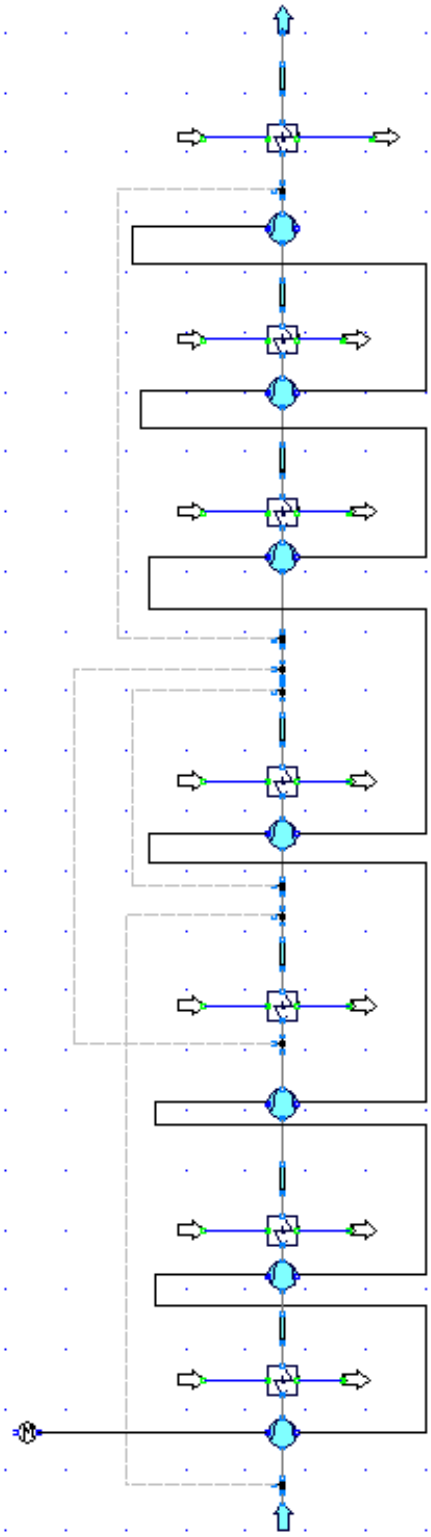

**Figure B1: 7-section compressor model simulated in IPSEpro**

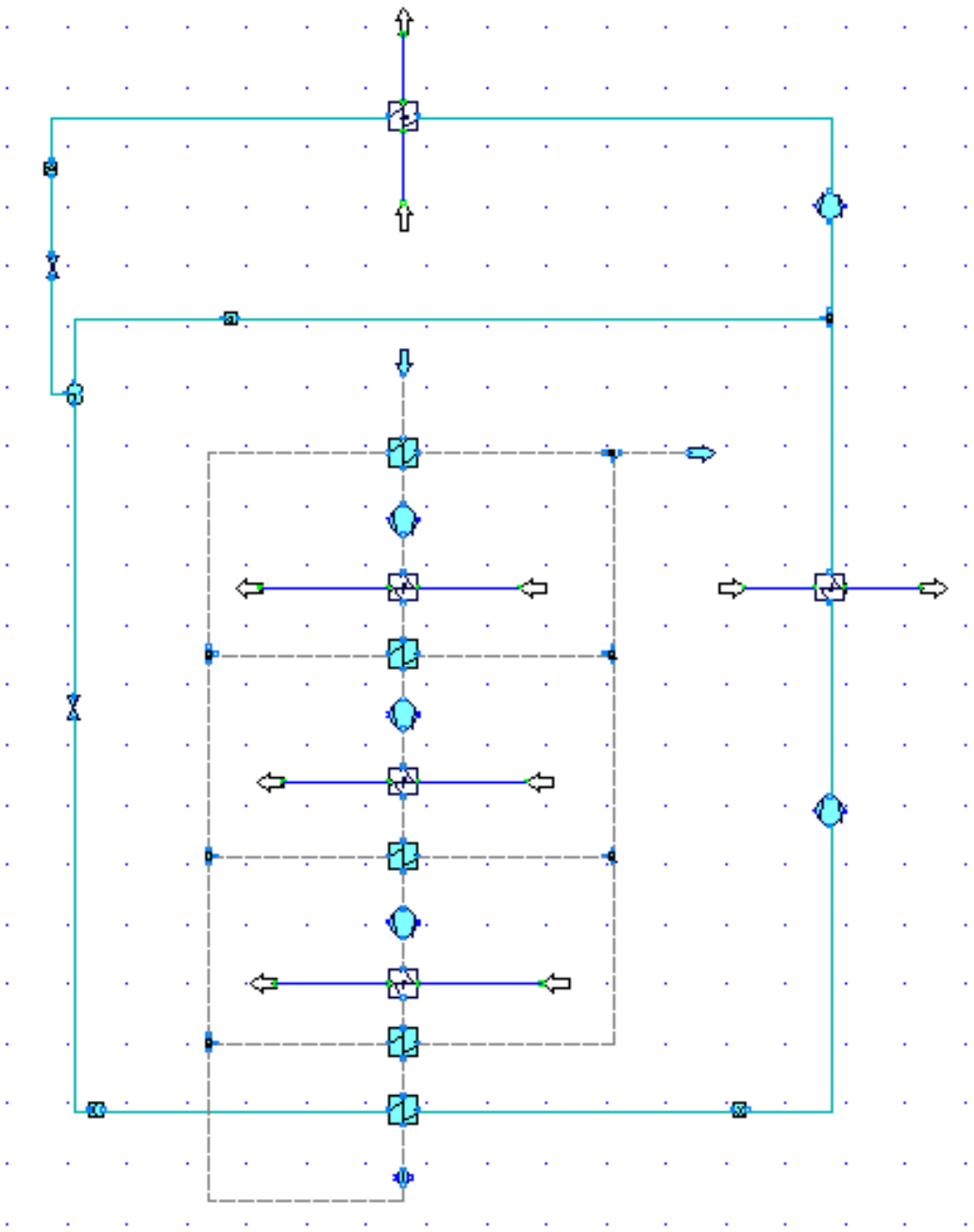

**Figure B2: Simplified cryogenic system with 3 $CO_2$ compressors and recirculated cold $CO_2$, simulated in IPSEpro**